Reviews in Mineralogy & Geochemistry
Vol. 88 pp. 567-636, 2022



# Geochronology of Diamonds

**Karen V. Smit*, Suzette Timmerman**
*Department of Earth and Atmospheric Sciences*
*University of Alberta*
*Edmonton T6G 2E3 Alberta, Canada*
*Now at the University of the Witwatersrand: *karen.smit@wits.ac.za, suzette@ualberta.ca*

**Sonja Aulbach**
*Institute of Geosciences*
*Goethe-Universität*
*Frankfurt am Main, Germany*
*s.aulbach@em.uni-frankfurt.de*

**Steven B. Shirey**
*Earth and Planets Laboratory*
*Carnegie Institution for Science*
*5241 Broad Branch Road NW, Washington DC 20015, U.S.A.*
*sshirey@carnegiescience.edu*

**Stephen H. Richardson**
*Department of Geological Sciences*
*University of Cape Town*
*Rondebosch 7701, South Africa*
*steve.richardson@uct.ac.za*

**David Phillips**
*School of Geography, Earth and Atmospheric Sciences*
*The University of Melbourne*
*Parkville, VIC 3010, Australia*
*dphillip@unimelb.edu.au*

**D. Graham Pearson**
*Department of Earth and Atmospheric Sciences*
*University of Alberta*
*Edmonton T6G 2E3 Alberta, Canada*
*gdpearso@ualberta.ca*

## INTRODUCTION

Diamond crystallization ages are essential information for science and industry, leading to an understanding of how, why, and where diamonds form in Earth and how best to find them. Such knowledge is of prime importance for constraining the source and mobility of volatile-rich diamond-forming fluids in the mantle and the nature of the geodynamic processes that release these fluids.

1529-6466/22/0088-0011$10.00 (print)
1943-2666/22/0088-0011$10.00 (online)
http://dx.doi.org/10.2138/rmg.2022.88.11

Geochronology using radiogenic isotopes relies on the differential partitioning of parent and daughter elements into different phases, including minerals and melts, and determining the time elapsed after parent–daughter fractionation and closure of the system. However, the purity of monocrystalline diamond presents a fundamental problem: the diamonds themselves have such low abundances of the elements of interest that precise and accurate age determinations are precluded. Therefore, dating the formation of diamond has to rely on dating its inclusions, an effort which started nearly 50 years ago and since then has undergone a profound evolution. The reliance on inclusions to obtain diamond ages is predicated on the hypothesis that the encapsulating diamond prevents further isotopic exchange between the mineral inclusion and the surrounding mantle.

In the 1970s, sulfides were the first inclusions for which age determinations were attempted using Pb isotopes (Welke et al. 1974; Kramers 1979). Due to low U–Th content, only Pb–Pb model ages are obtainable for sulfides. Diamonds from the Finsch and Kimberley kimberlites (Kaapvaal craton, South Africa) gave Pb–Pb model ages in excess of 2 Ga, much older than their Cretaceous host kimberlites. Even though the analytical data were subject to large blank corrections, as well as uncertainties in mantle Pb growth curves, these results provided some of the first evidence that diamonds are xenocrysts in the host kimberlite (Kramers 1979).

Richardson et al. (1984) produced ~3.3 Ga Sm–Nd and Rb–Sr model ages on composites of harzburgitic garnet inclusions from Kimberley and Finsch diamonds. In addition to proving that diamonds occur as xenocrysts in kimberlite, these results also clearly indicated that diamonds are billions of years old and established a Paleoarchean age for the continental lithospheric mantle sources for the diamonds.

Richardson and co-authors subsequently provided age constraints for many diamond suites from South Africa, Botswana, Australia, and Russia (e.g., Richardson 1986; Richardson et al. 1990, 1993; Richardson and Harris 1997). At the time of Richardson's Sm–Nd and Rb–Sr work, single grains of garnet or clinopyroxene from gem-quality monocrystalline diamonds needed to be grouped together with other similar grains—each broken from its own diamond host—in order to obtain sufficient Sm, Nd, Rb, and Sr to generate a signal on the mass spectrometer. This problem appeared to have been overcome in the late 1980s, when Burgess et al. (1989) and Phillips et al. (1989) reported $^{40}Ar/^{39}Ar$ ages for single clinopyroxene inclusions in diamonds from the Premier kimberlite (*Cullinan Mine*) in South Africa. However, subsequent work revealed unforeseen Ar redistribution problems with the approach used at the time, which has limited wider application of the technique (Burgess et al. 2004). Nevertheless, the $^{40}Ar/^{39}Ar$ method has proved useful for detrital diamond provenance studies (Phillips et al. 2004, 2018; Laiginhas et al. 2009).

In the mid-1990s, the analytical methods developed for Re–Os on whole-rock samples (e.g., Shirey and Walker 1998) were miniaturized and modified so that single sulfide inclusions (typically between 2 and 10 µg but also larger) could be analyzed, obviating the need to use composites (Pearson et al. 1998b; Pearson and Shirey 1999). Since the initial Re–Os study on Koffiefontein (Kaapvaal craton) sulfide-bearing diamonds (Pearson et al. 1998b), Re–Os has become the most widely used chronometer for determining diamond ages world-wide (e.g., Richardson et al. 2001; Westerlund et al. 2006; Richardson and Shirey 2008; Aulbach et al. 2009a,c, 2018; Smit et al. 2010, 2016; Wiggers de Vries et al. 2013; Gress et al. 2021a,b).

The recent advent in mass spectrometry of $10^{13}$ Ohm feedback resistors in Faraday cup current amplifiers, resulting in more sensitive detectors (Koornneef et al. 2014), has made it possible to measure the isotopes of Sm, Nd, Rb, and Sr at the extremely low amounts in which they occur in single garnet and clinopyroxene inclusions. This technique has been applied to inclusions in diamond from Botswana and South Africa (Koornneef et al. 2017; Timmerman et al. 2017; Gress et al. 2021a, b, c), affording the clearer detection of multiple diamond-forming events within a given mantle region, in particular when used in conjunction with Re–Os dating

of sulfide inclusions in the same diamond suite (e.g., Gress et al. 2021b).

A new method that shows promise in this evolving field is the dating of fluid-rich fibrous diamonds using the U–Th/He isotope system (Timmerman et al. 2019c; Weiss et al. 2021). Fluid-rich mircoinclusions contain sufficient $^{235,238}$U and $^{232}$Th that decay over time to $^{4}$He. Where mineral inclusions are used to date monocrystalline gem-quality diamonds, fluid inclusions can be used to date fibrous diamonds and give important constraints on whether they formed contemporaneously or in separate events.

In the 35 ensuing years since the Richardson et al. (1984) study, the ages of diamonds from almost every significant diamond-producing locality have been determined from their mineral inclusions. This allows viewing diamond formation less as an isolated event in the mantle under each mine, and more in the geological context of global tectonothermal events, such as the supercontinent cycle.

In this chapter we describe the radioisotope systems used for diamond geochronology and the principles on which they are based. Different approaches to using mineral inclusions for age constraints have different implications regarding accuracy and equilibration between diamond-forming fluids, the inclusions themselves and their host lithologies. Practical considerations of determining and interpreting diamond ages, including sources of uncertainty, the relationship of the dated inclusions to their host diamond, other (e.g., non-geochronological) evidence for ancient diamond ages, and a practical formalism for diamond ages are reviewed. A final discussion of terranes where diamond ages have been applied to constraining the geological evolution of continents illustrates one of the reasons why diamond ages are important.

## DATING PRINCIPLES AND GLOSSARY

### Terminology

Since the production of the first radiometric ages (Rutherford 1905) geologists have debated the significance of the event being *'dated'* by geochronology. All geochronology comes down to accurately determining the time of parent–daughter fractionation. The geological meaning of this fractionation often leads to multiple interpretations and disagreements.

Diamonds are typically dated to understand the time of crystallization: when carbon atoms in a fluid or melt took the form of a diamond crystal lattice. Dating the crystallization age of diamond is one of the most significant challenges in geochronology, and a practice that has generated much debate in the geological literature (e.g., Pidgeon 1989; Richardson 1989; Navon 1999; Pearson and Shirey 1999).

Dating diamond is difficult because the diamond lattice itself cannot be directly dated. There are several reasons for this. Despite being composed of nearly pure carbon, the ages of the vast majority of diamonds are older than the time-span accessible to $^{14}$C dating (~50 k.y.). Radioactive trace elements with much slower decaying radionuclides such as K, Rb, Sm, Re, and U do not substitute directly into the diamond lattice itself, but may instead be hosted in fluid and mineral inclusions (e.g., Weiss et al. 2022, this volume; Stachel et al. 2022a, this volume).

Even though fluid inclusions hold promise for radiometric dating, the radioisotopes of interest are often present in such low abundances in gem diamonds that precise isotopic measurement is precluded (e.g., McNeill et al. 2009; Melton et al. 2012; Krebs et al. 2019; Timmerman et al. 2019a). When present in higher concentrations in fibrous or fluid-rich diamonds, these radioisotopes may show complex isotopic systematics that are not always conducive to absolute age determination (Klein-BenDavid et al. 2010, 2014). Recently, however, fibrous fluid-rich diamonds have been successfully dated with U–Th/He systematics (Timmerman et al. 2019c; Weiss et al. 2021).

Mineral inclusions trapped inside diamond during growth are most frequently used for radiogenic isotope analyses. These inclusions are rare in gem-quality diamonds and often tiny—less than 100 μm. The geological events that give the least ambiguous dates involve the crystallization of a mineral at high enough temperatures to reset any pre-existing chronological information and chemically homogenize the isotopic system being considered. This is followed by very rapid cooling, to '*freeze in*' the element distribution created at the time of crystallization, allowing the geochronometer to be '*set*'. The challenge of determining the time of diamond crystallization can be well illustrated by considering some of the assumptions underlying the various types of radiometric age calculations.

To assist the non-specialist reader in understanding the differences, advantages and disadvantages in these calculations, we provide some definitions of the various terms used, prior to the main discussion. These ideas will be amplified with examples given through consideration of the different dating techniques.

***Decay constant and half-life.*** The decay constant ($\lambda$) can be thought of as the probability that a given nuclide will decay over some specified period of time, usually expressed in units of time$^{-1}$. The decay constant ($\lambda$) for $^{187}$Re is given as:

$$\lambda = 1.6689 \pm 0.0031 \times 10^{-11}\ a^{-1}\ \text{(Selby et al. 2007)}$$

where a = year

The term '*half-life*' ($t_{1/2}$) is slightly more tangible because it is given in units of years (for geological systems) and is expressed as the time taken for the original number of parent atoms to decrease by half. Re-arrangement of the standard equation for radioactive decay leads to the relationship between the half-life and the decay constant being given as:

$$t_{1/2} = 0.693/\lambda$$

***Parent–daughter ratio.*** The ratio of the unstable radioactive '*parent*' nuclide to the stable '*daughter*' nuclide produced by radioactive decay, e.g., $^{187}$Re to $^{187}$Os, $^{147}$Sm to $^{143}$Nd.

***Common.*** All the stable isotopes of an element, including the pre-existing daughter isotope, that are inherited at the time the isotopic system is closed. Radioactive decay adds new atoms of the daughter isotope to the *'common'* or extant isotopes of the element. In K–Ar geochronology this is equivalent to '*extraneous'* (includes excess and inherited) Ar.

***Isotopic system closure.*** The time at which atomic diffusion of parent or daughter isotope effectively ceases, at the sample-scale being considered, e.g., at the micron-scale of the lattice of a given mineral, or at the mineral-to-mineral scale of a rock. In the case of a single mineral trapped in a diamond it can be argued that '*closure*' of the system occurs when diamond encloses an inclusion and isolates it from isotopic exchange with its surroundings, because the diamond lattice prevents any measurable diffusional exchange with the components of the entrapped mineral. In such a case, isotopic closure can be argued to reflect the '*date of diamond crystallization*'.

If, however, the daughter nuclide is a gas ($^{40}$K–$^{40}$Ar or U–Th–$^{4}$He decay) or a highly incompatible element in the mineral lattice (e.g., Pb produced from the decay of U in zircon or rutile), the daughter nuclide may diffuse to the interface between the diamond and the inclusion over million-to-billion-year residency at mantle temperatures. In these cases, failure to analyze the whole system—the gas liberated on releasing the inclusion from the diamond or the fluid film at the inclusion-diamond interface—will yield an erroneous time since diamond crystallization.

***Initial isotopic ratio.*** The isotopic ratio of the daughter element, e.g., $^{187}$Os/$^{188}$Os$_i$ existing at the time of system equilibration and closure by igneous or metamorphic mineral crystallization. Subsequent accumulation of the daughter isotope by radioactive decay

produces a new, more radiogenic isotopic ratio compared to the initial isotopic ratio. In the case of mineral inclusions in diamond, this is the isotopic ratio of Sr, Nd or Os, that the inclusion possessed at the time of diamond encapsulation. This ratio can be calculated from the age of diamond formation, the measured isotopic composition of the daughter element and the parent/daughter isotopic ratio.

**Types of ages—what is being dated and what is in a name?**

Prior to an assessment of accuracy and precision, the most important consideration about any geological age is an understanding of *what event is being dated*. In the context of diamond geochronology, the resulting age may reflect any, or a combination of:

i. the instant of diamond crystallization, or the time of percolation of diamond-forming fluids into the host mantle,

ii. cooling of the diamond and its dated inclusion to a certain temperature after diamond formation,

iii. crystallization of a '*protogenetic'* mineral now included in diamond, prior to its encapsulation in the diamond,

iv. mixing of geochemical signatures of different fluid and solid components that are mobilized during the events that cause diamond formation.

Below we will consider the main types of geological ages employed in diamond dating studies. For a more complete explanation of the principles involved, the reader is referred to Reiners et al. (2018).

***Model ages.*** A model age traces the time of divergence of the isotopic evolution of a system (*rock or mineral*) from an assumed reference reservoir—e.g., the primitive mantle or mantle with a chondritic composition—due to a change or fractionation of the parent–daughter isotope ratio in response to a geological event such as partial melting. For example, a Re–Os model age will give the time of separation from a primitive or depleted mid-ocean ridge basalt (MORB)-like mantle source, in other words, the time of initial melt formation. This is because Re is 'mildly' incompatible and partitioned into the basaltic melt during mantle melting, whereas Os is 'strongly' compatible and remains in the residue.

Model ages often *do not* reflect the time of diamond formation; and *in the simplest case* reflect the time that the isotopic evolution of the mineral diverged from a given reservoir. For example, model ages obtained for lithospheric mineral inclusions would reflect separation of the source mantle from the convecting asthenospheric mantle. In many cases that is likely to be the time of cratonic lithospheric mantle formation because of the accompanying, extensive parent/daughter fractionation. In the case of a peridotitic garnet inclusion in a diamond, its Nd isotope model age is a calculation of the length of time required for the garnet to develop its measured Nd isotopic composition (at its measured Sm/Nd ratio) with two main assumptions:

1. that it was derived from a stated reference mantle source, and

2. there was a single stage evolution. More complex two-stage model ages are possible but are rarely used in diamond dating studies.

The two options for a reference mantle reservoir are usually a mantle with time-averaged Sm–Nd isotopic characteristics similar to the parent–daughter ratio of chondritic meteorites—a $T_{CHUR}$ model age—or a mantle source slightly depleted in melt components—a $T_{DM}$ model age. In effect, the calculation estimates the intersection of the time-integrated Nd isotope evolution of the sample, with that of the chosen reference reservoir. The resulting '*model age*', in the case of peridotitic garnet, may estimate the time of melt depletion or metasomatic enrichment of the garnet-bearing source , if it occurred close to the time of melt depletion. A third assumption is involved if we relate either of these events to the simultaneous crystallization of the host diamond.

In reality, many model ages integrate the *time-averaged effects* of multiple events, including any significant pre-history of an inclusion, where it inherits some isotopic evolution different from the assumed host reservoir before the diamond-entrapment event. Model ages must be treated with caution due to these underlying assumptions and the problems caused by possible protogenetic inclusions with significant prior histories, though the reader is referred to the recent discussion of these issues by Pamato et al. (2021) and the sections below.

Most sulfides take in very large amounts of *common* Os from their environment that becomes integrated with the *radiogenic* Os. Most mantle sulfides (and inclusions in diamonds) have experienced significant pre-history, and in the case of eclogitic source rocks, acquired radiogenic Os between formation of the oceanic crustal protolith and diamond formation during or after subduction. Even if such a pre-existing sulfide is later isotopically '*reset*' during diamond crystallization, retention of a radiogenic initial isotopic ratio and possible loss of Re from the sulfide at the time of resetting will lead to a model age calculation that will *not reflect* the diamond crystallization age when calculated with reference to a model evolution curve for the primitive or depleted mantle.

The most robust model or absolute ages are given by systems where a particular mineral may have little or almost no pre-existing radiogenic or *common* daughter isotope. This is generally the case with U–Pb ages acquired from zircon. It is also the case where the mineral is old enough with such an elevated parent–daughter isotopic ratio, such as some sulfides with extremely high Re/Os, that its evolution relative to the assumed reference reservoir has a very steep slope. In such cases, very little uncertainty results from the nature of the assumed parent reservoir. Conversely, great caution must be given to model ages in systems where the isotopic evolution of a sample diverges only slightly from its assumed parent reservoir (i.e., where the parent–daughter fractionation is subtle), because the very similar parent–daughter isotope ratios lead to little divergence of the sample from the parent reservoir and large uncertainties depending on the choice of reference reservoir (e.g., mantle that is chondritic, depleted, or enriched).

***Isochron ages.*** Isochrons are graphical constructs that rely on the cogenetic relationship between a whole rock and its mineral constituents, a suite of different rocks or, in the case of diamond geochronology, mineral inclusions. The conventional diagrams plot the parent/daughter isotope ratio of the system on the *x*-axis and the daughter isotope ratio on the *y*-axis (Fig. 1). A suite of minerals all derived from the same rock—or geologic event generated in a larger mantle region with the same initial isotope ratio—will evolve to produce linear relationships whose slope is proportional to the time since the system was homogenized. Isotopic homogenization is attained or approached, typically above the closure temperature of

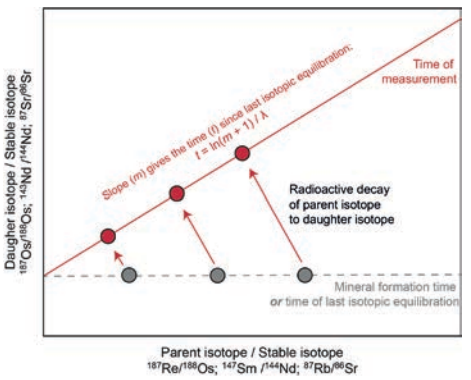


**Figure 1.** Principles of a conventional isochron diagram. The *x*-axis displays the ratio of the radioactively decaying isotope to a stable isotope of the daughter. The minerals with higher amounts of parent and/or lower amounts of daughter plot further to the right. The higher the content of parent isotope, the more daughter isotope is produced. These minerals plot at a higher position on the *y*-axis, which is the ratio of the radiogenic daughter to the same stable daughter isotope as on the *x*-axis. Radioactive decay preserves the slope that is generated by different amounts of parent relative to daughter in the different minerals. The slope of a line fitted through the present-day measured isotopic ratios, and the independently determined decay rate (accepted by the scientific community as a constant), yield the time since last isotopic equilibration.

the isotopic system of interest, especially if aided by a fluid or melt. The isotopic evolution of these mineral systems is then isolated by cooling of a hot rock to below the closure temperature, where inter-mineral diffusive equilibrium effectively ceases. The displacement of the different samples along the line is a positive correlation with their parent–daughter isotope ratio.

Isochrons require analyses of at least two samples to define a straight line, and more than two samples are highly preferred. Isochron ages are preferred over model ages, though they too require certain assumptions to be met for ages to be valid. Isochron ages also require careful interpretation, especially when the scatter in the data exceeds that expected from analytical uncertainties alone. For instance, a key requirement for the isochron approach is that all samples should start out with the same initial isotopic ratio so that they develop statistically significant linearity required of a *'true'* isochron relationship. This is rare enough in diamond dating that the term '*linear data array'* is used, which more accurately reflects the evident geological scatter.

For diamond inclusion dating, the attainment of initial isotopic '*equilibrium*' or uniformity is probably the single most difficult assumption to satisfy. Unlike a rock outcrop, we do not know the spatial relationship of the diamonds and their inclusions to each other in the mantle. We have to use additional data such as diamond internal structure (growth zones), inclusion chemistry and nitrogen aggregation systematics in the diamonds to relate different diamonds to each other. Even with these criteria, it is likely that one of the largest sources of uncertainty in diamond inclusion isochron dating is within '*over-dispersed*' datasets. This is where the uncertainties are dominated by the fact that inclusions from different diamonds may not have identical initial ratios during diamond formation, and only partial isotopic equilibration was achieved (Fig. 2).

Multiple inclusions within the same diamond growth zone are more likely to have the same initial ratio than even multiple inclusions from different growth zones within the same diamond (e.g., Wiggers de Vries et al. 2013). In the case of protogenetic inclusions, high melt/fluid–rock ratios during diamond formation should help to homogenize the isotopic ratio of the system, but any remaining variation will make a contribution to the statistical scatter and resulting uncertainty on the isochron regression.

Despite these caveats and challenges, many of which reflect natural mineralogical variability of samples beyond the control of the analyst, it is still possible to recover valuable age information from the isochron arrays defined by diamond inclusion suites. Geologically significant ages can be obtained as long as inclusions from the same diamond formation event are regressed together, as illustrated by the various examples dealt with in the remainder of this chapter.

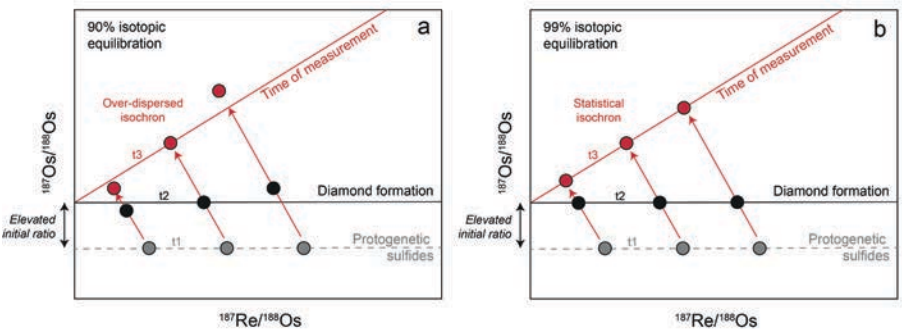


**Figure 2.** Illustrative isochron diagrams at 90 and 99% chemical diffusive equilibration. With increasing isotopic equilibration, the statistical quality of the isochron increases (see better alignment of datapoints with the isochron in **b)** because of closer adherence to a '*uniform initial ratio'* required to produce a statistically perfect isochron. Modified from Pamato et al. (2021).

## RADIOGENIC ISOTOPIC DATING METHODS AND APPLICABLE INCLUSION TYPES

### $^{40}Ar/^{39}Ar$

The possibility of dating diamonds using the $^{40}Ar/^{39}Ar$ laser probe technique was first investigated by Burgess et al. (1989) and Phillips et al. (1989). The ability to analyze single inclusions represented a major advance at the time compared to Rb–Sr and Sm–Nd analyses (e.g., Richardson et al. 1984; Richardson 1986), which required composites of several tens to hundreds of inclusions to achieve reasonable age precision.

***Principles.*** The $^{40}Ar/^{39}Ar$ dating method is a variant of the K-Ar technique and is based on the natural decay of $^{40}K$ to $^{40}Ar$, with a half-life of 1250 m.y. (McDougall and Harrison 1999 and references therein). In the case of the $^{40}Ar/^{39}Ar$ method, the parent $^{40}K$ isotopic content is determined indirectly with the stable isotope $^{39}K$ converted to $^{39}Ar$ by neutron irradiation in a nuclear reactor. The $^{40}Ar^*/^{39}Ar$ ratio is then proportional to age, when calculated relative to one or more co-irradiated neutron fluence monitors (reference minerals) of known age. Here, $^{40}Ar^*$ refers to radiogenic $^{40}Ar$ produced from $^{40}K$ decay. As the atmosphere contains 0.93% Ar (by volume), most rock/mineral samples include some proportion of atmospheric Ar adsorbed on mineral surfaces or contained within the crystal lattice. Atmospheric Ar has a measured $^{40}Ar/^{36}Ar$ ratio of 298.56 ± 0.31 (Lee et al. 2006), and measurement of $^{36}Ar$ can be used to correct $^{40}Ar_{total}$ for (assumed) atmospheric Ar contamination. The assumption of an initial atmospheric $^{40}Ar/^{36}Ar$ ratio can be tested using standard isochron plots, or, more typically, $^{36}Ar/^{40}Ar$ vs. $^{39}Ar/^{40}Ar$ correlation diagrams. If a mineral contains common argon with a composition above the atmospheric ratio, the additional $^{40}Ar$ is termed extraneous (excess or inherited) argon. The age of a sample is then given by the age equation:

$$t_{unk} = \frac{1}{\lambda}\ln\left(F \times J_{ref} + 1\right)$$

where unk = unknown;
$\lambda = 5.543 \times 10^{-10}$ yr$^{-1}$ (Steiger and Jäger 1977);
$F = {}^{40}Ar^*/{}^{39}Ar$;
ref = reference mineral (or fluence monitor);
$J$ = $J$-value:

$$J = \frac{(e^{\lambda t_{ref}} - 1)}{F_{ref}}$$

Commonly used reference minerals include the Fish Canyon Tuff sanidine (FCTs = 28.201 Ma; Kuiper et al. 2008), Alder Creek Rhyolite sanidine (ACRs = 1.816 Ma; Niespolo et al. 2017) and Mt Dromedary biotite (GA1550 = 99.125 Ma; Phillips et al. 2017). The irradiation process also produces so-called interfering isotopes such as $^{40}Ar$ from K and $^{36}Ar + {}^{39}Ar$ from Ca. Correction for these interfering isotopes is accomplished by analyzing co-irradiated, zero-age K-glasses and/or salts (e.g., $CaF_2$, $K_2SO_4$, KCl).

Argon is a noble gas, and its retention in a mineral lattice is a function of temperature, grain size (or more accurately diffusion dimension) and cooling rate. Typical closure (or blocking) temperatures for key K-bearing minerals are ~300 °C in biotite, ~400 °C in muscovite and ~550 °C in hornblende (McDougall and Harrison 1999 and references therein). As the $^{40}Ar/^{39}Ar$ method has a lower closure temperature than most of the other methods described herein, it is used for both geochronology and thermochronology (McDougall and Harrison 1999 and references therein).

***Inclusion types.*** The $^{40}Ar/^{39}Ar$ method is applicable to K-bearing minerals. Common K-bearing phases such as micas and feldspars are rare or absent as inclusions in diamonds. However, many clinopyroxene inclusions of both eclogitic (omphacite) and peridotitic (Cr-diopside) parageneses, contain small quantities of K, typically ~1000 ppm, with percent levels of potassium (~1.5 wt%) reported for some inclusions (Harlow and Veblen 1991; Harlow 1997). Elevated potassium levels have also been reported for eclogitic garnet inclusions from Orapa diamonds (Burgess et al. 1989, 2004). Clinopyroxene inclusions of eclogitic paragenesis are generally more abundant than the peridotitic Cr-diopside inclusions (Stachel and Harris 2008), but both types have been the target of $^{40}Ar/^{39}Ar$ dating studies. Bulanova et al. (2004) identified inclusions of yimengite [$K(Cr,Ti,Mg,Fe,Al)_{12}O_{19}$], a rare potassium magnetoplumbite mineral, in a diamond from the Sese kimberlite (Zimbabwe). Thus, other relatively K-rich mineral inclusions may be suitable candidates for $^{40}Ar/^{39}Ar$ dating.

***Practical applications.*** Initial attempts to determine diamond ages using $^{40}Ar/^{39}Ar$ laser probe methods involved analyses of eclogitic clinopyroxene inclusions from Cullinan (formerly Premier) Mine diamonds, which had been cleaved to expose the inclusions (Burgess et al. 1989; Phillips et al. 1989). The two studies yielded analogous average ages of 1198 ± 28 Ma (2σ) (Phillips et al. 1989) and 1185 ± 95 Ma (2σ) (Burgess et al. 1989), respectively—indistinguishable from the eruption age of the Premier kimberlite (~1.2 Ga; Kramers and Smith 1983). Prior to this, Richardson (1986) determined a Sm–Nd age of 1150 ± 60 Ma, for pooled eclogitic inclusions from Cullinan diamonds and the $^{40}Ar/^{39}Ar$ ages were therefore interpreted as the time of diamond formation.

However, subsequent $^{40}Ar/^{39}Ar$ analyses of similarly (partially) exposed clinopyroxene and garnet inclusions in diamonds from Orapa, Jwaneng (Botswana), Udachnaya (Russia) and Argyle (Australia), revealed unexpected complexities with this experimental approach, with most ages intermediate between the kimberlite eruption event and Sm–Nd (and later Re–Os) diamond formation ages (Richardson et al. 1990; Burgess et al. 1992). The favored explanation for this behavior was diffusion of pre-eruption radiogenic Ar ($^{40}Ar^*$) to the diamond/inclusion interface region during mantle residence, with partial to complete loss of this component when the diamond was cleaved to expose the inclusion (Burgess et al. 1992). Step-heating $^{40}Ar/^{39}Ar$ analyses of clinopyroxene inclusions extracted from their host diamonds produced similar age results, but with lower temperature steps yielding older apparent ages than the fusion steps (with minor exceptions) (Phillips et al. 2004; Phillips and Harris 2008). The 'intermediate' age results were attributed to partial Ar diffusion to the diamond/inclusion interface and defect structures in the clinopyroxene inclusions; this process is discussed in more detail in the section on '*Diffusion of elements from inclusion to inclusion-diamond interface*'.

The $^{40}Ar/^{39}Ar$ dating of exposed or partially exposed inclusions produces only minimum estimates of diamond formation ages. To determine diamond genesis ages, Burgess et al. (1992) suggested laser drilling to encapsulated inclusions within diamonds, to recover radiogenic Ar located in both the diamond/inclusion interface and the clinopyroxene inclusion. The difficulty with this approach is that diamond becomes opaque (black) in response to neutron irradiation, which makes locating buried inclusions a non-trivial issue. To address this issue, Burgess et al. (1994) ground and polished selected diamond faces to within ~0.5 mm of the inclusion and marked inclusion positions using laser spots. Using this method, Burgess et al. (1994) and Bulanova et al. (2004) reported $^{40}Ar/^{39}Ar$ ages for clinopyroxene-bearing diamonds from the Venetia kimberlite and yimengite-bearing diamond from the Sese kimberlite, respectively. Burgess et al. (2004) also attempted to laser-drill garnet- and clinopyroxene-bearing diamonds from the Orapa kimberlite but were unsuccessful as the inclusions were too deeply buried. Instead, these authors carried out furnace step-heating analyses of the Orapa diamonds, which released Ar in two pulses, one corresponding to Ar release from melting of the inclusion and decrepitation of the diamond (1200–1800 °C) and the second during diamond graphitization

(>2000 ºC). Some of the Venetia and Sese diamonds produced ages approaching the time of host kimberlite eruption (Bulanova et al. 2004; Burgess et al. 2004), possibly due to decrepitation of the polished surface prior to analysis (Bulanova et al. 2004). However, three Orapa diamonds yielded ages of ~1.0 Ga, similar to previous Sm–Nd diamond formation ages (Richardson et al. 1990), with other Orapa ages possibly supporting Re–Os ages of ~2.9 Ga (Shirey et al. 1999). One Venetia inclusion-bearing diamond gave an unrealistically old age of ~4.6 Ga, suggesting that at least some diamonds may contain excess Ar. Clearly, further studies involving laser drilling and/or furnace step-heating are required to investigate the utility of the $^{40}Ar/^{39}Ar$ method for dating diamond formation events.

Despite the challenges in dating diamond formation events, the observation that exposed inclusions often give ages approaching the times of host kimberlite eruption highlighted the possibility of constraining the provenance of detrital diamond deposits (Burgess et al. 1997; Phillips et al. 2004, 2017; Phillips and Harris 2008, 2009; Laiginhas et al. 2009). This rather unique application of the $^{40}Ar/^{39}Ar$ method is documented in more detail in the section below on provenance studies of detrital diamond deposits.

**U–Th/He**

The potential of the U–Th/He method for dating minerals was first recognized by Strutt (1905), and only much later applied to dating diamonds (Kurz et al. 1987). Through *in vacuo* crushing and step-heating experiments, Kurz et al. (1987) showed that monocrystalline diamonds had limited variation in $^{3}He$ but large variation in $^{4}He$, even within individual diamonds from Orapa. This variability could not be explained by alpha implantation alone, but was probably caused by differences in U–Th and/or $^{4}He$ concentrations in different diamond growth zones. With assumptions about the U–Th content, Kurz et al. (1987) estimated that monocrystalline Orapa diamonds were at least 500 Ma old, thereby showing that U–Th/He isotopes have potential for dating diamonds, and confirming earlier studies that diamonds are much older than the kimberlite (Kramers 1979; Richardson et al. 1984).

***Principles.*** The U–Th/He dating system is based on the decay of radioactive isotopes where $^{4}He$ atoms are created by capturing two electrons by α-particles. Most of the $^{4}He$ on Earth is formed by decay of U and Th ($^{4}He$ from longer-lived decays such as $^{147}Sm \rightarrow {}^{143}Nd$, is of lesser importance in diamonds, because only single α-particles are produced per decay):

$$^{238}U \rightarrow {}^{206}Pb + 8\alpha$$

$$^{235}U \rightarrow {}^{207}Pb + 7\alpha$$

$$^{232}Th \rightarrow {}^{208}Pb + 6\alpha$$

Alpha-particles from U and Th decay are formed in a decay chain via several intermediate radionuclides. The intermediate radionuclides with relatively long half-lives ($^{231}Pa$, $^{234}U$, $^{230}Th$) can be fractionated from $^{235}U$ and $^{238}U$, caused by differences in chemical properties of the various elements (e.g., Th, U, Pa), resulting in an imbalance called secular disequilibrium. This can occur during crystallization/partial melting and is important for many minerals when the crystallization period of a mineral is shorter than ~5× the half-life of the intermediate daughter nuclide (e.g., Farley 2002).

Secular disequilibrium is negligible for dating fluid inclusions in fibrous diamonds for two main reasons:

1. trace elements (U, Th) are primarily located in fluid inclusions in diamond (Timmerman et al. 2019; Krebs et al. 2019) and there is likely no fractionation between the diamond-forming fluid and encapsulated fluid inclusions;
2. after 5× the longest half-life ($^{234}U$; 5× = 1.23 million years) any initial disequilibrium returns to a secular equilibrium (Bourdon et al. 2003) and all studied fibrous diamonds and their fluid inclusions are significantly older than 1.23 million years.

Therefore, the total radiogenic $^{4}$He (including the usually negligible $^{147}$Sm decay for completeness) is defined as:

$$^{4}\mathrm{He} = 8\,^{238}\mathrm{U}\left(e^{\lambda.238t}-1\right)+7\,^{235}\mathrm{U}\left(e^{\lambda.235t}-1\right)+6\,^{232}\mathrm{Th}\left(e^{\lambda.232t}-1\right)+1\,^{147}\mathrm{Sm}\left(e^{\lambda.147t}-1\right)$$

where:

$\lambda_{238} = 1.55125 \times 10^{-10}$ yr$^{-1}$
$\lambda_{235} = 9.8485 \times 10^{-10}$ yr$^{-1}$
$\lambda_{232} = 4.9475 \times 10^{-11}$ yr$^{-1}$
$\lambda_{147} = 6.54 \times 10^{-12}$ yr$^{-1}$

This equation can be iteratively solved for time using the software package HelioPlot (Vermeesch 2010), which is also incorporated into IsoPlotR (Vermeesch 2018).

Formation of $^{4}$He by radioactive decay of Sm is negligible and $^{235}$U can be expressed as $^{238}$U/137.88 at present-day. Therefore, $^{4}$He production can be approximated by a simplified formula (see supplementary information in Timmerman et al. 2019c for derivation). Because diamond-forming fluids often contain '*common*' $^{4}$He, U–Th/He ages are considered to be maximum ages unless a 'common' $^{4}$He correction is made. This issue can potentially be solved when cogenetic samples form an isochron array, or by using the measured stable $^{3}$He concentration and assuming an initial $^{4}$He/$^{3}$He ratio.

$$^{4}\mathrm{He} = t\left(1.29\mathrm{e}^{-9}\,^{238}\mathrm{U}+2.97\mathrm{e}^{-10}\,^{232}\mathrm{Th}\right)$$

$$\frac{^{4}\mathrm{He}}{^{3}\mathrm{He}}\mathrm{measured} = \frac{^{4}\mathrm{He}}{^{3}\mathrm{He}}\mathrm{initial} + t\,\frac{\left(1.29e^{-9}\,^{238}\mathrm{U}+2.97e^{-10}\,^{232}\mathrm{Th}\right)}{^{3}\mathrm{He}}$$

The closure temperature of the U–Th/He system varies for different minerals, it is one of the lowest closure temperatures of all radiogenic systems, with temperatures of ~100 °C for apatite (Lippolt et al. 1994; Wolf et al. 1996; Warnock et al. 1997) and ~600 °C for garnet (Dunai and Roselieb 1996). Although diamond is formed above the U–Th/He closure temperature, diffusion rates for He (He > U–Th) in diamond are extremely slow: $\pm 4 \times 10^{-21}$ cm$^2$/s (Shelkov et al. 1998) to $1.8 \times 10^{-19}$ cm$^2$/s (Weiss et al. 2021). Due to these slow diffusion rates in diamond, the U–Th/He system is effectively closed in diamond, and makes it an ideal mineral for U–Th/He dating.

One of the limiting factors in U–Th/He dating applications of diamonds is the ability to precisely and accurately measure the low U, and Th abundances in diamonds. The lack of diamond reference materials hampers the ability to assess the accuracy of direct laser ablation measurements of diamonds. Induced neutron activation techniques have been used (e.g., Schrauder et al. 1996) but this approach renders the diamond unusable for noble gas measurements. The application of the method has been considerably helped by the advent of the '*off-line*' laser ablation ICP-MS measurement approach that allows pre-concentration of analytes to orders of magnitude higher than possible using conventional laser ablation ICP-MS approaches (McNeill et al. 2009; Klein-BenDavid et al. 2010).

***Inclusion types.*** Polycrystalline and fibrous diamonds have significantly higher concentrations of trace elements and noble gases compared to monocrystalline gem-quality diamonds. This difference is thought to be due to the fact that fibrous diamonds contain abundant fluid inclusions (Navon et al. 1988; Weiss et al. 2022, this volume), suggesting that trace elements and noble gases are primarily located in these fluid inclusions rather than in the diamond lattice itself. Because the abundances of U, Th are in the ppt range for monocrystalline gem-quality diamonds (McNeill et al. 2009; Krebs et al. 2019; Timmerman et al. 2019a), the accuracy and precision of these measurements is likely to remain one of the largest sources

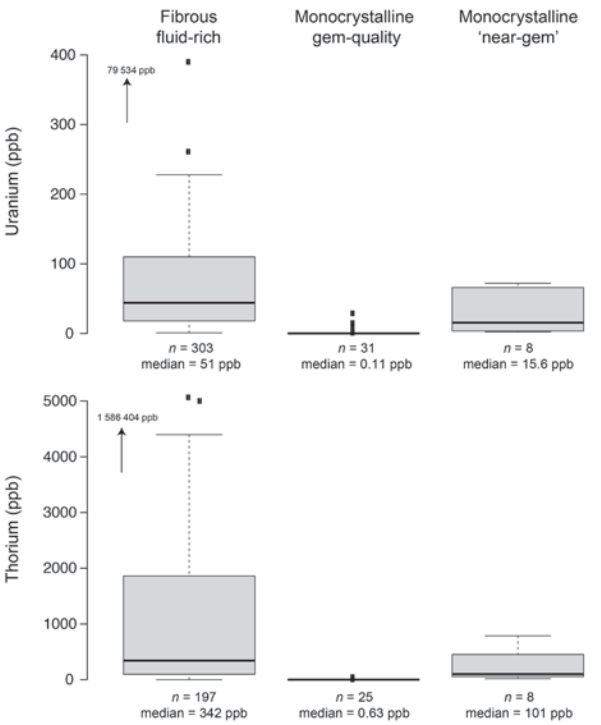


**Figure 3. '**Box and whisker' plots of the U and Th contents in fibrous fluid-rich diamonds compared to monocrystalline gem-quality and near-gem diamonds. Because the abundances of U and Th are prohibitively low in monocrystalline gem-quality diamonds, the U–Th/He method is limited to fibrous diamonds that have higher U–Th concentrations. Plotted using the data compilation in Weiss et al. (2022b).

of uncertainty in U–Th/He age determination of gem diamonds. This currently limits the U–Th/He method to 'fluid-rich' fibrous diamonds with higher U–Th concentrations (Fig. 3).

Polycrystalline diamonds—such as carbonado and framesite—have much smaller crystal sizes (generally smaller than 100 µm) and in such small diamonds, diffusion of He and implantation of $^{4}$He from the host rock needs to be taken into consideration (Ozima et al. 1991). Furthermore, polycrystalline diamonds have abundant mineral inclusions and He is unlikely to be released from mineral inclusions during crushing, resulting in lower apparent ages (Burgess et al. 1998).

***Practical applications.*** Despite the recognition in the 1980s that the U–Th/He method may be useful for dating diamonds (Kurz et al. 1987), it was not until 1998 that the first diamonds were analyzed for both U and He (Burgess et al. 1998). In these early studies He was released by crushing diamond in a vacuum (Burgess et al. 1998, 2009). Larger fragments that remained after crushing were irradiated and analyzed for U ($^{134}Xe_U$) using an extended Ar(–Kr–Xe) step-heating method (Burgess et al. 1998) or analyzed for U and Th by neutron activation (Schrauder et al. 1996).

Early He isotope studies on diamonds showed the importance of cosmogenic $^{3}$He accumulation in alluvial diamonds residing near Earth's surface for long periods. Cosmogenic $^{3}$He near the outside of the rough diamond (Honda et al. 1987; Lal 1989) adds to nucleogenic $^{3}$He that accumulates through the neutron bombardment of Li ($^{6}$Li(n,αβ)$^{3}$He) (Honda et al. 1987; Kurz et al. 1987). It was also recognized that the outer ~30 µm of a diamond crystal are affected by implanted $^{4}$He from U–Th decay of minerals in host rock for the diamond (Shelkov et al. 1998; Fig. 4).

Based on fragment sizes, modeling, vacuum crushing and step heating of fibrous diamonds, it was recognized that crushing is not an efficient way to extract all He from the diamond (releasing 4–20% of the total He), resulting in an underestimation of the age (Timmerman et al. 2019c). This is because α particles ejected from fluid/mineral inclusions can diffuse over a distance of a few μm and may accumulate within the diamond lattice, depending on how long the diamond resides in the mantle. The effects of α-ejection distance from fluid inclusions (12 μm) and He release from mineral inclusions (14–15 μm) were modeled and, in the case of two diamonds from the Democratic Republic of the Congo (DRC), α-ejection and/or fluid inclusion abundance were shown to be more important factors for He accumulation than α-implantation near the diamond surface (Fig. 4; Timmerman et al. 2019c).

The first U–Th/He dating study on fibrous diamonds (Timmerman et al. 2019c) assumed a closed system with negligible He diffusion ($D = 4 \times 10^{-21}$ cm$^2$/s; Shelkov et al. 1994), which provided a minimum age. Recently, the upper limit of He diffusion was estimated based on U, Th, and He contents of measured diamonds, an assumed initial R/Ra and a major craton stabilization age of 2.6 Ga and gives an upper diffusion rate of $1.8 \times 10^{-19}$ cm$^2$/s (Weiss et al. 2021). Taking He diffusion into account gave an upper age limit, and showed saline high density fluid (HDF)-bearing diamonds from Finsch and the Kimberley mines (also known as '*De Beers Pool*') are within error of kimberlite eruption ages (Weiss et al. 2021). On the other hand, silicic and carbonatitic HDF-bearing diamonds from Congo (Timmerman et al. 2019c), Finsch and Kimberley (Weiss et al. 2021) are significantly older than kimberlite eruption, with the oldest carbonatitic metasomatic event occurring between 0.75 and 2.6 Ga (Weiss et al. 2021). These age results show that not all fibrous diamonds formed shortly before kimberlite eruption, as was previously suggested from consideration of their N aggregation systematics and the similarity of their Sr isotope and trace element signatures to kimberlitic melts (e.g., Smith et al. 2012 and references therein).

Major improvements in our understanding of He evolution in the continental lithospheric mantle are still required to provide more accurate initial ratio constraints and model ages, though data are becoming available (e.g., Timmerman 2018; Timmerman et al. 2019b; Pernet-Fisher et al. 2019; Broadley et al. 2021). Corrections for initial trapped $^4$He using the measured amount of nucleogenic $^{21}$Ne and the mantle $^{21}Ne^*/^4He^*$ production ratio are possible and require evaluation. The influence of micro mineral inclusions and the relative release of mantle and radiogenic He during crushing *versus* heating also need further investigation.

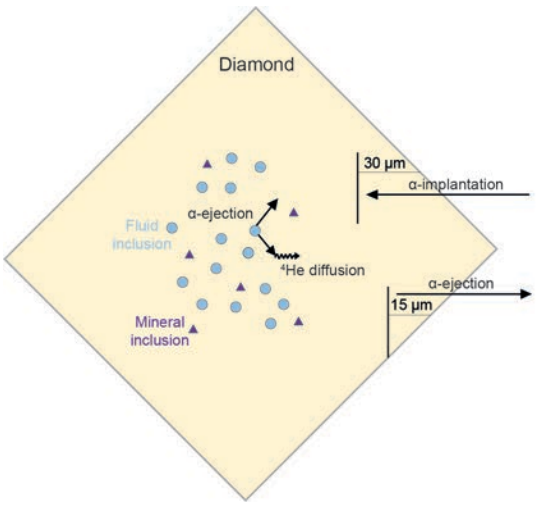


**Figure 4.** Processes influencing the $^4$He budget in diamond. This includes α-implantation into diamond from the host rock and α-ejection from diamonds and its fluid inclusions. Fluid and mineral inclusions are not to scale. Implantation and ejection distances are average values. Modified from Timmerman et al. (2019c).

**U–Pb and Pb–Pb**

The earliest studies aimed at dating inclusion-bearing diamonds began in the 1970s and focused on the U–Th–Pb isotope system in sulfides. Early analyses needed large numbers of inclusions due to the high procedural blanks at the time, and also suffered from large uncertainties in the mantle growth curve for Pb. It was another two decades before *in situ* techniques enabled further work on the Pb–Pb model ages.

***Principles.*** The U–Th–Pb system encompasses three separate chronometers based on the decay chains of the long-lived parent isotopes $^{238}U$, $^{235}U$ and $^{232}Th$, which terminate in daughter isotopes $^{206}Pb$, $^{207}Pb$ and $^{208}Pb$ respectively. Natural Pb has three stable radiogenically derived isotopes and only one stable non-radiogenic isotope $^{204}Pb$. The latter is by far the least abundant Pb isotope, typically ≤1.4% of common Pb. The U and Th decays (see equations above) produce three equations of the same form that can be used to determine an age:

$$^{206}Pb = {}^{238}U\,(e^{\lambda_{238}t} - 1) \text{ where } \lambda_{238} = 1.55125 \times 10^{-10}\ yr^{-1}$$

$$^{207}Pb = {}^{235}U\,(e^{\lambda_{235}t} - 1) \text{ where } \lambda_{235} = 9.8485 \times 10^{-10}\ yr^{-1}$$

$$^{208}Pb = {}^{232}Th\,(e^{\lambda_{232}t} - 1) \text{ where } \lambda_{232} = 4.9475 \times 10^{-11}\ yr^{-1}$$

One of the key advantages of this system is that the two U–Pb age equations can be combined into a Pb–Pb equation whereby U is eliminated as a variable. In this equation, the (present-day) $^{235}U/^{238}U$ term is assumed to be constant, although we now know it is not exactly constant. In principle only the Pb isotopic composition of a sample needs to be measured to obtain a $^{207}Pb/^{206}Pb$ age:

$$\left(\frac{^{207}Pb}{^{206}Pb}\right) = 1/137.88\left[\frac{(e^{\lambda_{235}t} - 1)}{(e^{\lambda_{238}t} - 1)}\right]$$

In practice, both U and Pb concentrations are normally measured in order to compare U–Pb and Pb–Pb ages as a check on closed system behavior. This can be illustrated on a U–Pb Concordia diagram (Wetherill 1956) where the Concordia curve represents the locus of points of equal $^{206}Pb/^{238}U$ and $^{207}Pb/^{235}U$ ages. For a concordant mineral sample, the $^{207}Pb/^{206}Pb$ age is the most precise and accurate of such absolute age determinations because any analytical errors in measurement of the U/Pb ratio have been eliminated.

This approach is ideal for mineral inclusions in diamond such as zircon (Kinny and Meyer 1994) and perovskite (Hamilton et al. 2003) that carry significant amounts of U and Th but largely exclude Pb at the time of crystallization. $CaSiO_3/CaTiO_3$ polymorphs (Bulanova et al. 2010), and rutile inclusions in diamond (Schmitt et al. 2019) have also been analyzed, however, the occurrence of these phases as inclusions in diamond is extremely rare.

Sulfides and clinopyroxene are the most commonly encountered inclusion in diamonds that contain measurable Pb. Because sulfides do not incorporate U and Th, only Pb–Pb ages are obtainable, based on an expansion of the radiogenic $^{207}Pb/^{206}Pb$ term in the Pb–Pb equation to include initial or common Pb:

$$\frac{\left[\left(\frac{^{207}Pb}{^{204}Pb}\right)_p - \left(\frac{^{207}Pb}{^{204}Pb}\right)_i\right]}{\left[\left(\frac{^{206}Pb}{^{204}Pb}\right)_p - \left(\frac{^{206}Pb}{^{204}Pb}\right)_i\right]} = 1/137.88\left[\frac{(e^{\lambda_{235}t} - 1)}{(e^{\lambda_{238}t} - 1)}\right]$$

where subscripts p and i refer to present and initial isotope ratios respectively.

There is no certain way of establishing the prevailing (initial) Pb isotope ratios for mantle sources from which the sulfide inclusions are derived. Theoretical mantle growth curves therefore need to be constructed for plausible values of $^{238}U/^{204}Pb$ ($\mu$) and Th/U ($\kappa$) from which Pb–Pb model ages can then be determined. Such growth curves can be single-stage or multi-stage and lead to model age uncertainty just from the choice of growth curve alone. Alternatively, where an array of data can be regressed, for multiple inclusions, secondary Pb–Pb isochrons could be used to establish ages. No such datasets are currently available as sulfides are typically analyzed for Re–Os isotopes and the Re–Os separation chemistry (Pearson et al. 1998b) is not easily adapted for low-blank Pb isotope measurement, though in theory it could be achieved.

A variety of instrumental techniques are available for making U–Th–Pb isotope measurements. In order of development, they are isotope dilution thermal ionization mass spectrometry (ID-TIMS), secondary ion mass spectrometry (SIMS) [or Sensitive High Resolution Ion MicroProbe (SHRIMP)] and laser ablation inductively coupled plasma mass spectrometry (LA-ICP-MS). Of these, ID-TIMS is the most precise and accurate absolute dating technique but requires inclusion dissolution, chemical separation of U (Th) and Pb, and different instrumental protocols for each element. Conversely, SIMS/SHRIMP and LA-ICP-MS are *in situ* techniques requiring matrix-matched standards to be run in parallel with samples. The latter techniques are therefore less precise and accurate but do offer greater spatial resolution within individual sectioned inclusions.

***Inclusion types.*** The U–Th–Pb dating technique is applicable to two main categories of inclusions. The more useful but least abundant type are silicate and oxide minerals that incorporate lithophile U and Th and exclude (initial or common) Pb. These are minerals such as zircon ($ZrSiO_4$), perovskite ($CaTiO_3$), breyite ($Ca_3Si_3O_9$), the Ca-TiSiO$_3$ phases, and rutile ($TiO_2$), in which $U^{4+}$ and $Th^{4+}$ substitute for $Zr^{4+}$ and $Ti^{4+}$. The less useful but most abundant type are sulfide minerals that incorporate substantial chalcophile Pb but exclude (parent) U and Th. These are various forms of monosulfide solid solution and its exsolution products, principally pyrrhotite ($Fe_{1-x}S$), pentlandite ($[Fe,Ni]_9S_8$) and chalcopyrite ($CuFeS_2$) in which $Pb^{2+}$ readily substitutes for $Fe^{2+}$ and $Cu^{2+}$. Sulfide inclusions of both peridotitic (high Ni, Os) and eclogitic (low Ni, Os) parageneses have been recognized. However, a robust division of peridotitic sulfides into harzburgitic versus lherzolitic types remains elusive. Lead contents of sulfide inclusions from global localities measured by SHRIMP range from <1 ppm to 1,500 ppm (Eldridge et al. 1991; Rudnick et al. 1993). Eclogitic sulfides were found to have the lowest and peridotitic sulfides the highest Pb concentrations but with considerable overlap at the low abundance end (Eldridge et al. 1991; Rudnick et al. 1993). The latter observation is borne out by other Re–Os studies of sulfide inclusions. For example, sulfide inclusion Pb concentrations measured by ID-TIMS for three eclogitic diamonds from Cullinan (Richardson and Shirey 2008) and two diamonds, one eclogitic and one peridotitic, from Letseng (Shirey and Richardson 2011) were indistinguishable from total procedural blank (10 pg).

***Practical applications.*** In the earliest work, Welke et al. (1974) investigated a single composite of 'black' sulfide inclusions from the ~1153 Ma old Premier kimberlite (Cullinan Mine, South Africa). The mixed diamond composite containing inclusions of unknown paragenesis was burnt to produce an inclusion residue for U–Pb analysis by ID-TIMS. Unfortunately, the analytical data were subject to large blank corrections in addition to uncertainties in model mantle growth curves but the data suggested an age for the sulfides of around 1.5 Ga. Subsequently, Kramers (1979) extended this approach to similar 'black' sulfide inclusion composites from Cullinan, Finsch and the four mines in Kimberley—Bultfontein, De Beers, Dutoitspan, Wesselton—sometimes collectively referred to as '*De Beers Pool*'. The data for Cullinan yielded a Pb–Pb model age closer to the 1153 Ma kimberlite emplacement age based on mantle Pb growth curves in favor at the time (Cumming and Richards 1975;

Stacey and Kramers 1975). In contrast, the Finsch and Kimberley data gave significantly older Pb–Pb model ages in excess of 2 Ga for diamonds from Cretaceous kimberlites. These results provided some of the first solid evidence that the diamonds were ancient and thus xenocrysts in the host kimberlite (Kramers 1979).

It took another two decades before the advent of *in situ* techniques enabled further work on the Pb–Pb model ages of sulfide inclusions in diamonds. In the early 1990s, the then novel SHRIMP at Australian National University (ANU) was used to investigate individual sulfide inclusions from a range of African and Siberian kimberlite localities (Eldridge et al. 1991; Rudnick et al. 1993; Hamilton et al. 1997). While the sulfide inclusions in these studies could be assigned to eclogitic and peridotitic parageneses based on Ni and Pb contents and in some cases coexisting minerals, the limitations of Pb–Pb model age interpretation became increasingly apparent. This problem was particularly clear for eclogitic sulfides with more radiogenic Pb isotopic compositions that gave anomalously young (relative to kimberlite emplacement) or future model ages. On the other hand, peridotitic sulfides varied in age between young and much older ages up to a maximum of 2.5 Ga.

Unfortunately, mantle Pb growth curves suffer from complex assumptions that limit their geochronological utility. Despite these limitations, the global set of Pb–Pb model ages for sulfide inclusions reported by Eldridge et al. (1991) and Rudnick et al. (1993) indicated that eclogitic diamonds are generally younger than peridotitic diamonds (for a more detailed review, see Pearson and Shirey 1999). Note, however, that there is considerable overlap between eclogitic and peridotitic sulfide-inclusion bearing diamond ages at the young end of the published Pb–Pb model age spectrum (Eldridge et al. 1991; Rudnick et al. 1993; Hamilton et al. 1997; Pearson and Shirey 1999) suggesting that *'young' (i.e., non-Archean)* peridotitic sulfide inclusion-bearing diamonds from Cretaceous kimberlites such as Koffiefontein and Finsch may be lherzolitic rather than harzburgitic (Shirey and Richardson 2011; Harvey et al. 2016). For example, the Finsch kimberlite carries diamondiferous lherzolite xenoliths in addition to (disaggregated) harzburgitic diamond host rocks (Shee et al. 1982).

*In situ* U–Pb dating using ion microprobe techniques (SIMS/SHRIMP) has been applied to silicate and oxide inclusion minerals such as zircon, perovskite and rutile with some success. However, the abundance of these accessory minerals as inclusions in diamonds is extremely low. So far only one zircon inclusion in a small diamond from the Mbuji Mayi kimberlite in the DRC has been successfully dated using the SHRIMP instrument (Kinny and Meyer 1994). The zircon yielded a $^{206}Pb/^{238}U$ age of 628 ± 12 Ma, based on the average of three spot analyses, as compared to a late Cretaceous kimberlite emplacement age of 70 ± 1 Ma (Schärer et al. 1997). Surprisingly, U, Th and Pb concentrations in the center of the crystal were found to vary by a factor of two (U = 360–660 ppm; Th = 250–560 ppm; Pb = 40–80 ppm) suggesting little internal redistribution of U and Th or loss of Pb (Kinny and Meyer 1994). However, the possibility that radiogenic Pb could have been partially lost by diffusion to the inclusion–diamond interface could not be entirely discounted and remains an issue to be addressed in future studies (Kinny and Meyer 1994; Pearson and Shirey 1999). Furthermore, the absence of any other inclusion phases in this diamond meant that little could be said about its paragenetic association and conditions of formation beyond speculating that the inclusion was eclogitic (Kinny and Meyer 1994) and the host diamond was most likely of continental lithospheric origin.

In a similar one-off study using the SHRIMP II instrument at the Geological Survey of Canada, a perovskite inclusion in a diamond from the Sytykanskaya kimberlite (Siberia) was investigated by Hamilton et al. (2003). Five spot analyses showed a twofold range of U (70–130 ppm) and Th (1,200–2,900 ppm) concentrations. Mean $^{206}Pb/^{238}U$ and $^{208}Pb/^{232}Th$ ages of around 350 ± 20 Ma were obtained, well within error of the 344 Ma host kimberlite age (Davis et al. 1980). The same small diamond was reported to carry olivine and chromite inclusions consistent with a peridotitic paragenesis but further work is needed to verify

the syngenetic versus epigenetic nature of this perovskite inclusion (Hamilton et al. 2003). However, the perovskite-structured phase goldschmidtite ($KNbO_3$) has been reported as an unaltered inclusion in a diamond from Koffiefontein, South Africa (Meyer et al. 2019) indicating that such minerals can be syngenetic.

Within a broader study of some 20 sublithospheric diamonds from the Collier-4 kimberlite in the Juina district, Brazil, one CaTi-perovskite + breyite inclusion was dated using the Cameca IMS1270 ion microprobe at Edinburgh University (Bulanova et al. 2010). The inclusion yielded a relatively well-constrained $^{206}Pb/^{238}U$ age of 101 ± 7 Ma (Bulanova et al. 2010) within error of the kimberlite emplacement age of 93 ± 2 Ma (Heaman et al. 1998). This is the first absolute age for a sublithospheric diamond with an inferred oceanic crustal protolith (Bulanova et al. 2010) subducted beneath the Amazonian craton in Cretaceous time (Harte and Richardson 2012).

A suite of rare rutile inclusions in eclogitic diamonds from the Mir kimberlite, Siberia, were dated using the Cameca IMS1270 ion microprobe at the University of California, Los Angeles (Schmitt et al. 2019). Rutile inclusions with the highest U concentrations (up to 23 ppm) yielded a mean U–Pb concordia age of 375 ± 7 Ma for 19 spot analyses. This age is slightly older than U–Pb ages of 362–357 Ma for Mir zircon megacrysts (Davis et al. 1980; Spetsius et al. 2002) but within the published range (376–346 Ma) for regional kimberlite magmatism (Kjarsgaard et al. 2022, this volume). It also differs substantially from Re–Os isochron ages of 0.9 and 2.1 Ga for eclogitic and lherzolitic sulfide inclusion-bearing diamonds from Mir (Wiggers de Vries et al. 2013). Schmitt et al. (2019) offer four possible scenarios to explain this difference. While their preferred interpretation is that the rutile U–Pb age is a valid diamond crystallization age, they do allow the possibility of diffusive Pb loss whereby incompatible radiogenic Pb could accumulate at the inclusion-diamond interface (see Fig. 9C in Schmitt et al. 2019). If correct, the latter interpretation would be consistent with the recent identification of hydrous-silicic fluid films (which could harbor radiogenic Pb and other cations) around silicate and oxide mineral inclusions in gem diamonds from global sources (Nimis et al. 2016).

**Sm–Nd and Rb–Sr**

Dating inclusion-bearing diamonds using the combined Sm–Nd and Rb–Sr isotope systems first became feasible in the early 1980s. It was around this time that elucidation of the oceanic mantle array and bulk earth evolution curve (Allègre et al. 1979; DePaolo and Wasserburg 1979; Jacobsen and Wasserburg 1980) allowed for sensible interpretation of the correlated Nd and Sr isotopic signatures of kimberlite-borne mantle xenoliths and xenocrysts. Both Nd and Sr tend to reside in the same mantle minerals (garnet and clinopyroxene) and can be analyzed in the same samples using sequential ion exchange column chemical separation and mass spectrometric techniques. Furthermore, Sm, Nd, Rb and Sr are all variably incompatible elements and their geochemical behavior and relative partitioning between different silicate phases is well understood.

***Principles.*** The Rb–Sr dating technique is based on β decay of $^{87}Rb$ to $^{87}Sr$ with a long half-life (50 b.y). Given strong fractionation of Rb from Sr during various igneous differentiation processes, Sr isotope ratios can increase quite rapidly in phases with high Rb/Sr:

$$\left(\frac{^{87}Sr}{^{86}Sr}\right)_p = \left(\frac{^{87}Sr}{^{86}Sr}\right)_i + \left(\frac{^{87}Rb}{^{86}Sr}\right)(e^{\lambda_{87}t} - 1)$$

where

$\lambda_{87} = 1.42 \times 10^{-11}$ yr$^{-1}$ (conventional value; Steiger and Jäger 1977),
$1.397 \times 10^{-11}$ yr$^{-1}$ (refined experimental value; Rotenberg et al. 2012),
and subscripts p and i refer to present and initial isotope ratios, respectively.

Rubidium is an alkali element, highly mobile in aqueous fluids, and has only two isotopes ($^{85}$Rb, $^{87}$Rb), making it difficult to correct for instrumental mass fractionation. The high abundances of Rb that are typical of crustal environments relative to the mantle mean that great care must be taken to guard against secondary, laboratory-origin contaminants or natural Rb enhancement due to secondary alteration (e.g., via cracks in the diamond). Conversely, Sr is an alkaline earth element that is less mobile in aqueous fluids. Strontium has four isotopes ($^{84}$Sr, $^{86}$Sr, $^{87}$Sr, $^{88}$Sr), providing separate reference isotope ratios for mass fractionation correction ($^{86}$Sr/$^{88}$Sr) and isotope dilution ($^{84}$Sr/$^{88}$Sr). The precision of Rb–Sr age determinations is thus ultimately constrained by how well intrinsic Rb concentrations can be measured.

The Sm–Nd dating technique is based on the α-decay of $^{147}$Sm to $^{143}$Nd, which has a very long half-life of 106 billion years. Combined with minimal fractionation of Sm from the geochemically similar Nd, neodymium isotope ratios tend to increase very slowly over time:

$$\left(\frac{^{143}\mathrm{Nd}}{^{144}\mathrm{Nd}}\right)_{\mathrm{p}} = \left(\frac{^{143}\mathrm{Nd}}{^{144}\mathrm{Nd}}\right)_{\mathrm{i}} + \left(\frac{^{147}\mathrm{Sm}}{^{144}\mathrm{Nd}}\right)(e^{\lambda_{147}t} - 1)$$

where
$\lambda_{147} = 6.54 \times 10^{-12}$ yr$^{-1}$
and subscripts p and i refer to present and initial isotope ratios, respectively.

Samarium and Nd are both rare earth elements (REE) that are much less mobile in aqueous fluids than Rb or Sr. Both Sm and Nd have seven isotopes that are more than enough to correct for isobaric interferences and provide separate reference isotope ratios for mass fractionation correction and isotope dilution. However, the precision of Sm–Nd age determinations remains limited by the small spread of parent/daughter ratio observed for REE that are only two atomic numbers apart. This problem is exacerbated by the longer half-life of $^{147}$Sm relative to $^{87}$Rb, $^{187}$Re or $^{238}$U.

The most precise and accurate instrumental technique for Rb–Sr and Sm–Nd isotope measurements is isotope dilution for accurate measurement of parent/daughter abundances by thermal ionization mass spectrometry (ID-TIMS) to obtain isotopic compositions. *In situ* techniques using these isotope systems are generally not favored for diamond dating studies, on account of the very small quantities of Sr and Nd present in silicate inclusions and the five- to six-figure precision required for meaningful measurements of Sr and Nd isotope ratios.

Given the very low Rb contents of mantle minerals such as garnet and clinopyroxene, $^{87}$Rb/$^{86}$Sr ratios measured for these inclusion phases are insignificant and age corrections are negligible. Present-day measured $^{87}$Sr/$^{86}$Sr ratios are effectively equivalent to initial $^{87}$Sr/$^{86}$Sr ratios at the time of diamond encapsulation and independent Rb–Sr ages are therefore unobtainable. However, $^{87}$Sr/$^{86}$Sr ratios can serve as a proxy for initial $^{143}$Nd/$^{144}$Nd ratios to check whether inclusions from different diamonds dated using the Sm–Nd isochron approach are indeed cogenetic.

***Inclusion types.*** The use of the Rb–Sr and Sm–Nd isotopic systems is generally applicable to two important silicate inclusion minerals, namely, garnet and clinopyroxene. In garnet, $Sm^{3+}$ and $Nd^{3+}$ replace $Mg^{2+}$ and $Fe^{2+}$ (and $Ca^{2+}$) on the X site via coupled substitution. At the same time, $Sr^{2+}$ readily substitutes for $Ca^{2+}$ whereas the much larger $Rb^{+}$ cation (like $K^{+}$) is crystallographically excluded at the time of crystallization. In diopside and omphacite, $Sm^{3+}$ and $Nd^{3+}$ replace $Mg^{2+}$ and $Fe^{2+}$ on M1 via coupled substitution whereas $Sr^{2+}$ substitutes for $Ca^{2+}$ on M2 while a very small amount of $Rb^{+}$ can be accommodated alongside $K^{+}$ in place of $Na^{+}$ on M2.

Subcalcic Cr-pyrope garnet is the most important carrier phase of both Nd (2–10 ppm) and Sr (2–25 ppm) in harzburgitic diamonds from type localities such as Finsch and Kimberley

(Richardson et al. 1984; Viljoen et al. 2014) ), but Sr content extends to almost 50 ppm in similar garnets from xenoliths and diamonds from Siberia (Shimizu and Sobolev 1995; Pearson et al. 1995; Shimizu et al. 1997). In lherzolitic diamonds, calcium-saturated Cr-pyrope garnet and Cr-diopside are both carrier phases for Nd (1–2 ppm and 2–4 ppm, respectively) whereas diopside is the dominant carrier phase for Sr (≥ 100 ppm) as observed in some Cullinan diamonds (e.g., Richardson et al. 1993). In eclogitic diamonds, pyrope-almandine garnet and omphacite are significant carrier phases for both Nd (1–8 ppm and 1–20 ppm, respectively) and Sr (1–30 ppm and 50–1800 ppm, respectively) as observed in studies of diamonds from the Argyle, Cullinan, Finsch, Jwaneng, Orapa and Letlhakane localities (Richardson 1986; Richardson et al. 1990, 1999; Smith et al. 1991; Timmerman et al. 2017). The Nd and Sr contents of other common silicate (olivine, orthopyroxene), oxide (chromite) and sulfide (pyrrhotite) inclusion phases are negligible. Kyanite has also been measured (Mei Yan Lai and Suzette Timmerman, unpublished data) and contains negligible amounts of either element. In sublithospheric inclusions, Sr and Nd abundances are high enough to be analyzed, but the potential for geochronology is still being evaluated (Pearson et al. 2007; Thomson et al. 2016). Rare mineral inclusions of, e.g., breyite, rutile, and loparite could potentially contain high enough Sr and Nd contents for isotope analysis. A compilation of Rb–Sr and Sm–Nd contents for worldwide lithospheric diamond inclusions is given in Stachel et al. 2022a, this volume)

***Practical applications.*** The use of Sm–Nd and Rb–Sr isotopic systems differs substantially according to the paragenesis of the diamond suite to be dated. In the case of harzburgitic diamonds, garnet is the only significant carrier phase for Sm, Nd and Sr while Rb is crystallographically excluded. Furthermore, such garnets show little spread in low (i.e., strongly sub-chondritic) Sm/Nd ratios for a given locality (Richardson et al. 1984; Shimizu and Richardson 1987). This means that Sm–Nd isochron ages are unobtainable for harzburgitic diamond suites from type localities like Kimberley and Finsch. However, such low Sm/Nd ratios lend themselves to the Sm–Nd model age approach by virtue of their shallow evolution curves relative to the reference reservoir, as seen on a standard Nd isotope evolution diagram. This is the approach adopted by Richardson et al. (1984) in obtaining Paleoarchean Nd model ages of 3.4–3.3 Ga (or 3.5–3.4 Ga for a depleted mantle source) for suites of several hundred subcalcic garnet inclusion-bearing diamonds from the Cretaceous Kimberley and Finsch kimberlites.

While the reliability of such Paleoarchean model ages for Finsch and Kimberley harzburgitic diamonds has frequently been questioned (Pidgeon 1989; Pearson et al. 1995; Shimizu and Sobolev 1995; Navon 1999; Pearson and Shirey 1999; Spetsius et al. 2002), these challenges have for the most part been shown to be unsustainable based on the following considerations. First, the use of composites of subcalcic garnet inclusions to obtain enough material for reasonably precise Nd and Sr isotope analysis (based on then available instrumental techniques) has been criticized as producing averages with no direct age significance. However, the extremely unradiogenic Nd isotopic character of these averages, as well as independent replication of results, precludes a wide distribution of individual inclusion values (Richardson et al. 1984; Caro et al. 2008), though this apparent uniformity is not present in every suite (Koornneef et al. 2017). Second, the highly radiogenic Sr isotope signature of unencapsulated subcalcic garnet macrocrysts (from disaggregated garnet harzburgite host rocks) contrasts with the markedly less radiogenic Sr in inclusions and strongly supports the long-term isolation of the inclusions by encapsulation in diamond and storage in the old-thick-cold continental lithospheric mantle beneath the Kaapvaal craton since the Paleoarchean (Fig. 5; Richardson et al. 1984; Boyd et al. 1985; Shirey and Richardson 2011).

In the case of lherzolitic diamonds, Sm and Nd (and Sr) are partitioned between calcium-saturated Cr-pyrope garnet and (modally rare) Cr-diopside with garnet acquiring the highest and diopside the lowest Sm/Nd ratios. Lherzolitic diamond suites are therefore suitable for obtaining Sm–Nd isochron ages while Sr isotopes provide a means for verifying whether

inclusions from different diamonds are cogenetic. This is the approach adopted in the early 1990s, again using composites of similar inclusions, for dating lherzolitic diamonds from the Cullinan Mine (Richardson et al. 1993) and harzburgitic to lherzolitic diamonds from Udachnaya (Richardson and Harris 1997). In both studies, Sm–Nd isochron ages of approximately 2.0 Ga were obtained notwithstanding some variation in garnet initial $^{87}Sr/^{86}Sr$ (discussed more in Pearson and Shirey 1999) attributed to a contribution of radiogenic Sr from one or more extraneous grains in some composites. The ages thus obtained for lherzolitic diamond formation would be consistent with major refertilization of the continental lithospheric mantle via melt metasomatism associated (for example) with widespread Bushveld magmatism at that time (Richardson et al. 1993; Shirey et al. 2002; Richardson and Shirey 2008).

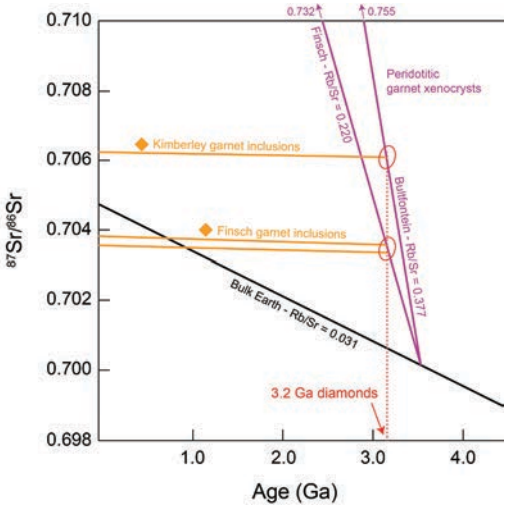


**Figure 5.** Strontium isotope evolution diagram for composite garnet inclusions from Kimberley and Finsch. Garnet inclusions in Finsch and Bultfontein (Kimberley) diamonds have $^{87}Sr/^{86}Sr$ ratios that intersect with the Sr isotope evolution curve for peridotitic garnet xenocrysts at around 3.2 Ga, here termed '*Sr model ages*'. These same composite garnet inclusions yielded 3.4–3.3 Ga Sm–Nd model ages, that indicate the age of the earliest Kaapvaal lithospheric mantle. Modified from Richardson et al. (1984).

In the case of eclogitic diamonds, Sm, Nd and Sr are invariably partitioned between pyrope–almandine garnet and omphacite, with other accessory phases such as kyanite, rutile and corundum being of little importance. Again, garnet exhibits the highest Sm/Nd ratios, and omphacite the lowest Sm/Nd ratios, whereas Sr isotopes provide the means for verifying whether inclusions from the same diamond or different diamonds are cogenetic. This approach was first applied in the 1980s to suites of eclogitic diamonds from Argyle, Cullinan, Orapa and Finsch at a time when composites of similar inclusions were still required to obtain enough analyte for TIMS analysis of small mineral inclusions (Richardson 1986; Richardson et al. 1990). Even so, the Sm–Nd isochron relationships obtained were sufficiently robust to indicate that eclogitic diamond formation only became prevalent in the Proterozoic. Further corroboration of these results was provided by work on a set of big individual inclusions from Finsch diamonds, which yielded Sm–Nd model ages of 2.4–1.4 Ga albeit with large errors (Smith et al. 1991). The last study of composite eclogitic inclusions was on diamonds from Jwaneng (Richardson et al. 1999), and this approach essentially came to an end with the advent of single sulfide inclusion Re–Os dating in the late 1990s (Pearson et al. 1998b, 1999a,b; Pearson and Shirey 1999).

Two decades later, technological advances in mass spectrometry, in particular the use of $10^{13}$ Ω resistors in ion current amplifiers (Koornneef et al. 2014), have rejuvenated the Sm–Nd isochron approach to dating eclogitic and peridotitic diamond formation. Using single garnet and clinopyroxene inclusions in Letlhakane and Orapa diamonds, Timmerman et al. (2017) have documented multiple eclogitic diamond growth events from the Proterozoic

to the Cretaceous that can be related to regional tectono-magmatic events. The key to this work has been to group individual inclusions on separate Sm–Nd isochrons according to their trace element chemistry, Sr isotope ratio, and nitrogen aggregation state of the host diamond (Timmerman et al. 2017). The grouping of inclusions for Sm–Nd isochrons based on similar chemical characteristics was subsequently applied to single harzburgitic and lherzolitic garnet inclusions from Venetia diamonds. Two separate isochrons—2.95 and 1.15 Ga—were defined based on differences in model ages, CaO contents and REE patterns, and were linked to fluid-dominated metasomatism and basaltic melt-dominated metasomatism, respectively (Koornneef et al. 2017). The Archean isochron age array consisting of low Sm/Nd garnets was not detected in an earlier study of composite harzburgitic-lherzolitic garnets from Venetia (Richardson et al. 2009), though the presence of an older Archean component was inferred from the initial $^{143}Nd/^{144}Nd$ ratio. In addition, over a quarter of the individual inclusions showed higher Sm/Nd and $^{143}Nd/^{144}Nd$ ratios than the earlier composite study, highlighting the need to re-evaluate pooled isochron ages and analyze individual inclusions (Koornneef et al. 2017).

The single inclusion approach for silicate inclusions in diamonds is clearly the way of the future (Gress et al. 2021a,b,c). The most compelling results will ultimately come from the analysis of rare coexisting (but non-touching) garnet and clinopyroxene inclusions from the same growth zone within a diamond. In rare instances where sulfide inclusions exist in the same growth zone as either garnet or clinopyroxene, the Sm–Nd and Re–Os systems yield the same ages within analytical uncertainty. This provides confirmation that the isochron ages reflect the diamond growth event (Gress et al. 2021b).

**Re–Os**

With the advent of new analytical tools in the 1990s, in particular the development of high-precision negative thermal ionization mass-spectrometry (Creaser et al. 1991; Völkening et al. 1991), the Re–Os isotope system became a commonly used dating tool and isotopic tracer. Several reviews through the years discussed the application of the Re–Os isotope system in cosmochemistry and high-temperature geochemistry and the dating of mantle peridotites and eclogites (Shirey and Walker 1998; Pearson 1999; Carlson et al. 2008; Rudnick and Walker 2009; Aulbach et al. 2016; Becker and Dale 2016; Harvey et al. 2016; Luguet and Reisberg 2016; Luguet and Pearson 2019; Reisberg 2021).

Because Re is mildly incompatible during partial melting of peridotite—whereas Os is compatible—this system is particularly suitable for dating of melt depletion events leading to the formation of lithospheric mantle. This leads to large differences in the Re/Os of melt and residue, which then evolve to highly radiogenic and unradiogenic $^{187}Os/^{188}Os$, respectively (Shirey and Walker 1998). Thus, this system was quickly adopted to date mantle samples, such as mantle xenoliths (e.g., Walker et al. 1989; Pearson et al. 1995; Pearson 1999) and exhumed lithospheric mantle sections (e.g., Reisberg and Lorand 1995; Saal et al. 2001). The high partition coefficients for Re and Os into sulfide and the possibility of their strong fractionation made the Re–Os system a likely candidate for the dating of single sulfide inclusions in diamonds. The first attempt at dating sulfides on Koffiefontein diamonds (Pearson et al. 1998b) was immediately successful—producing Archean and Proterozoic ages that eventually proved to be major eclogitic diamond forming events in the Kaapvaal craton. This study also yielded one of the first convincing young peridotitic diamond ages, matching the mantle residence suggested for this diamond from nitrogen aggregation systematics. A very useful aspect of the Re–Os system is being able to relate the sulfide inclusions in diamonds to the sulfides in their eclogitic and peridotitic hosts, i.e., a paragenetic distinction, because of clear differences in the concentrations of Re and Os in these two lithologies (Pearson et al. 1998), and because of the difference in their major element compositions (e.g., Deines and Harris 1995) that can be analyzed from the same digestion that is used for Re–Os isotopes.

***Principles.*** Use of the Re–Os isotope system as a geochronometer is based on the β-decay of $^{187}Re$:

$$^{187}Re \rightarrow {}^{187}Os + e^{-} + 1 \text{ electron antineutrino}$$

As such, this chronometer is suitable for dating via the isochron approach, with the usual premise that the samples used in the regression formed, or isotopically re-equilibrated, at the same time, in the same source, and that the system remained closed afterwards.

$$\left(\frac{^{187}Os}{^{188}Os}\right)_p = \left(\frac{^{187}Os}{^{188}Os}\right)_i + \left(\frac{^{187}Re}{^{188}Os}\right)\left(e^{\lambda_{187}t} - 1\right)$$

where
$\lambda_{187} = 41.5 \times 10^{-9}$ yr$^{-1}$
and subscripts p and i refer to present and initial isotope ratios, respectively

System closure is often not met by mantle-derived samples such as peridotite xenoliths (e.g., Walker et al. 1989; Pearson et al. 1995), which have scattered Re–Os isotope systematics due to their open system behavior up to and even beyond eruption to Earth's surface. This is because subsequent to melt depletion, the continental lithospheric mantle remained open to interaction with fluids or melts carrying Re, making Re more susceptible to secondary overprinting than Os. There is also a lack of isotopic equilibration of isolated accessory phases controlling Os (see Luguet and Pearson 2019 for a detailed review). It is, however, this peculiarity of Os ± Re strongly partitioning into sulfides and alloys (Lorand and Luguet 2016) that has given rise to the application of Re–Os geochronology to individual sulfide inclusions in diamond. Although many diamond suites have been shown to be of Archean or Proterozoic age (see section '*Categorization of ages*'), and diamond is considered the ultimate chemically inert container, inclusions in diamond do not always yield statistically precise isochrons. This is because diamond is precipitated during secondary processes involving fluid or melt ingress, which requires homogenization of the Os reservoir in the pre-existing mantle and that of the incoming fluid or melt, a process that produces cogenetic diamonds with some scatter in the initial Os isotopic composition (see section '*Protogenetic versus syngenetic debate*').

As an alternative to *'linear data arrays'*, Re–Os model ages can be calculated, preferably for ancient diamonds that host sulfides with extremely high Re/Os (e.g., Richardson et al. 2001), although model ages by themselves can be subject to large uncertainties. This is because the model age approach requires the source composition (often some primitive or chondritic upper mantle composition) to be known rather well back in time. Projection to the mantle evolution curve can have large age uncertainty for young samples due to mantle heterogeneity (e.g., Luguet and Pearson 2019) and large age uncertainty for old samples—especially those with low Re/Os ratios—due to projection errors intersecting the mantle composition. The latter problem does not hold for sulfides with very high Re/Os (eclogitic), whose Os isotope evolution intersects mantle evolution curves at a high angle, producing minimal differences in calculated model ages. Two types of model ages—$T_{MA}$ and $T_{RD}$—may be calculated (Shirey and Walker 1998; Walker et al. 1989) (Fig. 6). A $T_{MA}$ age dates the time of separation from a reference reservoir such as an upper mantle with a primitive or chondritic (chon) composition using measured $^{187}Re/^{188}Os$ and $^{187}Os/^{188}Os$:

$$T_{MA} = 1/\lambda \times \ln\left[\left(\frac{^{187}Os/^{188}Os_{chon} - {}^{187}Os/^{188}Os_{sample}}{^{187}Re/^{188}Os_{chon} - {}^{187}Re/^{188}Os_{sample}}\right)\right] + 1$$

A $T_{RD}$ age also dates the time of separation from a reference reservoir, but assumes that Re is perfectly incompatible and is completely extracted during partial melting (i.e., $^{187}Re/^{188}Os = 0$).

Using the measured $^{187}Os/^{188}Os$ yields:

$$T_{RD} = 1/\lambda \times \ln \left[ \left( \frac{^{187}Os/^{188}Os_{chon} - {}^{187}Os/^{188}Os_{sample}}{^{187}Re/^{188}Os_{chon}} \right) \right] + 1$$

An inherent assumption in the application of $T_{RD}$ ages is that Os in the sample is unradiogenic. The resultant age is a minimum age that deviates increasingly from $T_{MA}$ the smaller the degree of melt extraction (and by definition, the smaller the resulting Re/Os fractionation), and with elapsed time. In mantle peridotite residues produced from very large degrees of melting, where Re/Os has been reduced to nearly zero, $T_{RD}$ should equal the $T_{MA}$ model age. In mantle xenoliths that have been overprinted by interaction with their host magma, typically involving Re addition, a third model age ($T_{RD}$, erupt) is calculated, by subtracting the amount of $^{187}Os$ added by the decay of $^{187}Re$ since emplacement of the host magma, and using this initial $^{187}Os/^{188}Os$ to calculate $T_{RD}$ (Pearson et al. 1995; Fig. 6). This model age is not applicable to sulfide inclusions in diamond that have remained closed systems since encapsulation. While the underlying principles have not changed, potential pitfalls and best practices have been finessed through the years, along with further developments in sample preparation and analytical protocols. The reader is referred to Rudnick and Walker (2009), Meisel and Horan (2016), Luguet and Pearson (2019), Pearson et al. (2021) and Reisberg (2021) for recent updates.

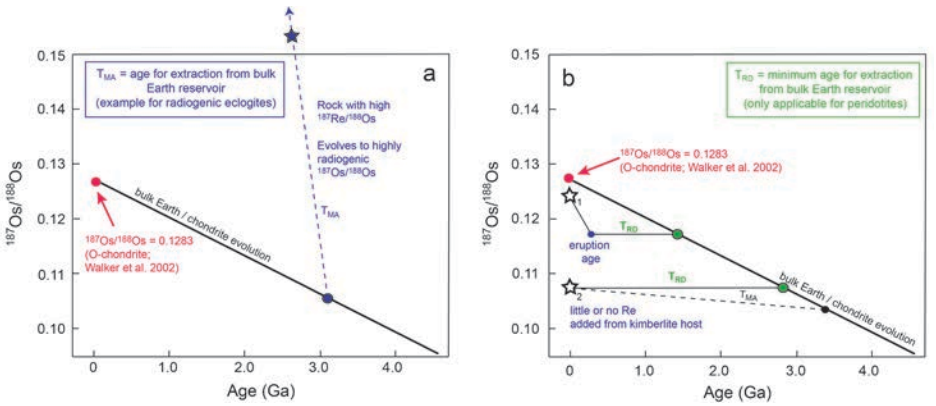


**Figure 6.** Graphical illustration of Re–Os model ages, that are calculated by projection back to a primitive mantle or bulk Earth (chondrite) evolution curve (Shirey and Walker 1998; Pearson and Shirey 1999). Both types of model ages give the time of extraction from a bulk Earth reservoir, and may not necessarily give the time of diamond formation. For eclogitic rocks and sulfides that have high Re/Os, $T_{MA}$ ages are calculated. For peridotite rocks and sulfides, $T_{RD}$ ages are more appropriate since the sample Re/Os isotopic ratio is significantly reduced by melt extraction. Because the mantle has become more isotopically heterogeneous with time, projection back to a bulk Earth evolution curve can have large age uncertainties for young samples.

***Inclusion types.*** Rhenium and Os are highly siderophile elements, which, in the absence of metal phases, behave in a strongly chalcophile manner, such that they are concentrated in—and their behavior is controlled by—sulfide minerals (Mitchell and Keays 1981; Lorand 1989; Fleet et al. 1996; Lorand and Luguet 2016). Combined with the fact that sulfide minerals are the most common inclusions in diamond (Harris and Gurney 1979), the potential of the Re–Os isotope system as a diamond dating tool was recognized early on (Pearson et al. 1998b, 1999a,b; Pearson and Shirey 1999). Because melts have high Re/Os and low Os concentrations, whereas residues have low Re/Os and high Os concentrations, it follows that peridotitic diamonds contain sulfides with higher Os contents (median 42 ppm, $n$ = 52) than sulfides in

eclogitic diamonds (median 0.034 ppm, $n$ = 82; Aulbach et al. 2016), which formed in a host rock that is the metamorphic equivalent of a mantle-derived melt, i.e., basalt. Sulfide-bearing eclogitic diamonds are more difficult to date for two reasons: (1) Os concentrations may be too low to obtain precisions sufficient for meaningful age calculation, depending on the size of the inclusion and total Os available for analysis, and (2) they invariably form in a high-Re/Os rock that has evolved to radiogenic $^{187}Os/^{188}Os$ by the time of eclogitization and diamond formation (Richardson et al. 2001; Aulbach et al. 2009c). This implies that meaningful model ages, requiring assumptions on the isotopic evolution (Re/Os) of the source, cannot be calculated with any confidence, and age constraints must rely on the isochron approach. An exception are sulfide grains with low common Os contents, where a large proportion of the measured Os is $^{187}Os$ from the *in situ* decay of $^{187}Re$ and from which absolute ages may be obtained (Richardson et al. 2001), as described in more detail below. The low amount of Os available for measurement in that study (20–120 fg) means that these are analytically highly challenging measurements to make. Additional challenges common to both peridotitic and eclogitic sulfide inclusions are discussed in section '*Sources of uncertainty*'.

***Practical applications.*** The first constraints on diamond formation ages via Re–Os dating of sulfide inclusions were presented in Pearson et al. (1998b) who obtained an age for mineral inclusions in a single peridotitic Koffiefontein diamond that yielded a date similar to the kimberlite emplacement age. In this same study, five eclogitic inclusions yielded ages of ~1.05 ± 0.12 Ga and 2.9 Ga, depending on the interpretations of this small data set. This was followed by a steady succession of papers reporting Re–Os isotope systematics of sulfide inclusions in diamond that recorded ages spanning the range from close to craton formation to eruption of the host kimberlite (see worldwide data compilation: Smit et al. 2021: https://doi.org/10.7939/DVN/DRAJGT). These studies are reviewed in more detail in a later section. To date, Re–Os dating of whole sulfide inclusions liberated by breaking the host diamond is performed in only few laboratories world-wide because the small amount of analyte requires ultra-low blanks and therefore ultraclean reagents and laboratories, coupled to sensitive, state-of-the-art mass spectrometers that are dedicated to the analysis of small samples. Initiated at the Carnegie Institution for Science in Washington DC (Pearson et al. 1998b), the technique has since only been adopted at The University of Durham (UK) and the University of Alberta (Canada).

## SOURCES OF UNCERTAINTY WHEN DETERMINING DIAMOND FORMATION AGES

While diamonds, as chemically inert containers, offer ideal conditions for closed-system evolution of their inclusions, it can be difficult to ascertain whether the inclusions formed at the same time in the same mantle source, or alternatively were isotopically re-equilibrated in response to the same event. That is, whether the inclusions are cogenetic with each other and with the diamond. Given the protogenetic origin of many inclusions (e.g., Nestola et al. 2014, 2019; Smit et al. 2016, 2019b; Aulbach et al. 2018), isotopic re-equilibration between the various inclusions comprising an isochron is typically required to obtain a meaningful age (see section *'Protogenetic versus syngenetic debate'* below). This can only be achieved, imperfectly, if the mantle volume is affected by events with high fluid–rock or melt–rock ratios (Aulbach et al. 2018). Because of the requirement of isotopic homogenization of a pre-existing reservoir, there is often significant scatter in the initial ratios defined by either mantle rocks or inclusions from diamonds, which inevitably deteriorates the quality of the isochron. Below we discuss some of the factors that may contribute to uncertainty in isochronous relationships, including partial isotopic re-equilibration, open system behavior, and analytical considerations such as over/under spiking.

**Protogenetic versus syngenetic debate**

A long-standing premise for diamond dating has been that the inclusions and the diamond co-crystallized from the same diamond-forming fluid. In other words, that there is a *syngenetic* relationship between diamond and inclusion, as opposed to the diamond incorporating a pre-existing (*protogenetic*) mineral grain. The assumption of a *syngenetic* relationship has traditionally been based on textures observed in diamond inclusions that show that the diamond's cubo-octahedral morphology has been imposed onto the inclusion (Harris 1968; Harris and Gurney 1979; Harris et al. 2022, this volume). Epitaxial crystallographic relationships between inclusions and diamond (e.g., Mitchell and Giardini 1953) can also be a key indicator of this *syngenetic* link. For example, most sulfide inclusions show cubo-octahedral morphologies (Harris et al. 2022, this volume) that are not expected for sulfide minerals, but rather are imposed by the host diamond, either onto (*partially?)* molten sulfides, or where sulfide compositions dictate that trapping maybe sub-solidus, by simultaneous growth with the diamond dominating the surface energy. These textures were traditionally interpreted as syngenetic, meaning that the sulfide and diamond precipitated from the same fluid/melt.

Later work showed that some inclusions could have a *syngenetic* interface with diamond even if crystallographic evidence suggests the inclusion was *protogenetic* (Agrosi et al. 2016). Similarly, Archean ages for sulfides enclosed in Paleozoic mantle zircon were interpreted as evidence that diamond sulfide inclusion-based ages are unrelated to diamond growth (Spetsius et al. 2002). Thus there is increasing evidence that mineral inclusions in diamonds can be pre-existing rather than *syngenetic*. Observations of compositional features of inclusions requiring a multi-stage evolution of their mantle source prior to their incorporation into diamond have led to concerns about the meaning of inclusion ages with respect to the diamond formation event (Nestola et al. 2017; Davies et al. 2018).

In the previous sections, we discussed the ample compositional evidence for pre-history of both silicate and sulfide inclusions prior to their incorporation in diamond. The faceted nature and small size—relative to the grain size of mantle xenoliths—of most inclusions in diamonds may belie an origin as dissolution-remnants of larger "protogenetic" crystals. However, this lack of syngeneity does not preclude a diamond formation age being obtained from inclusion-based dating studies. Because diamond formation is associated with fluids and melts, minerals from the surrounding rocks are either incorporated during partial melting, or fluid-enhanced diffusion takes place so that isotopes are re-equilibrated (Nestola et al. 2019; Pamato et al. 2021). Isotopic equilibration can also be achieved if the inclusion recrystallizes as the diamond is precipitated at high fluid– or melt–rock ratios during major diamond formation events (Aulbach et al. 2018). Such mineral inclusions are better referred to as *synchronous* inclusions (Nestola et al. 2017), and due to re-equilibration at the time of diamond formation will still yield geologically relevant diamond ages.

Implicit in this discussion, is the recognition that model ages obtained for a mineral inclusion in diamond are insufficient to define a diamond formation age. As discussed above (section '*Dating Principles*'), model ages provide the minimum age of the continental lithospheric mantle rather than the diamond age. In systems where a high degree of radiogenic common Os is likely to be inherited by the inclusion, even if growing synchronously with the diamond, model ages are potentially less reliable. Conversely, an isochron or age array can be interpreted to date a diamond formation event, so long as the assumptions behind the approach are broadly met. The robustness of sulfide Re–Os isochron ages has been recently demonstrated by age-equivalent Sm–Nd isochrons from the same diamonds (Gress et al. 2021b). The issues relating to dating diamonds using the isochron approach are similar to those posed by dating any metamorphic rock where new minerals may have grown perhaps by metasomatism of some components. A large-scale diamond-formation event with high fluid–rock ratios can explain why inclusions in diamonds are sometimes considered *cogenetic*—they retain similar initial radiogenic isotope compositions—even if they are sampled as spatially unrelated

xenocrysts (e.g., Allègre 2008). In smaller-scale events with lower fluid–rock ratios, isotopic compositions are expected to show scatter due to the open-system environment in the mantle, with repeated metasomatic events causing elemental fractionation and isotopic overprint. The observation in most isochron diagrams is that inclusions tend to show some scatter around the linear regression, suggesting that inclusions are from sources with varying initial radiogenic isotope ratios that were imperfectly re-equilibrated and mixed during diamond formation, all leading to higher uncertainties in the determined age. Even so, this scattered age is likely to be a useful approximation of the age of the diamond-forming event.

**Sources of uncertainty in silicate studies**

***Diffusion of elements from inclusion to inclusion-diamond interface.*** Diffusion is faster at higher temperatures. For this reason, diffusion of elements between mineral inclusions and the inclusion–diamond interface or fluid film may occur during mantle residence, possibly causing elemental fractionation and changed parent/daughter isotopic ratios over time. In this case, the mineral inclusions themselves will no longer represent 'closed' systems and may not yield diamond formation ages.

One example of diffusion is the loss of argon from clinopyroxene inclusions during mantle residence. Analyses of exposed or extracted clinopyroxene inclusions yield $^{40}Ar/^{39}Ar$ ages close to kimberlite eruption, with most ages between the times of kimberlite eruption and diamond formation (e.g., Burgess et al. 1994, 2004; Phillips et al. 2004, 2018; Phillips and Harris 2008, 2009). The favored explanation for this behavior was diffusion of pre-eruption radiogenic Ar ($^{40}Ar^{*}$) to the diamond/inclusion interface region during mantle residence, with partial to complete loss of this component when the diamond was cleaved to expose the inclusion (Burgess et al. 1992). However, step-heating experiments have shown that lower temperature steps yield older apparent ages than the fusion steps (Phillips et al. 2004; Phillips and Harris 2008). These steps indicate that the diffusional behavior is more complex. Partial accumulation of pre-eruption Ar in defect structures within the clinopyroxene lattice is suggested with concomitant or subsequent partial Ar diffusion to the diamond/inclusion interface. Fracturing around the inclusion in response to changing pressure and temperature during the eruption process (Bulanova et al. 2004; Burgess et al. 2004; Phillips et al. 2004; Phillips and Harris 2008) is likely the cause. Therefore, laser drilling to enclosed inclusions or furnace graphitization of the diamond plus inclusion is required to sample the radiogenic Ar residing at both the interface and within the inclusion. As there are technical challenges with both approaches, the $^{40}Ar/^{39}Ar$ method has not been widely used to determine diamond formation ages.

Lead loss is common in U-bearing minerals, due to the different chemical behavior of U compared to its daughter Pb isotopes, as well as alpha-recoil damage in the mineral. A recent U–Pb study on rutile inclusions from Mir eclogitic diamonds yielded ages consistent with kimberlite eruption (Schmitt et al. 2019) and are much younger than Re–Os isochron ages for sulfide inclusions from eclogitic diamonds of the same pipe (Wiggers de Vries et al. 2013). Pb loss from rutile into cracks, a Pb-rich phase on inclusion margins, or Pb loss into a fluid film surrounding inclusions (Nimis et al. 2016) cannot be excluded. Currently, the (trace element) composition of the fluid film is unknown and therefore it is not known whether there is a differential Pb isotopic composition. Thus, the rutile inclusions were suggested to record diamond formation shortly before kimberlite eruption (Schmitt et al. 2019). However, as U partitions into rutile 250× more strongly than Pb (Foley et al. 2000), if Pb is lost to a fluid film then U–Pb dating of rutile likely does not record diamond formation. Other studies of high U–Pb inclusion phases in diamond have given similarly young ages (Hamilton et al. 1997) similar to kimberlite emplacement, indicating that this may be a common phenomenon, at least for rutile and $CaTiO_3$ perovskite inclusions. In contrast to U–Pb, diffusion rates and partition coefficients of Sm and Nd are similar to each other, in the same order of magnitude, suggesting limited parent–daughter fractionation between inclusion and fluid film. Further *in situ* studies are required, but currently there is no evidence for significantly modified Nd isotopic compositions of silicate inclusions through loss of elements to a fluid film or into cracks.

***Extraneous argon.*** *'Excess Ar'* is defined as $^{40}Ar$, apart from atmospheric $^{40}Ar$, that is incorporated into rocks and minerals by processes other than *in situ* radioactive decay of $^{40}K$ (McDougall and Harrison 1999). Excess Ar results in $^{40}Ar/^{36}Ar$ values above the atmospheric ratio of >298.56 (Lee et al. 2006), and may be identified from isochron plots. Inherited Ar is radiogenic Ar ($^{40}Ar^{*}$) that is included in rocks and minerals through contamination by older material or involves the retention of $^{40}Ar^{*}$ from a previous event (McDougall and Harrison 1999). Extraneous Ar is a term that includes both excess and inherited Ar.

If it is assumed that clinopyroxene inclusions extracted from their host diamond have lost all pre-eruption Ar, $^{40}Ar/^{39}Ar$ dating of the inclusions should yield the age of the host kimberlite (e.g., Phillips et al. 2004). If a clinopyroxene inclusion retains a proportion of the pre-eruption Ar, this Ar component is considered '*inherited*' Ar. In cases where $^{40}Ar/^{39}Ar$ ages are anomalously old compared to other dating methods or the age of the Earth, then the inclusions would be deemed to contain excess Ar. For example, Burgess et al. (2004) reported $^{40}Ar/^{39}Ar$ ages of >4.5 Ga for enclosed inclusions from an Orapa diamond and concluded that the inclusions (or diamond) must contain excess Ar.

***Inherited compositional characteristics and isotopic dis/equilibrium.*** There are many compositional features observed in silicate inclusions that require them to have resided in the continental lithospheric mantle prior to diamond formation. For example, common sinusoidal rare earth element (REE) patterns in harzburgitic garnet inclusions suggest a complex history, and are caused by LREE metasomatism in a melt-depleted peridotite prior to diamond formation (Stachel et al. 1998; Taylor et al. 2003) or interaction of the diamond-forming fluid with melt-depleted peridotite (Koornneef et al. 2017).

Large variations are observed in Sr isotope ratios between silicate inclusions in monocrystalline diamonds (e.g., Richardson et al. 1990), but also even within single fibrous diamonds (0.709–0.717; Klein-BenDavid et al. 2010). In particular, radiogenic $^{87}Sr/^{86}Sr$ ratios in garnet inclusions in diamond (Richardson et al. 1984, 1993; Timmerman et al. 2017), fluid inclusions in diamond (Klein-BenDavid et al. 2010,2014), and garnets recovered from the kimberlite host (Richardson et al. 1984) are unsupported by their low $^{87}Rb/^{86}Sr$ ratios. Initial ratios are well above ratios of the bulk Earth at that time (Richardson et al. 1990). This implies a multi-stage isotopic evolution of the diamond-forming fluid source and complicates using Rb–Sr for age constraints, resulting in Rb–Sr model ages that are unlikely to have geological significance (Timmerman et al. 2017).

The isotopic composition of relatively high atomic number elements like Sr do not change during high-temperature geological processes such as immiscibility or fluid–mineral fractionation during diamond growth. Based on trace elements and Sr–Nd–Pb isotopic compositions, an Archean metasomatized lithospheric mantle with phlogopite (high Rb/Sr) or subducted sediment (Mazzone and Haggerty 1986; Viljoen et al. 1996) can be the source of highly radiogenic Sr (Klein-BenDavid et al. 2010, 2014). More recent element fractionation in the metasomatized ancient source or mixing with depleted fluid/s can lower Rb/Sr ratios, providing a large range in $^{87}Sr/^{86}Sr$ ratios and radiogenic Sr that is unsupported by the present-day low Rb/Sr ratios. Rb–Sr isotopic compositions need to be treated with caution before being applied to diamond dating. However, they can still be useful since similar initial Sr isotope ratios are a good indicator that the inclusions are cogenetic, or protogenetic inclusions whose isotopic compositions have been equilibrated during the diamond-forming event and hence can be used to determine grouping for Sm–Nd isochron regressions.

As Sm and Nd show similar chemical behaviour, the radiogenic ingrowth of $^{143}Nd$ is less variable due to smaller relative differences in Sm/Nd ratios (Richardson et al. 1984). Since diffusion of Sm and Nd in garnet is about 75,000× slower than Os diffusion in sulfide at mantle temperatures of 1100 °C (Tirone et al. 2005), variability in initial $^{143}Nd/^{144}Nd$ ratios is more likely to be preserved in different silicate inclusions during diamond formation.

Samarium diffusion modeling by Nestola et al. (2019) indicates that a 0.1 mm garnet grain will reach equilibrium within 200,000 years at 1150 °C (which is considered to be the average temperature for diamond formation within the continental lithospheric mantle; Stachel and Luth 2015). At the same temperature, ~1 mm garnets, would take around 20 million years to equilibrate (Fig. 7). These diffusion calculations use the slowest diffusion coefficients in the literature (Van Orman et al. 2002), and equilibration times are two orders of magnitude faster if diffusion coefficients from Tirone et al. (2005) are used. Regardless, these equilibration times are significantly less than the uncertainty on most Sm–Nd diamond ages. Under hydrous mantle conditions during diamond growth, garnet would have even faster diffusion rates (Katayama and Karato 2008). Based on (anhydrous) garnet diffusion modeling and assuming protogenesis, Nestola et al. (2019) recommended that silicate inclusions in diamonds that are >100 μm in size and formed at temperatures <1000 °C should not be used for age determinations, though more diffusion data, relevant to the diamond growth environment, is needed to evaluate these criteria (Koornneef et al. 2017).

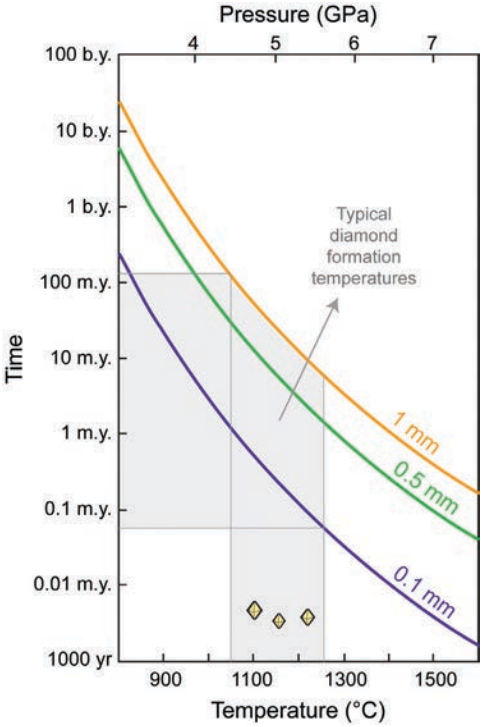


**Figure 7.** Samarium diffusion times for garnets of different sizes (0.1 mm, 0.5 mm, 1 mm), along a geotherm corresponding to 40 mW/m$^2$ surface heat flow. The **grey box** represents typical diamond formation conditions in the sub-continental lithospheric mantle ($T$ = 1150 ± 100 °C) (Stachel and Luth 2015). Equilibration times at these temperatures are roughly between 0.1 m.y and 100 m.y, which is within the typical uncertainties associated with diamond age determinations. For example, a 0.1 mm garnet grain will reach equilibrium within 200,000 years at 1150 °C, calculated using the slowest diffusion coefficients in the literature (Van Orman et al. 2002). Equilibration times are two orders of magnitude faster if diffusion coefficients from Tirone et al. (2005) are used. Diffusion coefficients have so far only been determined under anhydrous conditions, and diffusion may be even faster under hydrous conditions that may be more typical of diamond formation. Modified from Nestola et al. (2019).

## Sources of uncertainty in sulfide studies

***Pre-encapsulation history of sulfide inclusions.*** There are several eclogitic sulfide-derived isochrons with strongly radiogenic initial $^{187}Os/^{188}Os$, that exceed estimates for a coeval mantle with chondritic composition (Walker et al. 2002) at the time of diamond formation. These supra-chondritic initial $^{187}Os/^{188}Os$ ratios require ingrowth of $^{187}Os$ in a high Re/Os environment prior to diamond formation and sulfide entrapment. Given the eclogitic nature of these inclusions, this evolution plausibly occurred in the oceanic crustal protolith, and radiogenic Os was subsequently inherited when sulfide and diamond grew from subduction-related fluids or melts. Alternatively, since MORBs are sulfide-saturated (e.g., Patten et al. 2013),

the sulfides may have existed all through the evolution of the oceanic crust, and recrystallized upon metamorphism. Many eclogitic sulfides have Re/Os that is too low to account for their radiogenic $^{187}Os/^{188}Os$, suggesting that Re was lost during partial melting as the eclogite was invaded by diamond forming fluid (e.g., Westerlund et al. 2004; Smit et al. 2016).

Figure 8 illustrates how highly radiogenic $^{187}Os/^{188}Os$ recorded in eclogitic sulfide inclusions can be inherited from high Re/Os protoliths. Sulfide inclusions in the 650 Ma Zimmi diamonds, West African craton have highly radiogenic $^{187}Os/^{188}Os$ (1.5–2.2) and mass-independently fractionated sulfur isotopes that were generated in Archean protoliths subducted into the continental lithospheric mantle (Smit et al. 2016, 2019b). Neoproterozoic (~700–900 Ma) oceanic crust would require $^{187}Re/^{188}Os \geq 2000$ to evolve to these radiogenic $^{187}Os/^{188}Os$ within 100–200 million years, i.e., the assumed time between formation of the igneous precursors at an oceanic spreading ridge and their metamorphism during subsequent subduction. Various components of modern oceanic crust have highly variable $^{187}Re/^{188}Os$ ranging from 100s to 1000s (Peucker-Ehrenbrink et al. 2003). Eclogite xenoliths from the nearby Koidu kimberlite, which most likely formed in the Neoarchean (Barth et al. 2002; Aulbach et al. 2019), have $^{187}Re/^{188}Os$ from 2.4 to 159 (Barth et al. 2002). Such Archean oceanic crust could produce the $^{187}Os/^{188}Os$ measured in Zimmi sulfides in the two billion years after eclogite emplacement. Archean sulfur derived from associated subducted Archean sediments could explain the mass-independently fractionated sulfur isotopes. Fluid/melt fluxing of the mantle during Neoproterozoic subduction then facilitated partial melting, Re–Os isotopic re-homogenization, and Zimmi diamond formation.

In another example, eclogitic sulfide inclusions from both the 2.89 ± 0.06 Ga Kimberley and 1.89 ± 0.19 Ga Diavik diamonds (Richardson et al. 2001; Aulbach et al. 2009c) have radiogenic $^{187}Os/^{188}Os$ requiring Re/Os ~50–100. These Re/Os are lower than those typical of young oceanic crust (Re/Os up to ~1,000; Shirey and Walker 1998) but similar to oceanic crust which loses Re during the subduction, dehydration, and metamorphism (Becker 2000; Dale et al. 2007) that takes place within 10–200 million years after the oceanic crust is formed at a mid-ocean ridge (Fig. 8). This scenario can generate the initial $^{187}Os/^{188}Os$ ratios recorded in Kimberley and Diavik sulfide inclusions—0.156 ± 0.011 and 0.13 ± 0.10, respectively—and suggests eclogitic diamond formation shortly after or during subduction, where sufficient fluids are liberated to isotopically homogenize the Os isotopes in portions of the oceanic crust. Both these localities record coeval eclogitization, with eclogite xenoliths recording the same ages as craton amalgamation (Kaapvaal: Shirey et al. 2001; Menzies et al. 2003) and craton–margin collisional events (Slave: Schmidberger et al. 2007; Aulbach et al. 2009b).

***Evidence for isotopic equilibration of pre-existing sulfide inclusions.*** Osmium diffuses readily in sulfides and has a low closure temperature in pyrrhotite (Brenan et al. 2000) which favors the establishment of isotopic equilibrium with the diamond-forming fluid. Several diamond localities clearly show that pre-existing sulfides were isotopically re-equilibrated at the time of diamond formation, including Klipspringer eclogitic sulfides, Victor lherzolitic sulfides, and Zimmi eclogitic sulfides (Westerlund et al. 2004 ; Smit et al. 2016, 2019; Aulbach et al. 2018).

Based on 14 sulfide inclusions, a 718 ± 49 Ma age array (MSWD = 6.1) was obtained for Victor lherzolitic diamonds, with initial $^{187}Os/^{188}Os$ of 0.1177 ± 0.0016 (Aulbach et al. 2018). This initial ratio is less radiogenic than the convecting mantle at 720 Ma, indicating that at least a portion of the Os was inherited from older sources in the continental lithospheric mantle and that these sulfide inclusions precipitated or re-precipitated along with the Victor diamonds. The observation that an age array was obtained despite contributions from isotopically heterogeneous sources in the continental lithospheric mantle—a region known to experience repeated and ongoing metasomatism—suggests the participation of sufficient amounts of melt during sulfide-bearing diamond formation to allow for near-re-homogenization of Os isotopic compositions from various sources (Aulbach et al. 2018).

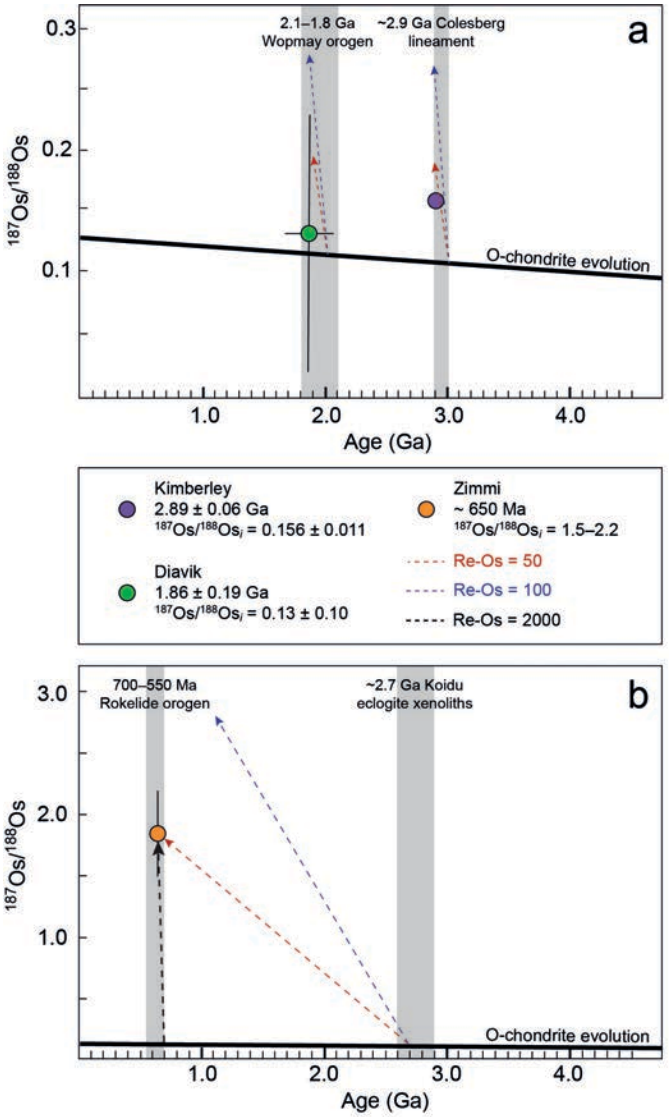


**Figure 8.** Os isotope evolution diagram for dated eclogitic diamonds from three localities: Kimberley, Kaapvaal craton (Richardson et al. 2001), Diavik, Slave craton (Aulbach et al. 2009c), Zimmi and Koidu, West African craton (Smit et al. 2016); illustrating ingrowth of radiogenic Os in (meta)basaltic protoliths with variably high Re/Os. For Kimberley and Diavik, subduction-related eclogitization of oceanic crust around 10–100 million years after its formation can explain the moderately radiogenic initial $^{187}Os/^{188}Os$ obtained from Re–Os isochrons. Eclogite xenoliths from Diavik have measured $^{187}Re/^{188}Os$ of 0.4 to 52 (Aulbach et al. 2009b), although the Re/Os of the igneous precursor prior to dehydration ± partial melting would have been higher (Becker 2000). At Zimmi, strongly radiogenic initial $^{187}Os/^{188}Os$ could be explained by remobilization of Os from an eclogite reservoir emplaced in Neoarchean time, as inferred for eclogite xenoliths from nearby Koidu, which have measured $^{187}Re/^{188}Os$ from 2.4 to 159 (Barth et al. 2002). Note trade-off between the age of the oceanic crust at the time of diamond formation and its Re/Os.

Similarly, five eclogitic sulfide inclusions from Klipspringer, South Africa, record a 2.55 ± 0.15 Ga isochron (MSWD = 0.87), with an elevated initial $^{187}Os/^{188}Os$ of 0.187 ± 0.046 (Westerlund et al. 2004). This initial Os isotope ratio requires pre-evolution in a high Re/Os environment, such as Archean eclogite in the continental lithospheric mantle. Ventersdorp magmatism at 2.7 Ga heated the lithosphere, causing partial melting of sulfide-bearing eclogite and homogenization of the Re–Os system, and resulting in isochronous relationships between these pre-existing sulfides (Westerlund and Gurney 2004; Westerlund et al. 2004).

***Exsolution of monosulfide solid solution to a low-temperature assemblage.*** At mantle conditions, sulfide exists as monosulfide solid solution (*mss*), that is Ni-rich in peridotitic diamonds and Ni-poor grading into Ni-rich pyrrhotite in eclogitic diamonds. Upon low-temperature re-equilibration, for example during transport to Earth's surface, *mss* exsolves into a low-temperature assemblage, typically consisting of pentlandite ($(Fe,Ni)_9S_8$), pyrrhotite ($Fe_{(1-x)}S$) and chalcopyrite ($CuFeS_2$) in varying proportions (e.g., Lorand and Grégoire 2006; Fig. 9). In addition, molybdenite ($MoS_2$) has recently been described in the Raman spectra of 73 out of 80 Mir eclogitic sulfides (Kemppinen et al. 2018; Smith et al. 2022, this volume). Molybdenum though, is not an uncommon trace element in eclogitic sulfides. For example, Diavik eclogitic sulfide inclusions have Mo contents between 44 and 160 ppm (Aulbach et al. 2012). During exsolution, both molybdenite and chalcopyrite concentrate towards the exterior surfaces of sulfide inclusions, as observed in backscattered electron images and EDS maps of sulfides (Fig. 10).

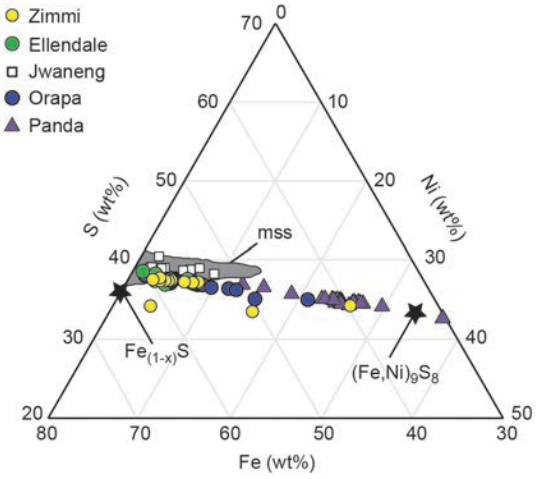


**Figure 9.** Compositions of sulfide inclusions in diamonds from different localities. Field for high temperature *mss*—monosulfide solid solution—from Ebel and Naldrett (1997). Pyrrhotite ($Fe_{(1-x)}S$) and pentlandite ($(Fe,Ni)_9S_8$) are low-temperature sulfides that are produced during exsolution. Data for Zimmi from Smit et al. (2016); Ellendale, Jwaneng and Orapa from Karen Smit (unpublished data) and Richardson et al. (2004); and Panda (Ekati Mine) from Westerlund et al. (2006).

It has been shown that during low-temperature re-equilibration, trace elements—including Re and Os—will partition differently between the different sulfide minerals, as observed in both orogenic peridotites and mantle xenoliths (van Acken et al. 2010; Holwell et al. 2011) and in sulfide inclusions in diamond (Richardson et al. 2001). As Re is preferentially partitioned into the combination of chalcopyrite + molybdenite relative to pyrrhotite + pentlandite, low-temperature re-equilibration has the potential to cause problems for Re–Os age dating if the whole inclusion is not recovered. This is a particular challenge when sulfides, due to their softness, break into multiple pieces during extraction from the diamond, as small fragments including Re-rich rims may be lost. Practitioners of the Re–Os sulfide method go to extraordinary lengths to ensure that they recover all the material liberated by cracking a diamond, because they have long been aware of these issues. This also means that great caution needs to be applied to Os isotope measurements made on all sulfides because of exsolution, especially by

laser-ablation approaches where polishing of thin sections or grain mounts is a pre-requisite for analysis. Indeed, some scatter observed in Re–Os data sets may be related to incomplete inclusion recovery and may be dominated by variation in the Re/Os ratio.

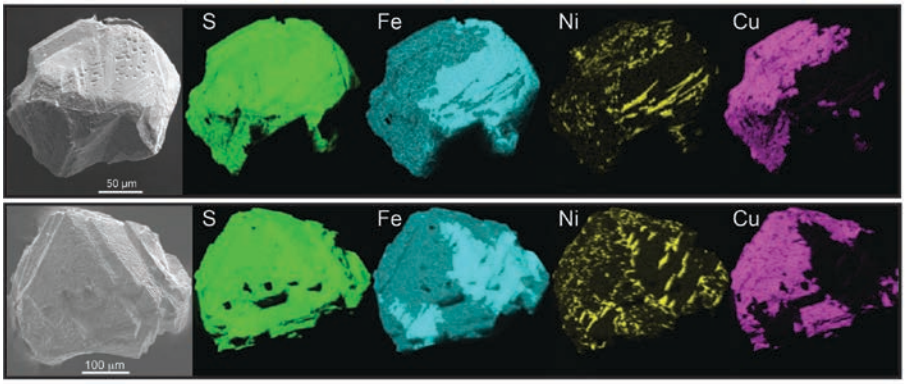


**Figure 10.** Energy-dispersive X-ray spectroscopy maps showing the spatial distribution of major elements in sulfide inclusions. During kimberlite eruption and cooling of monosulfide solid solution (*mss*), pentlandite- and chalcopyrite-rich sulfides are exsolved. Reproduced from Smit et al. (2016).

Increased scatter in Re–Os isotopic data naturally results in higher uncertainties on the determined age, but need not significantly affect the slope of the regression in a Re–Os isochron diagram. This is illustrated in the Re–Os isotope study of peridotitic sulfides from Ellendale (NW Australia) where one peridotitic sulfide falls off the main isochron formed by six other sulfides because it broke during extraction and was only partially recovered (Smit et al. 2010). Its higher $^{187}Re/^{188}Os$ is explained by sampling more Cu-rich portions of the sulfide, and incorporation of this sulfide in the isochron regression yields an identical 1426 Ma age, though the uncertainty on the age increases from 130 Ma to 390 Ma. In contrast, any effect on $^{187}Os/^{188}Os$ is typically minor because Re–Os fractionation during low-temperature re-equilibration occurs during eruption, and most kimberlites and lamproites are very young relative to the age of the diamond (Gurney et al. 2010). This is best demonstrated in sulfide DP9 from Kimberley (also known as '*De Beers Pool*'), where one fragment of this sulfide had double the Cu concentration and 30% higher $^{187}Re/^{188}Os$, while maintaining similar $^{187}Os/^{188}Os$ to the other fragments (Richardson et al. 2001). Regression of both fragments yields an isochron age equivalent to that of the kimberlite eruption.

Considering the potential for increased scatter in the Re–Os isotopic compositions of heterogeneous sulfides and the blocking temperatures well below the storage temperature in the lithospheric mantle, it is remarkable that the overwhelming majority of ages obtained on sulfide inclusions in diamonds appear to have geological significance. In rare cases where silicate and sulfide inclusions co-exist in the same diamond growth zone, similar ages have been obtained (Gress et al. 2021b), providing increased confidence in the robustness of inclusion-based diamond ages.

Homogenization of sulfide inclusions back to their high temperature *mss* mantle composition can be achieved by heating the diamond (and its inclusions) in a furnace (McDonald et al. 2017). By using this homogenization approach, Re–Os isotopes are more evenly distributed through the sulfide, and scatter resulting from incomplete recovery of the sulfide inclusion may be significantly reduced. Another benefit is that Re–Os isotope measurements can be done utilizing only part of the sulfide, so that the remainder of the inclusion can be used for other measurements. Sulfur isotope measurements by ion microprobe are however excluded, since there is currently no standard available for *mss*.

***Low Os content.*** Due to the mildly incompatible nature of Re, and the compatible nature of Os during partial melting, eclogitic sulfides formed in a metabasaltic source typically have higher Re/Os than peridotitic sulfides due to both higher Re and lower Os contents (see section on '*Re–Os*' above). Because eclogitic sulfides typically have lower Os than peridotitic sulfides, larger eclogitic sulfide grains need to be dissolved in order to measure enough Os to obtain acceptable measurement statistics and reduce blank corrections. Eclogitic inclusions are often barely large enough to achieve these measurement goals. Thus, during mass spectrometry, the total amount of $^{187}$Os available for ionization is extremely low, and when combined with the very low $^{188}$Os result in high in-run uncertainties on $^{187}$Os/$^{188}$Os. In particular, this is true for tiny (< 7 μg) eclogitic inclusions. Data compiled for several eclogitic sulfide suites show that eclogitic sulfides that weigh less than 7 μg (less than ~130 μm diameter), yield excessively high uncertainties in $^{187}$Os/$^{188}$Os (Fig. 11). Judging the size of sulfide inclusions can be difficult in some diamonds due to extensive "rosette" fractures that may surround the inclusion, leading to substantial over-estimates of inclusion size in some cases. The low total Os available for analysis in relatively small sulfide inclusions leads to more substantial blank corrections on both Os content and $^{187}$Os/$^{188}$Os (Fig. 11). This propagates through to higher uncertainties in final measured values compared to sulfides with higher Os content (either larger eclogitic inclusions, or peridotitic sulfides with higher Os concentration).

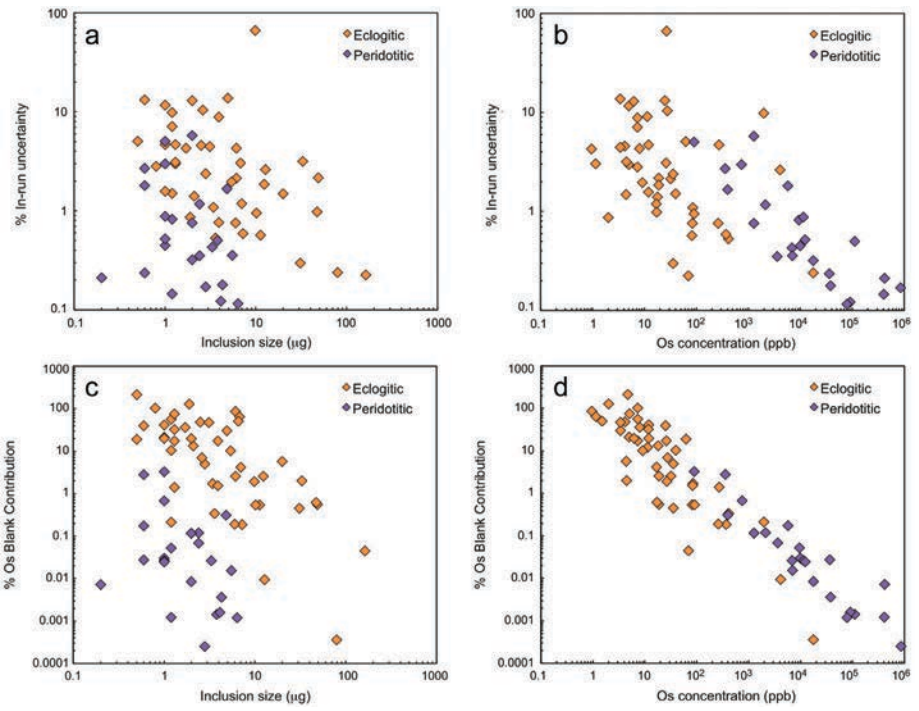


**Figure 11.** The influence of inclusion size and Os concentration on the **a,b)** in-run analytical uncertainty, and **c,d)** estimated blank contribution on the sulfide Os content. Smaller inclusions with lower Os concentration have the highest contribution of blank (*background*) Os. Smaller inclusions that give low Os ion yields during mass spectrometry have the highest in-run uncertainties. For small eclogitic sulfide inclusions from Sewa River and Victor, the in-run uncertainties and blank contributions were prohibitively high and no age determinations could be made. Peridotitic sulfides from Sewa River (Karen Smit, unpublished data), Victor (Aulbach et al. 2018) and Ellendale (Smit et al. 2010). Eclogitic sulfides from Orapa, Juina, Sewa River (Karen Smit, unpublished data), Zimmi (Smit et al. 2016), Victor (Aulbach et al. 2018) and Ellendale (Smit et al. 2010).

**Sources of uncertainty in both silicate and sulfide studies**

***Under/Over spiking.*** While isotope dilution is generally regarded as the '*gold standard*' of elemental abundance determinations, a weakness it has is the need for prior information on likely Re, Os, Sm, Nd, Rb, Sr concentrations and elemental ratios in the inclusions. An informed estimate needs to be made in order to calculate the appropriate amount of isotopic spike to be added prior to dissolution. For Re and Os in sulfides, such an estimate is typically based on whether it is eclogitic (Ni-poor) or peridotitic (Ni-rich). Sulfide paragenesis is determined prior to dissolution by EDS analyses of the sulfide, to get an approximation of the bulk Ni content. If the inclusion breaks during extraction, it is better to get a qualitative composition from an interior part of the grain to avoid the chalcopyrite-rich portions along the exterior. For Sm, Nd and Rb, Sr in silicates, the identity and paragenesis of the mineral inclusion can usually be recognized based on colour (and/or EMP analysis on a flat portion of the unpolished grain) and concentrations estimated based on the range observed in corresponding xenolith and xenocryst minerals.

For sublithospheric diamonds, where paragenetic distinction is not as simple, estimating the Re and Os concentrations in the inclusion can be more complicated. For example, Re and Os concentrations for two metallic inclusions in a CLIPPIR diamond (Smith et al. 2017, 2021) could not be accurately determined for practical reasons. To facilitate handling of these 50–100 μm inclusions, which are highly susceptible to electrostatic/magnetic forces, Os was distilled directly from the inclusions while they were still embedded in the cleaved diamond surface. Their weights were thus difficult to estimate and their Os contents much higher than expected. The resulting sample solutions were critically under-spiked. The very high isotope dilution error magnification (EM) applicable to these sample-spike mixtures meant that measured isotope dilution ratios were within EM-propagated error of the normal (unspiked) isotope composition. Under such circumstances the ability to determine precise Os isotopic compositions is unaffected because all that is being measured is the normal Os in the sample (i.e., negligible spike Os correction). In addition, the chromic–sulfuric reagent used for sulfide dissolution preferentially attacks the pyrrhotite and its dissolution efficacy on Fe–Ni metal, cohenite and other accessory phases such as Cr–Fe-oxide is unknown. Since the exsolution of the homogeneous Fe–Ni–C–S phase on exhumation to pyrrhotite, cohenite and Fe–Ni metal will fractionate Re from Os differently in each phase, actual concentrations and Re/Os ratio would have been impossible to interpret. Again, this effect does not hinder the determination of accurate Os isotopic compositions (Smith et al. 2017, 2021) but serves to illustrate the complexities that can be encountered.

Both over- and under-spiking can introduce substantial propagated uncertainties in concentration and isotopic ratios measurements. If the isotope dilution ratio (spike isotope/reference isotope; e.g., $^{190}Os/^{188}Os$, $^{150}Nd/^{146}Nd$, $^{84}Sr/^{86}Sr$) of the sample–spike mixture ($R_M$) is too high, it is very difficult to determine the natural isotopic composition of the sample. Conversely, if a sample is underspiked, error magnification on the abundance estimate increases more rapidly, though at minimal effect on the radiogenic isotope ratio (Fig. 12).

***Open system.*** Cracks that connect an inclusion to the diamond surface and permit exchange with fluids in the mantle and/or kimberlite, can compromise the goal of determining the diamond formation age. Although plastic deformation of diamond is more common at high temperatures in the mantle, brittle deformation is known to occur. Routine practice during age determinations is to exclude mineral inclusions with visible cracks to the diamond surface, however the presence of annealed cracks cannot always be ruled out despite cathodoluminescence investigation of the diamond surrounding the inclusion. Older cracks sealed with younger diamond growth have been documented from a few localities, and may certainly be more common (e.g., Taylor et al. 1995; Smith et al. 2014).

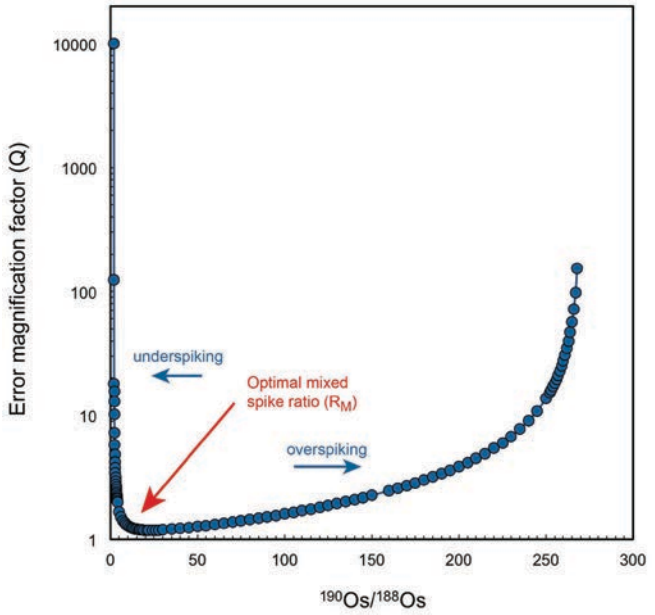


**Figure 12.** An informed estimate of Re, Os, Sm, Nd, Rb and Sr concentrations and elemental ratios in inclusions needs to be made in order to calculate the amount of isotopic spike to be added prior to dissolution. Both over- and under-spiking can introduce uncertainties in concentrations and isotopic ratios. For Re–Os isotope analyses, isotopic spikes typically contain $^{190}Os$ as the tracer isotope. If the $^{190}Os/^{188}Os$ in the sample-spike mixture ($R_M$) is too low, error magnification (Q) of the Os abundance estimate increases rapidly. If overspiking occurs (i.e., $^{190}Os/^{188}Os$ is too high) then it becomes difficult to determine the isotopic composition of the sample.

The only isotopic dataset that indicates connection to the diamond surface by obvious cracks is for six sulfide inclusions in Jagersfontein diamonds (Sonja Aulbach, unpublished data). Interestingly, the Re–Os isotopic compositions of these sulfides have a linear relationship and yield an imprecise age of 252.5 ± 41.9 Ma (Fig. 13). This age is significantly younger than the other diamond ages determined for Jagersfontein (1.7 Ga, 1.1 Ga; Aulbach et al. 2009a), but older than kimberlite eruption (86 Ma; Smith 1983). Thus, while inclusions in such diamonds can no longer inform us on diamond formation ages, they may still be interpretable. In this case, the age overlaps with those reported for strongly metasomatized peridotite xenoliths from the 84 Ma Bultfontein kimberlite (Giuliani et al. 2014), and may reflect isotopic resetting due to mantle metasomatism known to affect all continental lithospheric mantle sections prior to kimberlite eruption (Wass and Rogers 1980).

## CLASSIFICATION OF AGES BY TYPE OF DIAMOND SUITE

Diamond ages can be classified into types by the number of stones involved, the relationship of inclusions to growth zones in the diamond, the mineralogy of the inclusion(s), and way the ages are determined (e.g., model age vs. isochron age). Such classification can provide a useful framework for interpreting the ages geologically—especially because diamonds are xenocrysts physically removed from the geologic context of their mantle hosts by the nature of kimberlitic sampling, except for rare diamondiferous xenoliths.

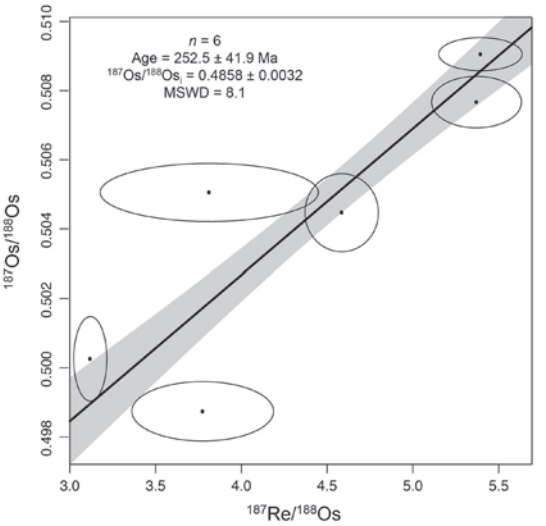


**Figure 13.** Jagersfontein isochron obtained from sulfides with visible cracks to the surface of the diamond. Six inclusions yield an imprecise date of 252 ± 42 Ma (Sonja Aulbach, unpublished data), which is younger than other diamond ages determined for Jagersfontein and significantly older than kimberlite eruption (86 Ma; Smith 1983). See text for further details.

## Single diamond ages

Although it would be ideal for each diamond dating study to have many diamonds with inclusions, the researcher is often confronted with few or maybe even only one propitious stone because diamonds with big enough inclusions for analysis are quite rare. Surprisingly, useful ages from sulfides using the Re–Os system can be obtained from just one diamond in four different ways. These ages are possible with the Re–Os system because of the huge range in the abundance of parent $^{187}$Re and daughter $^{187}$Os, whereas they are not always practical with the Sm–Nd or Rb–Sr systems because of the very limited range of parent to daughter abundance in these systems.

***Model ages.*** Model ages (see '*Principles*' section above for a general outline) are calculated from the measured isotopic composition of a sulfide inclusion and the Os isotopic evolution of some reference reservoir (typically the Earth's mantle, but also chondritic reservoirs). This calculation is essentially a correction for radiogenic growth of daughter $^{187}$Os using the time-averaged $^{187}$Re/$^{187}$Os ratio from the point at which the inclusion had the same isotopic composition as the reference reservoir. Uncertainty comes from a combination of factors: a) the uncertainty in the isotopic growth of the reference reservoir, b) analytical uncertainty in the Re/Os of the inclusion, and c) the assumption that the inclusion measured experienced a single-stage evolution on separating from the reference reservoir. While the insights that can be gained from just one determination can be quite remarkable (e.g., the ability to determine whether a sulfide originated in Mesoarchean lithosphere versus Paleoproterozoic lithosphere) the precision and accuracy are often only known to within 200–300 million years, and, thus, such model ages are not suited to unraveling fine-scale age differences. While model ages provide invaluable constraints on the stabilization age and evolution of diamond source rocks, one model age from a diamond inclusion does not necessarily date a diamond formation event.

Peridotitic sulfides nearly always have very high Os content and very low Re content. The low resultant $^{187}$Os/$^{188}$Os of peridotitic sulfides often gives *minimum ages* for the depletion or '*freezing-in*' of an initial Os isotopic composition. A good example is the one sulfide inclusion

in a diamond analyzed from Murowa (Zimbabwe craton). This sulfide produced a $T_{RD}$ of 3.25 Ga, within uncertainty of the oldest model age on a mantle xenolith from the same locality ($T_{RD}$ of 3.31 Ga). Although the model age obtained from the diamond may not necessarily reflect the time of diamond formation, these ages confirm the existence of protoliths older than the Mesoarchean in the Zimbabwean continental lithospheric mantle (Smith et al. 2009; Pearson et al. 2018), which had long been suspected due to Paleoarchean granite-greenstones, detrital zircons, and chromite deposits in the Zimbabwe craton (Dodson et al. 1988; Wilson 1990; Nägler et al. 1997; Zeh et al. 2014)

Peridotitic sulfides with very low Re/Os are often more reflective of the inclusion protolith, whereas isochrons (and model ages that are in agreement with isochrons) most likely reflect diamond formation (e.g., Pearson et al. 1999a,b). This could be the case for 3.5–3.1 Ga model ages from Udachnaya peridotitic sulfide inclusions that likely reflect the minimum age of the Siberian continental lithosphere rather than the age of diamond formation. Other age determinations for Udachnaya peridotitic diamonds give 2 Ga isochron ages (e.g., Richardson and Harris 1997), similar to the ages for eclogitic diamonds (Wiggers de Vries et al. 2013), granulite xenoliths (Koreshkova et al. 2008) and peridotite xenoliths (Doucet et al. 2015; Ionov et al. 2015).

Single eclogitic sulfides can produce model ages by extrapolation from their extremely high $^{187}Os/^{188}Os$, back to a bulk Earth or mantle growth curve. For eclogitic sulfides, the accuracy of the model age depends on the closed system behavior of Re and Os and thus the fidelity of the Re/Os ratio since entrapment in the diamond, as well as how much radiogenic Os has accumulated. Thus, while a model age can, in principle, be obtained on a single grain, prudence dictates use of multiple eclogitic sulfides on an age array (see below) to provide some indication that the Re/Os has not varied and to obtain more accuracy on the projection.

Model ages for the Sm–Nd system in silicate minerals also have the potential to reflect diamond growth if the Sm/Nd fractionation is substantial enough. Occasionally, single diamond model ages have successfully been obtained using the Sm–Nd system for sufficiently large silicate inclusions. For example, Smith et al. (1991) obtained a Nd model age of 2.11 ± 0.12 Ga for a websteritic clinopyroxene inclusion in a Kimberley diamond based on this approach. Model ages are less definitive where Sm/Nd fractionation is subtle relative to the reference reservoir, for example, the Cullinan lherzolitic garnets (Richardson et al. 1993).

***Radiogenic daughter (absolute) ages.*** Occasionally, sulfides are uncovered that contain only a radiogenically-derived isotope of Os—$^{187}Os$. These minerals contain no '*common*' or unradiogenic Os, which indicates that at the time of incorporation into the diamond the sulfide contained only Re and an unmeasurably small amount of Os. In a study of sulfides from the De Beers Pool diamonds in Kimberley (South Africa), Richardson et al. (2001) discovered five sulfide inclusions with these characteristics. These sulfides were so overspiked with the typical $^{190}Os$ spike that error magnification leads to large uncertainties in the exceptionally low Os concentrations. In this situation, $^{187}Re/^{188}Os$ values become extraordinarily high ($\gg$10,000) and fail to plot on conventional isochron diagrams with normal samples (cf. Richardson et al. 2001). Sulfides like these appear to be rare but they present an interesting case study in dating methodology.

***Core–rim ages.*** A common question that arises is how long it takes for a diamond to crystallize. When a diamond has grown with the fortuitous entrapment of several inclusions in different locations relative to the core and rim of the diamond, the minimum time for a diamond's growth can be estimated from the core–rim ages. The most detailed examples of this approach are on diamonds from the Siberian and Kalahari cratons. Wiggers de Vries et al. (2013) documented two main episodes of diamond crystallization (~2.1–1.8 Ga and ~1.0–0.9 Ga) in the Siberian craton (23$^{rd}$ Party Congress, Mir, and Udachnaya kimberlites). One diamond, sample 4239, had sulfides defining an isochron at the older, Paleoproterozoic

age in the core as well as sulfides defining the younger Mesoproterozoic isochron age in the rim. These age differences confirm that this diamond took around 1 billion years to form, probably in two distinct growth pulses of much shorter duration. Similarly, multiple episodes of diamond formation are present at Letlhakane and Orapa, with two diamonds containing inclusions in different growth zones showing age differences up to 2 b.y. (Timmerman et al. 2017). Sample LK75 from Letlhakane had a clinopyroxene in an intermediate growth zone that falls along a 2.3 Ga isochron and a garnet in the rim that falls along a 0.25 Ga isochron. Sample OR02 from Orapa had a garnet in an inner zone that falls along a 1.1 Ga isochron, and a garnet in the rim that is within error of the kimberlite eruption age.

These results demonstrate that these diamonds are aggregated products of at least two episodes of diamond growth. Unfortunately, these ages do not reveal the crystallographic growth rate of the diamond over a billion years. Such composite diamond crystals seem to be the norm—as can be seen from CL textural studies of many diamonds from kimberlites worldwide, where the most striking examples are monocrystalline diamonds with younger fibrous overgrowths (e.g., Petts et al. 2016; see also Jacob and Mikhail 2022, this volume; Weiss et al. 2022, this volume). Even if one were to obtain a perfect diamond where the intricate growth zones contained inclusions that were spaced at just the right interval to determine a zone-to-zone age, it is likely that the uncertainties for each zone would overlap enough to preclude the determination of a growth rate.

***Mineral isochrons.*** The gold standard for dating a diamond is the 'mineral isochron' approach, explained in more detail in the '*Principles*' section above. The value of mineral isochrons from single diamonds comes from the proximity of the mineral grains, which enhances the likelihood that they were in isotopic equilibrium at the time of closure of the isotopic system. In diamonds containing inclusions that define mineral isochrons, the date obtained is the time of system closure and the age of formation of the diamond because it records the blocking of interdiffusion between the mineral grains by the diamond.

Yellow, Type Ib alluvial diamonds from Zimmi (Sierra Leone) provide one of the clearest mineral isochron examples (Fig. 14). Smit et al. (2016) analyzed three different diamonds each with 3–4 separate sulfide inclusions, and each diamond yielded a 650 Ma age regression from its own '*linear data array*' whose individual uncertainties overlapped. Each diamond has a high but not identical initial $^{187}Os/^{188}Os$ (between 1.5 and 2.2) so it is not sensible to include all the data in one regression. Even with these differences in the initial $^{187}Os/^{188}Os$, this high or so-called 'radiogenic' $^{187}Os/^{188}Os$ requires long-term evolution of the sulfides in a high Re/Os eclogitic host and confirms that the Zimmi diamonds all formed during one diamond-forming episode in the continental lithospheric mantle.

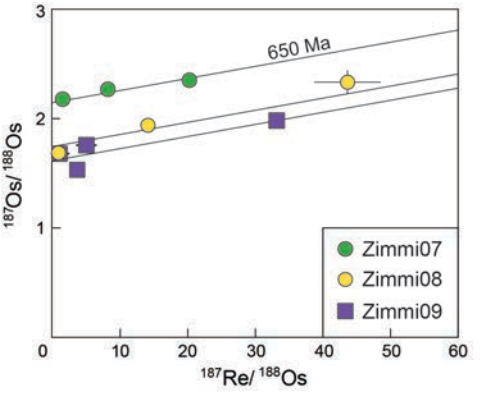


**Figure 14.** Three Zimmi diamonds—each with three to four sulfide inclusions—yielding identical 650 Ma ages. These data have too much scatter to meet the requirements for true isochrons, but are termed '*linear data arrays*'. Scatter is likely due to partial isotopic re-equilibration of pre-existing sulfides at the time of encapsulation in the diamond. Where not visible, uncertainties are smaller than the size of the symbol. Modified from Smit et al. (2016).

In peridotitic diamonds from the Ekati mine in the Slave craton, Westerlund et al. (2006) obtained sulfide Re–Os isochrons on five separate diamonds with 2–3 inclusions per diamond—all of which can be combined to give an aggregate 3523 ± 170 Ma isochron with 11 inclusions (Fig. 15). Because the sulfide isochrons can be regressed together with the inclusions from other diamonds, this multi-phase isochron firmly establishes the age of the oldest diamonds ever dated. Equally important, the elevated initial $^{187}Os/^{188}Os$ of the isochron is based on inclusions that crystallized in the outer growth zones of the diamonds—not their cores. This textural evidence supports the interpretation that the last stage of diamond growth was from fluids that had incorporated some radiogenic crustal Os derived from the recycling of oceanic lithosphere. The local vs global scale implications of this recycling are a source of debate.

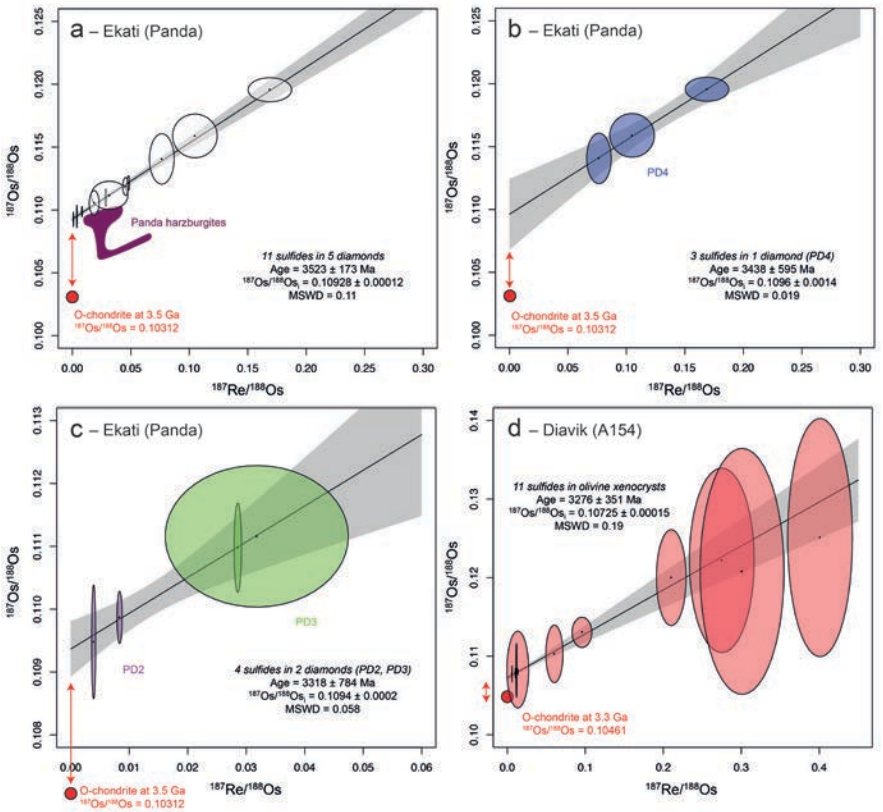


**Figure 15.** Re–Os isochron plots from sulfide inclusions in diamonds and harzburgites from the Ekati mine (Westerlund et al. 2006) and olivine xenocrysts from the Diavik mine (Aulbach et al. 2004). The Ekati and Diavik mines are both in the Lac de Gras area of the Slave craton and appear to contain diamonds of similar age range hosted in Paleoarchean lithospheric mantle. **a)** Eleven sulfides from five diamonds chosen for their co-linearity on the isochron plot. Three of these diamonds each have multiple inclusions which support the eleven-inclusion array as indicating that these diamonds formed at the same time from a fluid that equilibrated isotopically at the time of diamond crystallization. Note that this fluid has an initial $^{187}Os/^{188}Os$ that is significantly enriched relative to a depleted mantle that had evolved with a chondritic $^{187}Re/^{188}Os$. **b, c)** Detail of the three diamonds with sulfide mineral isochrons are shown in these two Re–Os isochron panels. **d)** Sulfides in individual olivine grains from Diavik have a similar age to the diamonds from Ekati, and a similar $^{187}Os/^{188}Os$ to the more scattered harzburgite xenoliths from Ekati (Westerlund et al. 2006). This corroborates the age of the lithospheric mantle in the Lac de Gras region and the enriched initial $^{187}Os/^{188}Os$ of the diamond-forming fluid that percolated through the lithospheric mantle beneath Ekati. These datasets show the importance of being able to obtain mineral isochrons or linear data arrays to bolster the accuracy of initial isotopic compositions.

Occasionally during sample preparation, a sulfide inclusion will break into several pieces leading to a serendipitous variant of the mineral isochron. Richardson et al. (2001) showed that two pieces from a single sulfide plotted on a single mineral isochron giving an age within uncertainty of the 85 Ma kimberlite eruption age. The weighted average of the two grains plotted on the 2.89 ± 0.26 Ga aggregate isochron for the single sulfides from 11 individual diamonds from Kimberley. This kind of mineral isochron is strong evidence that the inclusions remain totally isolated from alteration (and potential Re addition) during kimberlite eruption and throughout the 85 million years since. The exsolution of a monosulfide to an assemblage of sulfide minerals, each of which partitions the parent and daughter isotopes differently, will produce data that fall off isochrons unless the entire assemblage is extracted and analyzed as discussed above. Striving to recover as much of the sulfide inclusion as possible is critical to obtaining accurate ages.

**Multiple diamond ages**

When the supply of diamonds with inclusions is plentiful, a good test of a meaningful age is the adherence of the data to linearity on an isochron plot. This test is widely used in geochronology because it signifies that the individual minerals in igneous rocks or different rocks in an igneous complex were in isotopic equilibrium at the time of closure of the isotopic system. In other words, the diffusion length scale through the melt for equilibration before closure was much larger than the distance between the individual minerals or rocks. When these conditions are met or at least can be evaluated rigorously by the fit to linearity, a true '*isochron*' is obtained. In the case of inclusions, system closure is obtained by encapsulation within diamonds.

For suites of monocrystalline diamonds, the very low occurrence of sulfide and silicate inclusions within run-of-mine production implies that the majority of diamonds were growing apart in the mantle such that the inclusions might not have been in isotopic equilibrium, except through contact with diamond-forming fluids. Thus, data on an isochron diagram are unlikely to meet the true geochronological definition of an isochron or pass tests of rigorous fit to linearity. Instead, the term '*linear data array*' is used, to clearly differentiate data sets with more scatter than true isochrons.

***Composite isochron (linear data array) ages.*** The composite isochron age approach using combined Sm–Nd and Rb–Sr systems was adopted in the early 1990s for dating lherzolitic diamonds from Cullinan (Richardson et al. 1993) and harzburgitic-to-lherzolitic diamonds from Udachnaya (Richardson and Harris 1997). At that time, composites of tens of mostly small inclusions (average weight = 20 μg) were required to obtain enough material for sufficiently precise Nd and Sr isotope analysis by ID-TIMS. In principle, compositing or grouping of cogenetic inclusions with a range in major and trace element concentrations can reduce the spread in Sm/Nd ratio but will not affect the overall isochron relationship, so long as the inclusions are cogenetic and had the same initial isotope ratio. In practice, if non-cogenetic inclusions are composited, important information about multiple diamond-forming events at a single locality may be lost.

The most important feature of lherzolitic diamond suites (i.e., containing calcic Cr-pyrope and Cr-diopside) for dating purposes is the observed spread in Sm/Nd ratio of garnet inclusions which is positively correlated with calcium content and differs from pyroxene; Cr-pyrope acquires the highest and Cr-diopside the lowest Sm/Nd ratios. In the Cullinan study (Richardson et al. 1993), individual inclusions were grouped in different categories based on Ca, Cr, Ti and Na contents measured by electron microprobe on tiny fragments of each inclusion (Richardson et al. 1993), a more precise refinement of the previous selection method by optical properties. The best-defined lherzolitic garnet category had significant Ti and Na contents (up to 0.9% $TiO_2$, 0.2% $Na_2O$) and a distinctive reddish tinge. In rare bimineralic inclusion-bearing diamonds, this variety of garnet can be seen to coexist with bright emerald-green diopside with correspondingly higher Ti, Al, Cr and Na contents than pale emerald-

green diopside that can be paired with more calcic, pale-purple lherzolitic garnets. The best-defined lherzolitic garnet–diopside pair of composites gave a two-point Sm–Nd isochron age of 1.93 ± 0.04 Ga. The other three lherzolitic garnet composites with intermediate Sm–Nd ratios also lie on this isochron within larger analytical errors. However, the garnet and clinopyroxene composites show a significantly large range in initial $^{87}Sr/^{86}Sr$ ratio (0.7037–0.7058). In particular, the garnet composites with lower Sr contents extend to the higher end of this range, suggesting the presence of one or more grains with radiogenic Sr.

This compositional variability is not unexpected given the formation of lherzolitic diamonds in pre-existing continental lithospheric mantle via melt metasomatism of refractory garnet harzburgite laced with radiogenic Sr (Richardson et al. 1984), resulting in small-scale variability in initial isotope ratio for inclusions from different diamonds. The more conservative five-point Sm–Nd isochron age of 1.94 ± 0.10 Ga (Richardson et al. 1993) lies close to a 2.054 Ga U–Pb zircon age for the Merensky Reef of the Bushveld Complex (Scoates and Friedman 2008), suggesting that the Archean harzburgitic continental lithosphere was modified by Bushveld-type magmas (Richardson et al. 1993; Shirey et al. 2002; Richardson and Shirey 2008). Further Sm–Nd and Rb–Sr work on individual inclusions from global lherzolitic diamond localities is clearly warranted.

***Age arrays from single inclusions in multiple diamonds***. It is extremely rare to find multiple large inclusions within a single growth zone in one diamond. For this reason, it is the more usual case to analyze individual inclusions from different diamonds to obtain age constraints. The main requirements for a true isochron in all radiogenic isotope systems (see above), are that the inclusions are cogenetic, that they had identical initial radiogenic isotope ratios, and that the system remained closed and has not been disturbed since isotopic closure.

However, for inclusions in diamonds these conditions are often not precisely met. Observed variability is often greater than can be explained from experimental (analytical) uncertainty alone, especially due to the high analytical precision and sensitivity of modern mass spectrometry compared to older studies. This is usually attributed to the '*geological uncertainty*' that encompasses the natural variability of non-touching mineral grains that actually could have been tens of meters apart in the mantle. The uncertainties associated with these assumptions are discussed above in Section '*Sources of uncertainty when determining diamond ages'*. The resulting isochrons are referred to as '*over-dispersed*', with the variability likely coming from a variation in the initial isotopic ratio, e.g., due to incomplete isotopic re-equilibration (Fig. 2).

A cogenetic relationship for individual inclusions can be evaluated based on the characteristics of the host diamond growth zone—C isotopic compositions, N aggregation characteristics and subtle N abundance variations in growth zones as imaged by cathodoluminescence—or the compositions of the inclusions to be dated. Dating sulfide versus silicate minerals requires different approaches to evaluating that they belong to the same diamond generation event. The studies on Slave craton diamonds by Westerlund et al. (2006) and Siberian diamonds by Wiggers de Vries et al. (2013) are good examples of the latter feature; multiple inclusions in diamonds were extracted and correlated directly with separate episodes of fluid influx and hence diamond growth that could be seen as isotopically distinct or revealing significant differences in age for different zones (see section on 'core to rim analyses' above). '*Linear data arrays*' of $Re/^{188}Os$ versus $^{187}Os/^{188}Os$ have provided valid ages from the world's most significant diamond localities (see worldwide data compilation in Smit et al. 2021). Diamond ages ranging from the Paleoarchean through to the Neoproterozoic and even Mesozoic have been obtained, which mostly correlate to known geological processes (see section '*Geological applications: What diamonds and their ages have revealed* ').

For sulfides, it is critical before isotopic analysis to ascertain the peridotitic ([Ni] typically > ~6 wt%) vs. eclogitic ([Ni] typically < ~6 wt%) paragenesis by a non-destructive analytical technique, such as energy dispersive X-ray microanalysis on polished diamond plates or isolated sulfide grains released from the diamond. Besides being a first-order screen for potential

co-genesis, the paragenesis of the sulfide is critical to estimating the Os content of the sulfide so that an isotopic spike of the right concentration can be used in isotope dilution analyses.

For silicates, $^{147}Sm/^{144}Nd$ versus $^{143}Nd/^{144}Nd$ arrays are made from single garnet and clinopyroxene inclusions that are grouped at least by similar chemical characteristics in the same manner as composite isochron ages. In the study by Timmerman et al. (2017), eclogitic inclusions were additionally grouped by similar diamond host growth structure, nitrogen aggregation state, trace element abundances, and strontium isotope compositions. In the study by Koornneef et al. (2017) different peridotitic diamond populations from Venetia were distinguished by Sm–Nd depleted mantle model ages and subsequently by Ca contents of garnets. The group with model ages of 3.0 ± 0.1 Ga and CaO contents < 2.5 wt% had trace element patterns with higher LREE and lower HREE relative to the group with 1.1 ± 0.2 Ga model ages and CaO > 2.5 wt%. This resulted in two isochron ages (2.95 and 1.15 Ga) similar to the model ages. While some other Venetia garnet inclusions fall onto these isochrons, their model ages and/or different REE patterns do not justify including them. The difference between the mixed Sm–Nd isochron array at 2.30 ± 0.04 Ga of pooled inclusions from Venetia (Richardson et al. 2009) and isochron arrays of 2.95 ± 0.07 and 1.15 ± 0.11 Ga from individual inclusions (Koornneef et al. 2017) showcase the differences that can exist between composited grains and single grains on an isochron or '*linear data array*' (Fig. 16). In the former study, inclusions from diamonds of different ages might get combined; in the latter study, an atypical inclusion in one diamond might control the age obtained. In both cases, best practice dictates the use of other compositional information (e.g., mineral chemistry, Sr isotopic composition, diamond type and C isotopic composition) to regress inclusions from diamonds that have grown in the same episode of fluid infiltration. Of course, the main goal is to be able to resolve these different episodes as distinct outside the age uncertainties of each isochron.

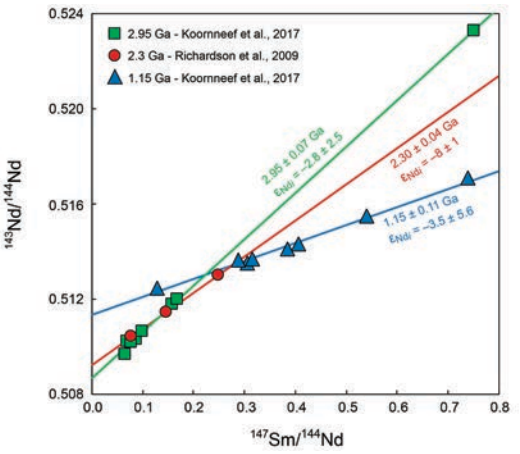


**Figure 16.** Samarium–Nd isochrons for peridotitic diamonds from Venetia (Kaapvaal craton). Garnet inclusions with similar Ca content and REE characteristics, from diamonds with similar $\delta^{13}C$-values, form two distinct '*linear data arrays*' at ~2.95 and 1.15 Ga (Koornneef et al. 2017). Three groups of composite garnet inclusions plot along a ~2.3 Ga '*linear data array*' that is intermediate between arrays obtained from individual inclusions (Richardson et al. 2009). There are additional inclusion data from Venetia that do not fit these two events. See text for further discussion.

## Practical definition for geologically meaningful diamond ages

Our discussion of diamond geochronology so far raises the question of what geological events are being dated with any ages, whether they are '*model ages*', '*single diamond ages*', or '*linear data arrays*'. Diamonds crystallize from carbon- and nitrogen-bearing fluids that pass though peridotites and eclogites. Isotopic closure is obtained when diamond grows and encapsulates the inclusion (see Stachel et al. 2022b, this volume for various diamond formation mechanisms), and essentially stops diffusive exchange between the inclusion and other minerals in the host rock or the fluid. For a '*model age*' from an inclusion in a diamond to represent the time of diamond formation, it should be considered as the time that the inclusion was in equilibrium with

a defined reservoir (such as an estimated mantle composition). It is then assumed that this time is similar to the time of encapsulation in the diamond. For any '*single diamond age*' obtained from multiple inclusions (core-to-rim, mineral isochron) or '*linear data array*' age, we must be dating individual sulfides or silicates that have shared a common geological history.

Since the overall goal of these different types of ages is to determine the time of diamond formation, the geological prehistory of any protogenetic (pre-existing) inclusion is secondary compared to the time of encapsulation by diamond as given by the model age, the core-to-rim age, the mineral isochron age, or the age of the linear data array. Considering the haphazard nature of mantle sampling during a kimberlitic eruption, the chaotic nature of diamond transport in the rising kimberlitic magma, and the distances over which an eruption occurs, it is remarkable that linear age arrays in suites of xenocrystic diamonds exist at all. The final important test is to see if the determined radiometric ages fit into the larger geodynamic history that might indicate when metasomatism and accompanying melts and fluids invaded the continental lithospheric mantle.

Diamond encapsulation shuts down parent–daughter fractionation and diffusive re-equilibration on the mineral inclusion scale—an event that can be dated geochronologically. Geological and experimental studies show that the dynamic nature of the mantle produces the melts/fluids that make diamonds in two basic ways: the dehydration of altered and hydrated slabs when they subduct into the mantle or the generation of melts/fluids during the adiabatic ascent of mantle plumes/upwellings. Often the age of the events that are capable of producing diamond-forming fluids can be determined independently through paleomagnetism studies, plate reconstructions, timing of volcanism, crustal evolution histories, or continental collision events. The alignment of the timing of such events with the ages obtained from diamond geochronology is tacit supporting evidence for the veracity of the diamond ages. Good examples from the Kaapvaal, Siberian, Slave, and West African cratons are given below.

**Indirect evidence for the antiquity of diamonds**

Besides the practical geological tests described above—meaning that the determined ages fit within the larger regional geological framework—there is abundant indirect and non-inclusion evidence that diamonds are indeed as old as the ages given by radiometric age determinations. Consideration of this evidence is useful in light of the generally accepted protogenecity of many inclusions, and previous arguments that diamonds are much younger than the inclusions that they host (e.g., Navon 1999; Spetsius et al. 2002).

***Diamond deposit age***. The first line of evidence is the occurrence of diamonds in volcaniclastic and sedimentary rocks that are known to be Archean and Proterozoic. Note though, that diamonds purportedly found as micro-inclusions in 4.252–3.058 Ga detrital zircon from the Jack Hills metasedimentary belt in Australia (Menneken et al. 2007) have since been identified as laboratory contamination (Dobrzhinetskaya et al. 2014).

The oldest known diamond-bearing sedimentary rocks are the 2.89–2.82 Ga gold-bearing Central Rand sequence of the Witwatersrand basin in South Africa (Wagner 1914; Williams 1932; Raal 1969). Diamond association with typical diamond indicator minerals was suggested to point to a kimberlitic source rock (Helmstaedt et al. 2010 and references therein). A similar association of diamonds and indicator minerals has recently been reported from 2.85 Ga conglomerates from the northern Slave craton (Timmerman et al. 2020). Diamonds in the 2.75 Ga Fortescue Group conglomerates in the Hamersley basin of the Pilbara craton in western Australia were linked to the recycling of diamond detritus into a once continuous basin connecting the Pilbara and Kaapvaal cratons (Helmstaedt et al. 2010).

Archean diamonds also occur in the Michipicoten greenstone belt in the Wawa-Abitibi Terrane of the Superior craton (Canada). Diamonds occur in 2.74–2.68 Ga lamprophyre dikes and metaconglomerates, and carry inclusions compositionally similar to diamonds from the worldwide cratonic lithospheric mantle (Stachel et al. 2006; Helmstaedt et al. 2010; Kopylova et al. 2011; Miller et al. 2012). The continental lithospheric mantle at 2.7 Ga could be shown to

be exceptionally thick (300 km) and refractory based on majorite components in harzburgitic garnet inclusions (Stachel et al. 2006), suggesting formation of a diamondiferous cratonic nucleus prior to 2.7 Ga amalgamation of the Superior craton (Stachel et al. 2006; Kopylova et al. 2011; Miller et al. 2012). Other work on Wawa diamonds showed a high proportion of mixed peridotitic and eclogitic inclusions in a single diamond, tentatively ascribed to mixing of subducted oceanic crust and mantle in a subduction environment (De Stefano et al. 2006). This is in accord with a potential subduction imprint revealed by slightly heavy C-isotopes of octahedral diamonds (Stachel et al. 2006).

In northern Brazil, Venezuela and Guyana, diamonds and gold are mined from the Roraima supergroup 1.95–1.78 Ga, although the diamonds appear to derive from >1.98 Ga conglomerates in the Arai Formation (Meyer and McCallum 1993; Reis et al. 2017; Bassoo et al. 2021). These diamonds have predominantly peridotitic inclusions, with a minor eclogitic population (Bassoo et al. 2021).

The Marange diamonds in eastern Zimbabwe occur in >1.1 Ga conglomerates of the Umkondo Group, and have also been locally deposited into softer Quaternary sediments (Hanson et al. 2004; Moore et al. 2009). The kimberlite source(s) for the diamonds have not been found and the age of the diamonds is unknown. However, from the age of the Umkondo conglomerates the diamonds are at least Proterozoic.

Although the vast majority of kimberlites have Phanerozoic ages, some diamondiferous kimberlites (e.g., 1.2 Ga Premier in South Africa; 1.1 Ga Wajrakarur in India and 1.1 Ga Kyle Lake in Canada; compilation in Kjarsgaard et al. (2022, this volume), and the richly diamondiferous Argyle lamproite in western Australia (Jaques et al. 1990) were emplaced in the Proterozoic, providing incontrovertible evidence for the antiquity of the diamonds contained therein.

***Nitrogen aggregation state***. The level of nitrogen aggregation in the diamond lattice provides an independent indication of the billion-year geological history of most diamonds. Substitution of nitrogen atoms into the diamond lattice, and later diffusion into aggregated nitrogen is described in detail in Green et al. (2022, this volume) to which the reader is directed for background. Diffusion of isolated substitutional nitrogen ($N_S^0$– C centers) and aggregation to 2N (A centers) and $N_4V$ (B centers with a vacancy – V) is dependent on three variables: temperature, time and nitrogen concentration. Concentration of A and B centers can be relatively well constrained using Fourier Transform Infrared (FTIR) spectroscopy. However, without information about the average temperature a diamond experienced over its geological history, nitrogen aggregation state can only be a blunt and imprecise chronometer at best.

For example, constructed isotherms for varying mantle residence times show that 1-billion-year time variation gives less than 50 °C temperature variation, which is smaller than the overall uncertainties for most geothermometers (Nimis 2022, this volume). Similarly, the presence of relatively unaggregated A centers in a diamond cannot be used as evidence for '*young*' diamond growth, since aggregation is much more dependent on temperature. The oldest dated diamonds from Ekati retain relatively unaggregated nitrogen (<30% B centers) over their 3.5 billion-year mantle history, likely due to their residence in a shallower (cooler) part of the Slave continental lithospheric mantle (Westerlund et al. 2006).

Despite these caveats, using the average temperatures for diamond growth obtained from mineral inclusions along with nitrogen aggregation characteristics in the host diamond (Stachel 2014; Nimis 2022, this volume), the billion-year mantle residence history of the majority of lithospheric Type IaAB diamonds is fully supported.

***Retarded isotopic growth of inclusions versus mantle minerals***. Another independent measure of diamond antiquity comes from the general isotopic uniqueness of mineral grains

included in diamonds observed by Richardson et al. (1984) who compared harzburgitic garnet inclusions from diamonds from Finsch ($^{87}Sr/^{86}Sr_i = 0.7037$) and Kimberley ($^{87}Sr/^{86}Sr_i = 0.7062$) with similar concentrate garnets separated from the Finsch ($^{87}Sr/^{86}Sr_i = 0.7073$ to 0.7321) and Bultfontein ($^{87}Sr/^{86}Sr_i = 0.7102$ to 0.7551) kimberlites (Fig. 5). The large difference in initial Sr isotopic composition indicated billions of years of encapsulation of the inclusion minerals in their diamond host compared to unencapsulated garnets of similar composition, especially at the very low measured $^{87}Rb/^{86}Sr$. This difference supported the more precise 3.4–3.3 Ga Sm–Nd model ages obtained on the harzburgitic garnet inclusions (that indicate the minimum age for the western Kaapvaal lithosphere). Pearson and Shirey (1999) summarized the Sr isotopic data for peridotitic and eclogitic garnet inclusion suites from Premier, Udachnaya, Orapa, and Argyle (Richardson 1986; Richardson et al. 1990, 1993, 1998; Richardson and Harris 1997), and noted that long lithospheric mantle residence time of billions of years is implicit in the Sr isotopic data and supports the Sm–Nd isochrons of these studies.

## GEOLOGICAL APPLICATIONS: WHAT DIAMONDS AND THEIR AGES HAVE REVEALED

### Detrital diamond deposits: provenance, glaciation, geomorphology, and plate reconstruction

Prior to the discovery of kimberlites in the Kimberley area of South Africa in 1871, all historical diamonds were recovered from alluvial deposits, most notably occurrences in India (e.g., Krishna River) and Borneo, Kalimantan Province (e.g., Spencer et al. 1988 and references therein). Alluvial diamond deposits are now known from many cratonic regions worldwide (Kjarsgaard et al. 2022, this volume). In some cases, the alluvial diamond deposits can be traced back to primary kimberlite or related rock sources (e.g., Kwango River – Lunda Norte kimberlites, Angola). However, many detrital diamond deposits have no clear relationships to known primary sources. Well documented examples include the deposits along the West Coast of southern Africa, alluvial occurrences across southeast Asia, southeast Australia, the Ural Mountains in Russia, the Krishna River in India, the Yuan region of China, and the Paraná Basin in Brazil (Kjarsgaard et al. 2022, this volume). These so-called '*headless*' placers have generated significant controversy and have spawned a number of '*non-traditional*' explanations for the source(s) of these diamonds. These include primary rock types other than kimberlites/lamproites and alternative diamond formation theories, for example, subduction in eastern Australia and Kalimantan, obduction of ophiolite complexes and meteorite impact (White et al. 2016 and references therein).

Determining the source(s) of detrital diamond deposits is important to exploration for primary diamond occurrences. Detrital sources also provide information on past kimberlite and related rock eruption episodes, erosional histories across source continental terranes, paleo-drainage patterns, glacial movements and the tectonic evolution of affected terranes. Conversely, knowledge of the age of the source kimberlites and/or related rocks provides an important constraint on the provenance of detrital diamonds. The actual host rocks of detrital diamonds provide minimum age constraints on the primary source(s) of contained diamonds. This information is particularly important for older sediments, given the limited number of available primary sources. In some cases, maximum age constraints have been provided by $^{40}Ar/^{39}Ar$ analyses of clinopyroxene inclusions extracted from detrital diamonds.

***Application of the $^{40}Ar/^{39}Ar$ method to provenance studies.*** The $^{40}Ar/^{39}Ar$ method presents an important tool for constraining the provenance of detrital diamond populations because it provides ages on single diamonds with silicate inclusions. While these genesis ages can be complicated by the loss of Ar to the diamond–inclusion interface during diamond residence in the mantle, or accumulation of pre-eruption Ar in lattice defects in the diamond, these ages can be useful when there is only partial Ar loss (Bulanova et al. 2004; Burgess et al. 2004; Phillips et al. 2004; Phillips and Harris 2008).

The basis for interpretation of $^{40}Ar/^{39}Ar$ ages obtained from detrital diamonds stems from a study of Orapa mine diamonds (Phillips and Harris 2008) where it was shown that many $^{40}Ar/^{39}Ar$ ages on clinopyroxene approached the age of the host kimberlite. In this study, eclogitic clinopyroxene inclusions were extracted from 26 diamonds. Of these, 35% (9 of 26) yielded $^{40}Ar/^{39}Ar$ ages within error of the age of the Orapa kimberlite (~90 Ma) (Phillips and Harris 2008). The remaining inclusions gave older apparent ages, up to 436 ± 84 Ma (2σ). Overall, 77% (20 of 36) of inclusion ages were within 50 Ma, and 92% (33 of 36) within 100 million years, of the age of the Orapa eruption event. Therefore, $^{40}Ar/^{39}Ar$ ages obtained from clinopyroxene inclusions represent maximum estimates for the time of source kimberlite eruption, although the youngest ages may approximate the time of kimberlite eruption. In the case of multiple diamond populations, only the youngest detrital population, or populations separated by ~100 million years, may be resolvable. This novel $^{40}Ar/^{39}Ar$ approach has been used to constrain the provenance of detrital diamonds from the West Coast of southern Africa (Namibia; Namaqualand, South Africa), the Urals in Russia, the NW Province alluvial deposits in South Africa and the Copeton alluvial deposit in Australia. Each of these deposits is discussed in turn.

***Revealing southern African paleo-drainage systems.*** Extensive diamond placer deposits are located along the west coasts of Namibia and Namaqualand (South Africa), with >120 million carats of gem-quality diamonds recovered (Oosterveld 2003). Considerable controversy exists as to the provenance of these deposits. The interior of Namibia hosts several kimberlite localities, but none are diamondiferous. The nearest primary diamond-bearing occurrences are located more than 700 km inland, on the Kalahari craton. This cratonic area hosts numerous kimberlites, with emplacement ages ranging from ~1350 Ma to ~80 Ma (Kjarsgaard et al. 2022, this volume). The two main competing theories for the origin of the West coast diamonds involve either: 1) erosion of distal Cretaceous/Jurassic kimberlites and orangeites, and transport of the diamonds to the West Coast via the paleo-Orange River (e.g., de Wit 1993, 1999; Bluck et al. 2005); or 2) recent erosion of Permo-Carboniferous (~300 Ma) glacial deposits (Dwyka Group), with the primary source of the diamonds being pre-Dwyka kimberlites on the Kalahari craton (e.g., Van Wyk and Pienaar 1986; Maree 1987, 1988; Moore and Moore 2004).

Phillips and Harris (2009) conducted $^{40}Ar/^{39}Ar$ step-heating experiments on 50 peridotitic and eclogitic clinopyroxene inclusions from Namibian diamond production. Ages ranged from 62 ± 30 Ma to 1441 ± 700 Ma, with the majority of ages <300 Ma. These data indicate that the majority of West Coast diamonds could not have been sourced from the Dwyka glacial deposits but were sourced from post-Dwyka kimberlites/lamproites. In addition, six inclusions yielded ages unique to Cretaceous (90–80 Ma) kimberlites on the Kalahari Craton. The authors concluded that the Namibian diamonds likely originated from erosion of Cretaceous/Jurassic kimberlites and/or lamproites (previously termed 'orangeites' or 'Group II kimberlites') located on the western part of the Kalahari Craton, with only minor contributions possible from syn-Karoo (e.g., Jwaneng, Botswana) and/or pre-Karoo (e.g., Venetia, National) kimberlites.

$^{40}Ar/^{39}Ar$ analyses of clinopyroxene inclusions extracted from Namaqualand diamonds (West Coast, South Africa) were conducted in two batches, the first using an older generation single-collector mass spectrometer and the latter using a state-of-the-art multi-collector mass spectrometer (Phillips et al. 2018). The two batches yielded similar results, with apparent ages ranging from 118 ± 44 to 3684 ± 191 Ma and 121 ± 15 Ma to 689 ± 5 Ma, respectively. Similar to the Namibia study, the majority of Namaqualand inclusions (88%) gave ages consistent with an origin from post-Dwyka kimberlites/orangeites, with few (if any) diamonds originating from >500 Ma kimberlites. However, in this case, no inclusion ages could be uniquely assigned to Cretaceous age Kalahari Craton kimberlites. Therefore, it was concluded that the Namaqualand diamonds were mainly sourced from older Cretaceous/Jurassic (~200–115 Ma) orangeites (also known as Group II kimberlites) and transported to the West Coast via the paleo-Karoo River (de Wit et al. 1992). In contrast, the Namibian diamonds appear to

have been sourced from both Cretaceous/Jurassic kimberlites (~90–80 Ma) and orangeites (~200–115 Ma) and were transported to the Namibian coast by the paleo-Kalahari River, which captured the paleo-Karoo River and formed a pre-cursor to the modern Orange River.

***New diamond sources in the East European craton***. Alluvial diamond deposits occur along the western margin of the Middle and North Ural Mountains in Russia and are located in Devonian (~400 Ma) sediments of the Takaty Formation (Kukharenko 1955; Bekker et al. 1970). Re–Os analyses of eclogitic sulfide inclusions from several diamonds produced an isochron age of 1280 ± 310 Ma (2σ), interpreted as the age of diamond formation (Laiginhas et al. 2009). $^{40}Ar/^{39}Ar$ analyses of eclogitic clinopyroxene inclusions from five Urals alluvial diamonds produced similar ages averaging 472 ± 28 Ma (2σ). These data constrain the ages of source kimberlites/lamproites to ~500–400 Ma. As there are no known kimberlites/lamproites of this age in the region, Laiginhas et al. (2009) suggested the existence of undiscovered primary sources in the Volga-Uralia terrane of the East European Craton.

***Glacial transport of diamonds in South Africa and Australia.*** Several alluvial diamond deposits occur in the North West Province of South Africa. These include unusual diamond-bearing gravels in the Lichtenburg-Ventersdorp area, which occur within sinuous ridges and in sinkholes above an erosional surface of the ~2.7 Ga Malmani dolomites (de Wit 2016 and references therein). Based on agate populations as well as Cambrian 'mantle' zircon ages of 664–489 Ma, and a $^{40}Ar/^{39}Ar$ clinopyroxene inclusion age of ~ 600 Ma, de Wit (2016) concluded that the diamonds were transported from Cambrian age kimberlites by Dwyka glaciers and deposited in paleo-eskers, to form the sinuous ridges in the area.

The Copeton alluvial diamond occurrence in New South Wales (Australia) is associated with Tertiary gravels underlying Tertiary basalts. The gravels are devoid of kimberlitic indicator minerals and some of the diamonds contain unusual calc-silicate mineral inclusions (Burgess et al. 1998; Davies et al. 2002). This has led to suggestions that the diamonds might be derived from local Tertiary leucitite and/or basaltic volcanism, with the diamonds originally formed in subducted oceanic slabs (Taylor 1990; Sutherland et al. 1994; Barron et al. 1998, 2011). Pearson et al. (1998a) obtained 3.4 and 2.1 Ga model ages from two peridotitic sulfides from Copeton diamonds, suggesting that they were of cratonic origin. Burgess et al. (1998) obtained $^{40}Ar/^{39}Ar$ ages from three clinopyroxene inclusions from two diamonds, all of which yielded similar ages averaging 340 ± 28 Ma. This result was considered to represent the age of the source kimberlite/lamproite. Given the lack of kimberlites/lamproites in the region, the absence of kimberlitic indicator minerals and the well-sorted nature of the diamond population, Burgess et al. (1998) raised the possibility that the Copeton diamonds could have originated from Antarctica, with subsequent northward transportation by Permian age glaciers.

**Diamond ages and craton evolution**

A worldwide association between ancient cratons and diamond occurrences has long been known (e.g., Kennedy 1964; Clifford 1966; Gurney and Switzer 1973; Boyd and Gurney 1986). Typical usage of the term '*craton*' refers to ancient portions of the Earth's crust that have been stable since 2.5 Ga, even though early work recognized the association of diamonds with ancient cratons of at least 1.5 Ga age (Kennedy 1964; Clifford 1966). This strict usage based on age is problematic since many '*cratons'* worldwide actually show significant evidence for later reworking during the Proterozoic and Phanerozoic. Instead of crustal age, an updated definition of 'craton' uses thickness of the stabilizing lithospheric mantle below continental crust, visualized through fast seismic shear wave speeds in global seismic velocity models. In the updated definition, cratons are regions of the Earth's continental crust that are underlain by 150–200 km thick continental lithospheric mantle providing long-term stability since at least 1 Ga (Pearson et al. 2021). Using this updated definition, around 63% of exposed continental crust and 18% of Earth's surface can be considered to be cratonic.

The association of diamonds with cratonic regions, and the intersection of peridotite-derived conductive geotherms with the diamond stability field, led to the suggestion that diamonds reside in the lithospheric mantle beneath cratons (e.g., Sobolev 1977; Boyd et al. 1985; Boyd and Gurney 1986; Haggerty 1986). The first sulfide Pb–Pb ages (Kramers 1979) and the first harzburgitic-garnet-inclusion-based diamond ages proved that diamonds originate in old lithospheric mantle (Richardson et al. 1984).

Diamonds have formed through nearly all of Earth's history (Figs. 17, 18), in distinct episodes that can often be linked to larger-scale tectonic processes (Richardson et al. 2004; Pearson and Wittig 2008; Shirey and Richardson 2011; Howell et al. 2020). Diamonds, and their formation ages, are the ideal time-resolved mantle samples that can provide an overview of continent formation and evolution. A classic example is how the creation, assembly, and modification of the Kaapvaal-Zimbabwe craton is reflected in the age and chemistry of multiple generations of diamonds formed and stored in its lithospheric mantle (Shirey et al. 2002, 2004).

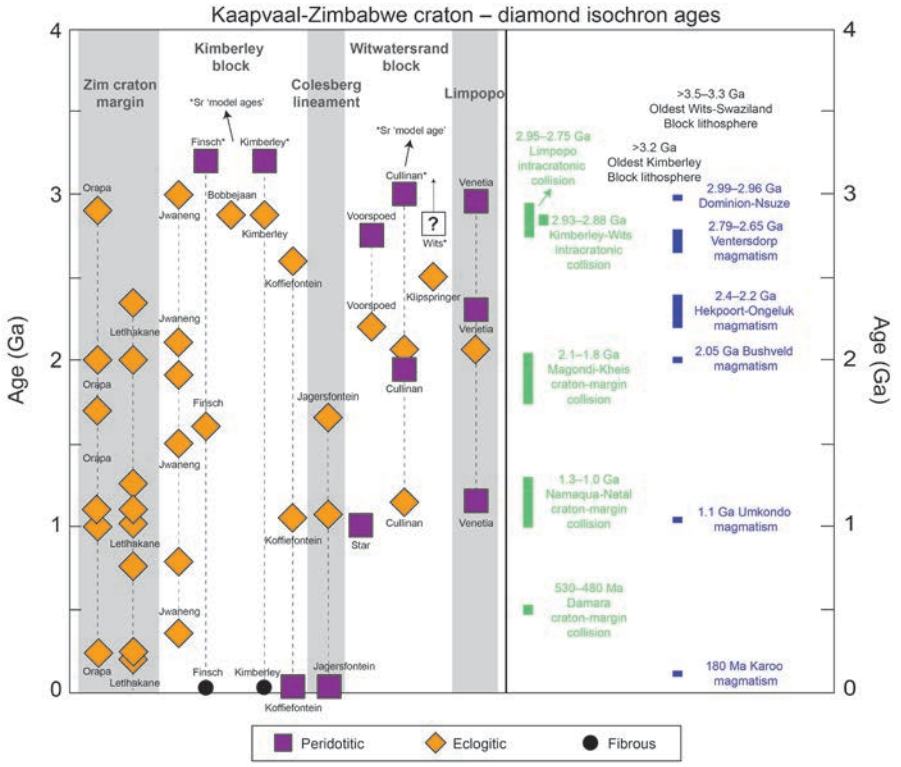


**Figure 17.** Isochron or *'linear data array'* ages for eclogitic and peridotitic diamonds, from the Kaapvaal–Zimbabwe cratons in southern Africa. Many localities have multiple growth events with diamonds forming in both eclogite and peridotite. Archean ages for Finsch, Kimberley and Cullinan diamonds are Sr 'model ages' (see Fig. 5). Diamonds occurring in Archean rocks in the Witwatersrand *'Wits'* Basin are shown as their minimum age (age of their sedimentary host rocks). Diagram updated and modified from Howell et al. (2020). See worldwide data compilation (Smit et al. 2021; https://doi.org/10.7939/DVN/DRAJGT) for an overview of all isochron ages, and their references.

## Formation of the first cratonic blocks, craton assembly and the onset of plate tectonics

Models for the formation of the thick buoyant lithospheric mantle beneath stable cratons range from *horizontal tectonic processes*, such as compressional thickening (Jordan 1978;

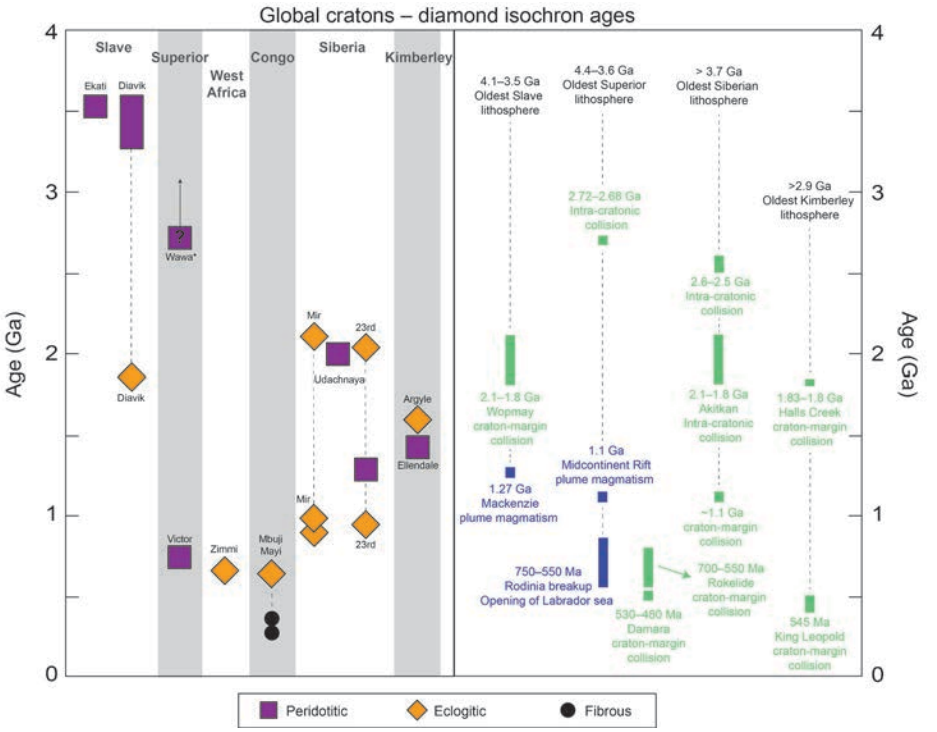


**Figure 18.** All isochron or *'linear data array'* ages for eclogitic and peridotitic diamonds, from global cratons. Diamonds occurring in Archean rocks at Wawa (Superior craton) are shown as the age of their sedimentary host rocks. Updated and modified from Howell et al. (2020). See worldwide data compilation (Smit et al. 2021; https://doi.org/10.7939/DVN/DRAJGT) for an overview of all isochron ages, and their references.

Wang et al. 2018; Pearson et al. 2021) accompanying Wilson cycle continental collision (Shirey and Richardson 2011) or stacking of subducted oceanic lithosphere (Helmstaedt and Schulze 1989; Pearson and Wittig 2008) to *vertical tectonic processes*, such as formation in mantle plumes (e.g., Aulbach 2012), melting at the base of oceanic plateaus (Nair and Chacko 2008; Reimink et al. 2014), or ambient mantle melting below hot ridges (Herzberg and Rudnick 2012). These divergent models have led to debate between proponents of horizontal versus vertical processes in the formation of the earliest continental lithosphere. As the only stabilized relicts of mantle left from the Archean, continental lithospheric mantle and the key minerals it contains (e.g., diamonds) provide important constraints on the geodynamics of the early Earth and the onset of plate tectonics—Earth's present, global, mantle-convection-driven process (Pearson et al. 2021).

The global record for diamond ages shows that prior to 3.0 Ga, only peridotitic diamonds formed, whereas after 3.0 Ga, eclogitic diamonds became prevalent (Figs. 17, 18). From this observation and supercontinent-style rifting of the Kaapvaal and Pilbara cratons at 3.2 Ga (Zegers et al. 1998; see summary in Van Kranendonk and Kirkland 2016), Shirey and Richardson (2011) suggested that the prevalence of eclogitic diamonds after 3.0 Ga resulted from the capture of eclogite and diamond-forming fluids in continental lithospheric mantle via subduction and continental collision, marking the onset of the Wilson cycle of plate tectonics. The absence of >3.2 Ga eclogite xenoliths and eclogitic diamonds from the lithospheric mantle in any craton may suggest that the earliest cratonic nuclei formed by non-Wilson cycle processes. Similarly, the presence of mass-independently fractionated sulfur in sulfide

inclusions from various cratons can be used to assess the role of plate tectonics in craton formation (Smit et al. 2019b). However, the absence of a true Wilson cycle does not rule out the presence of some form of more localized recycling or even shallow plate subduction, and the formation processes behind cratonic nuclei may differ from that responsible for the larger cratonic units extant today (Pearson et al. 2021).

The oldest known diamonds that inform us about the earliest craton formation processes are the 3.5–3.3 Ga Ekati and Diavik diamonds on the Slave craton (Westerlund et al. 2006; Aulbach et al. 2009c, 2011). Sulfide inclusions in diamonds from the Panda kimberlite (Ekati Mine) and their associated harzburgites have elevated initial Os isotopic compositions that are best explained by some form of crustal recycling (Fig. 15; Westerlund et al. 2006). However, the lack of both atmospherically-modified sulfur isotopes in the sulfide inclusions (Cartigny et al. 2009), and non-mantle O-isotopes in garnet peridotites (Regier et al. 2018) suggest that depleted peridotitic lithologies became part of the Slave continental lithosphere in a way that did not involve substantial surface material. This requirement is consistent with models proposed for formation of the earliest shallow Slave continental lithospheric mantle, by crust formation in an oceanic plateau setting (Reimink et al. 2014), or by collisional compression (Regier et al. 2018; Wang et al. 2018), followed by thickening via underplating of plume mantle residues (Griffin et al. 1999), dated to 3.27 ± 0.34 Ga (Aulbach et al. 2004). This plume model and the suggested timing are in excellent agreement with the recently reported 3.19 ± 0.12 Ga age obtained from detrital chromite linked to komatiite magmatism in the Slave craton (Haugaard et al. 2021).

Preservation of ultra-depleted residues juxtaposed with enriched signatures in diamond forming fluids coupled with the absence of trapped and recognizable oceanic lithospheric components (e.g., eclogite, MIF-sulfur) highlights the special mix of geologic conditions that converged to form one of Earth's earliest cratons. It is important to consider, however, that isolated evidence for Paleoarchean recycling processes in the Slave craton does not imply that Earth had already transitioned to sustained global plate tectonics.

Amalgamation of different cratonic nuclei, each with their own lithospheric mantle, into a larger stable cratonic region, a process that may well reflect the inception of the supercontinent cycle (e.g., van Kranendonk and Kirkland 2016) is reflected by diamond ages in the Kaapvaal–Zimbabwe craton. Kimberley, Bobbejaan, Jwaneng and Orapa eclogitic diamonds all record 2.9 Ga ages (Fig. 19) (Pearson et al. 1998b; Shirey et al. unpublished, 2013; Richardson et al. 2001; Richardson et al. 2004). These diamond ages overlap with the timing of subduction-collision along the Colesberg lineament that is recorded in crustal xenoliths (Schmitz et al. 2004), and the occurrence of 2.9 Ga diamondiferous eclogite xenoliths with basaltic to komatiitic compositions (Shirey et al. 2001; Menzies et al. 2003). Along with their enriched initial $^{187}Os/^{188}Os$ and atmospherically-modified sulfur isotopes (Orapa and Jwaneng; Farquhar et al. 2002; Thomassot et al. 2009) these 2.9 Ga eclogitic diamond ages suggest the involvement of enriched recycled components during diamond formation, likely derived from subducted oceanic lithosphere involved in amalgamation of the Kimberley and Witwatersrand blocks of the Kaapvaal craton.

**Craton modification associated with diamond growth**

The continental lithospheric mantle has been recognized as an important carbon reservoir, which, after initial melt extraction imposing highly refractory and reducing conditions, was gradually re-enriched in volatiles and sulfur and re-oxidized through infiltration of fluids and melts from passive upwelling, episodically impinging plumes and subducting slabs (e.g., Foley and Fischer 2017). We now know that lithospheric diamonds form during episodes of fluid infiltration into the lithospheric mantle keel in response to large-scale geotectonic processes (Figs. 17, 18), and studies of lithospheric diamonds are the key means to look at carbon cycling between the crust and mantle over the past 3.5 billion years.

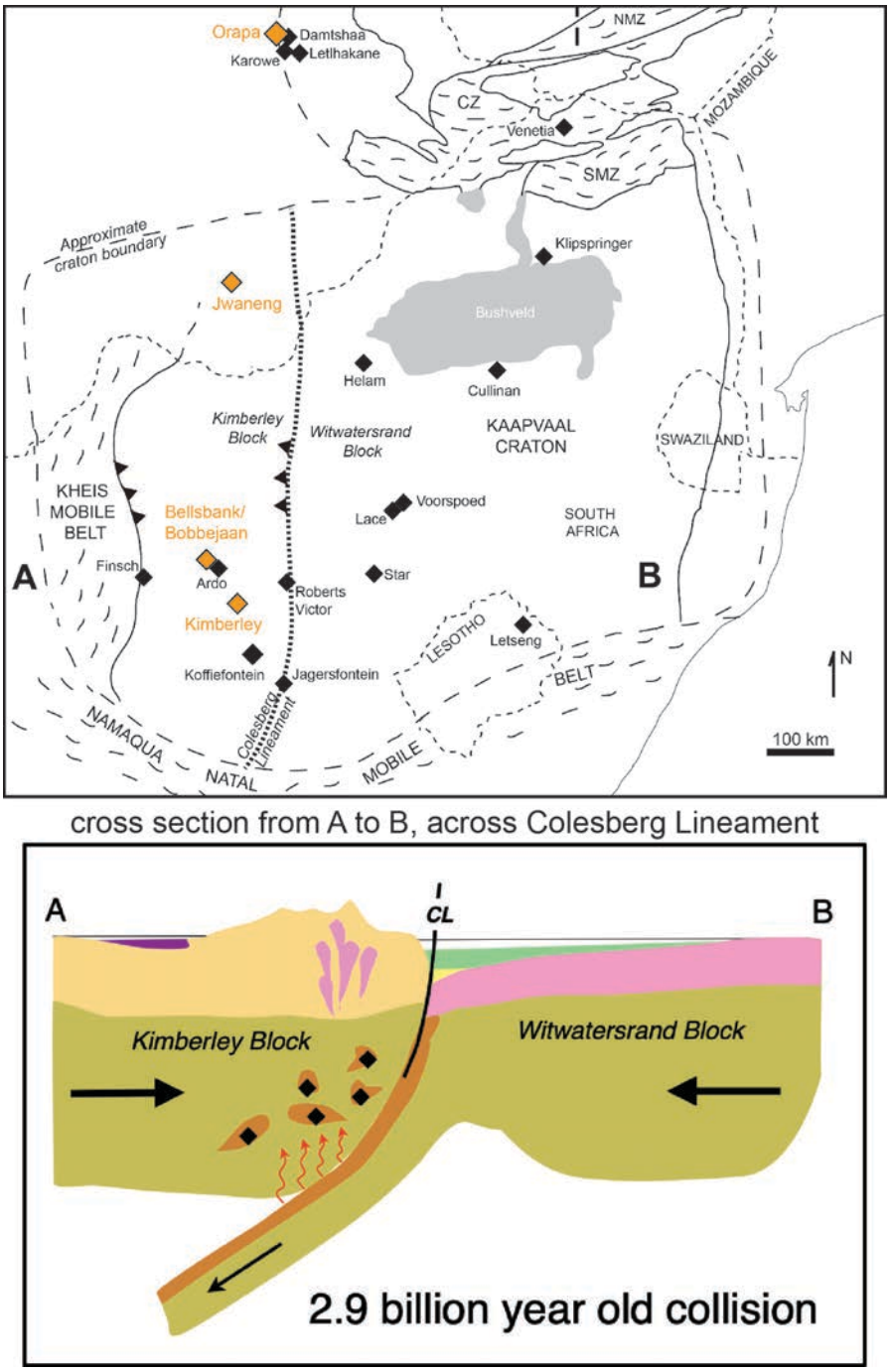


**Figure 19.** Eclogitic diamond formation at Orapa, Jwaneng, Bobbejaan and Kimberley (**orange diamond symbols**) associated with 2.9 Ga subduction and amalgamation of the Kaapvaal craton. Collision schematic from Shirey et al. (2013). See worldwide data compilation (Smit et al. 2021; https://doi.org/10.7939/DVN/DRAJGT) for an overview of all isochron ages, and their references.

***Subduction along craton margins.*** Diamond ages have changed our thinking about the association of diamonds with ancient continental mantle keels. Contrary to traditional thinking (e.g., Clifford 1966), diamond age determinations have shown that diamonds also form during active tectonism in the orogenic belts around cratons. Incorporation of such areas into the spectrum of Earth's lithosphere that has diamond potential has expanded diamond exploration targets and will continue to contribute to finding new economic diamond deposits (Sobolev 1985; Jaques et al. 1990). Eclogitic diamonds have become powerful tracers of supercontinent assembly, and how subduction introduces carbon-bearing fluids to the continental lithospheric mantle, thereby affecting its composition and stability (e.g., Shirey and Richardson 2011).

Perhaps the best example is the Argyle mine in Australia, where '*subduction along the Kimberley craton edge generated the world's biggest diamond deposit*' (Stachel et al. 2018a). Argyle is a famous supplier of pink and red diamonds (Shigley et al. 2001) and known for its exceptionally high diamond grades (Jaques et al. 1990; Rayner et al. 2018). Argyle occurs within the Proterozoic Halls Creek orogen (1.83-1.92 Ga; Hancock and Rutland 1984). The Argyle eclogitic diamonds formed at 1580 ± 30 Ma (Richardson 1986) in "close" temporal association with Halls Creek collisional processes, likely in Archean mantle (Luguet et al. 2009). On the other side of the Kimberley craton, ~20 Ma Ellendale lamproites occur in the King Leopold orogen. The lherzolitic Ellendale diamonds formed at 1426 ± 130 Ma, also in >2.9 Ga Archean mantle (Smit et al. 2010). The presence of Archean mantle below Argyle and likely Ellendale shows that early Proterozoic convergent orogens (Tyler et al. 1999; Griffin et al. 2000) play a key role in diamond formation within the cratonic mantle of the Kimberley craton, which extended beneath these areas.

Even if diamond-bearing kimberlites and lamproites do not erupt through the surface expression of an orogenic belt, there are several worldwide diamond localities that have allowed us to link diamond formation to known subduction processes along craton margins. The Diavik eclogitic diamonds formed at 1.86 ± 0.19 Ga (Aulbach et al. 2009c) coincident with collision and accretion of the Wopmay orogen along the western margin of the Slave craton (Hoffman et al. 1989), an event that is also recorded in eclogite xenoliths (Schmidberger et al. 2007; Aulbach et al. 2009b).

In southern Africa, there are several localities where diamonds formed in temporal or spatial association with the Magondi-Kheis and Namaqua-Natal orogens along the Kaapvaal craton margin. At Jagersfontein, five eclogitic diamonds record formation at 1.65 ± 0.18 Ga associated with the Kheis orogen along the western Kaapvaal craton (Aulbach et al. 2009a). Also at Jagersfontein, a second younger eclogitic population formed at 1070 ± 110 Ma, coincident with the Namaqua-Natal orogen along the southern Kaapvaal margin (Aulbach et al. 2009a). The effect of the Namaqua-Natal event on the continental lithospheric mantle is also evident in the diamonds from Koffiefontein (1048 ± 120 Ma; Pearson et al. 1998b) and Star (1000 ± 33 Ma; see worldwide data compilation in Smit et al. 2021; https://doi.org/10.7939/DVN/DRAJGT).

In West Africa, three eclogitic diamonds from Zimmi in Sierra Leone each yield identical ~650 Ma ages (Smit et al. 2016). Diamond formation is temporally related to subduction along the SW margin of the Man craton, recorded in the Rokelide orogen (700–550 Ma; Lytwyn et al. 2006). In Siberia, lherzolitic and eclogitic diamonds formed in the Paleoproterozoic (Richardson and Harris 1997; Wiggers de Vries et al. 2013) in association with the orogenies that created the 2.1–1.8 Ga Angara and Akitkan orogens (Cherepanova and Artemieva 2015 and references therein). In diamonds sampled by the 23rd Party Congress kimberlite, there are both 1.30 ± 0.29 Ga lherzolitic diamonds and 0.97 ± 0.31 Ga eclogitic diamonds (Wiggers de Vries et al. 2013). These Mesoproterozoic ages may be linked to subduction processes related to the assembly of the Rodinia supercontinent (Gladkochub et al. 2006).

Examples of diamond localities that occur in off-craton (or craton-margin) settings are George Creek, Sloan and other kimberlites in the Colorado-–Wyoming province (Otter 1989; McCallum et al. 1991; Chinn 1995), the Prairie Creek lamproite province in Arkansas (Dunn 2003), and Buffalo Head Hills in Alberta (Banas et al. 2007). However, there are no age constraints on any of these diamonds to determine whether diamond formation occurred due to influx of subduction fluids and melts, or whether they are older diamonds that survived in the mantle through tectonic reworking. Clearly these areas should be the targets of future dating projects.

***'Non-subduction' refertilization.*** Lherzolitic diamond formation is a widespread phenomenon (e.g., Richardson and Harris 1997; Smit et al. 2010; Aulbach et al. 2018) (see also worldwide data compilation in Smit et al. 2021), corresponding to ~12% of peridotitic-inclusion-bearing lithospheric diamonds and dominating the inclusion population at some locations (Stachel et al. 2018b, 2022a, this volume). Refertilization (or lherzolitization) of the initially depleted lithosphere (van Achterbergh et al. 2001; Pearson et al. 2002; Simon et al. 2007) and minor associated diamond growth likely occurred in the presence of small-volume melts, producing garnet inclusions with characteristic, generally mildly sinusoidal REE patterns (Stachel and Luth 2015). Lherzolitic diamond formation has been suggested to represent the deep and early component of the refertilization and re-oxidation of the lithosphere required for successful kimberlite eruption (Aulbach et al. 2018; Shirey et al. 2019). So far, all known lherzolitic diamonds formed during the Proterozoic, though additional dating studies may extend this age range.

Diamonds from the Venetia mine in the Limpopo belt (between the Kaapvaal and Zimbabwe cratons) have a range of ages from Neoarchean to Neoproterozoic. A Sm–Nd isochron array from pooled inclusions yielded a 2.30 ± 0.04 Ga age (Richardson et al. 2009). Isochrons constructed from individual inclusions from different diamonds gave 2.95 ± 0.07 and 1.15 ± 0.11 Ga (Koornneef et al. 2017) (Fig. 16). Richardson et al. (2009) interpreted the 2.3 Ga isochron age as mixing between 2 Ga Bushveld basaltic magmatism with older (>3 Ga) harzburgite. Similarly, diamond formation at 2.95 and 1.15 Ga were also ascribed to metasomatism in the continental lithospheric mantle, where Archean diamonds formed in association with rifting in the southern Zimbabwe craton, and Proterozoic diamonds formed during magmatism associated with the Umkondo large igneous province (Koornneef et al. 2017).

Udachnaya (*Siberia*), Cullinan (*Kaapvaal*), Ellendale (*Kimberley*) and Victor (*Superior*) all have Proterozoic lherzolitic diamonds. Ages for Udachnaya (2.01 ± 0.6 Ga; Richardson and Harris 1997) and Cullinan (1.93 ± 0.04 Ga; Richardson et al. 1993) diamonds were determined from composite silicates, and may represent an average diamond age. In the latter case, however, there is a strong association with Bushveld magmatism at 2.05 Ga (Richardson et al. 1993; Shirey et al. 2002; Richardson and Shirey 2008). Regardless, these localities show that peridotitic diamond formation is not restricted to Archean depleted harzburgite, but that re-enriched lherzolite is also an important economic diamond host, challenging existing paradigms (Stachel et al. 2018b). A Re–Os sulfide isochron shows that Ellendale lherzolitic diamonds formed at 1.43 ± 0.03 Ga, within Archean lithospheric mantle (Smit et al. 2010), however influx of carbon-bearing fluids and/or melts has not yet been correlated with known tectonic or magmatic events in the Kimberley continental lithosphere. The Victor lherzolitic diamonds formed at 719 ± 49 Ma (Aulbach et al. 2018), during rifting and breakup of the Rodinia supercontinent which promoted mobilization of fluids/melts into the Superior continental lithosphere. Trace elements in the Victor diamonds suggest a melt-like character to the diamond-forming fluid (Krebs et al. 2019). The one Koffiefontein diamond that formed at 69 ± 30 Ma in association with proto-kimberlite magmatism is also likely to be lherzolitic (Pearson et al. 1998b).

The Klipspringer diamonds (South Africa) are also a good example of diamond formation due to metasomatic reworking of the continental lithospheric mantle, although they are not lherzolitic. Here, eclogitic diamonds formed at 2.55 ± 0.15 Ga, likely due to partial melting of eclogite in response to Ventersdorp magmatism and heating at 2.7 Ga (Westerlund et al. 2004).

**Sublithospheric diamond ages**

Despite the extensive dating studies of mineral inclusions in lithospheric diamonds, the dating of sublithospheric diamonds is still in its infancy because mineral inclusions with sufficient Sm, Nd, U, Pb, Re, and Os are extremely rare and often small in size. Extant studies are limited as only four Re–Os and Sm–Nd model ages and two U–Pb ages have been obtained. However, as might be expected from geodynamic considerations, ages on sublithospheric diamonds display none of the Archean ages so prevalent in the lithospheric diamond populations—they are all Mesoproterozoic or younger.

A complication is that while lithospheric diamonds have inclusions that can be clearly defined by compositional similarity to major mantle minerals of peridotitic, websteritic, and eclogitic parageneses (Stachel et al. 2022a, this volume), sublithospheric diamonds do not (Walter et al. 2022, this volume). Ultrahigh PT phases such as Ca-silicate perovskite, majorite, bridgmanite, breyite, and ferropericlase-magnesiowustite are stable in the deeper mantle below the continental lithospheric mantle. These phases often revert to lower-pressure assemblages, display intermediate compositions between expected endmembers (e.g., Thomson et al. 2016), and have non-stochiometric solid solutions. Thus, while some inclusions can show a loose affinity to peridotitic or eclogitic precursors, other inclusions cannot be easily classified into the same simple parageneses as lithospheric diamonds (Stachel et al. 2022a, this volume). Sublithospheric phases that are suitable for U–Pb or Sm–Nd dating include breyite ($Ca_3Si_3O_9$ in walstromite structure), $CaTiO_3$, and majoritic garnet. Rare sulfides (Hutchison 1997; Hayman et al. 2005; Kaminsky et al. 2009; Smit and Shirey, unpublished; Bulanova et al. 2010) are also suitable for Re–Os dating. Ferropericlase is not datable with commonly-used radioactive decay systems.

The isotopic dataset for sublithospheric inclusions is currently biased by: 1) the type of inclusions, and 2) the location of the studied inclusions. Sampling biases aside, there is an increasing amount of evidence that the majority of recovered sublithospheric diamonds are associated with subducted material (Shirey et al. 2021; Walter et al. 2022, this volume). This is based on the carbon isotopic compositions of the diamonds themselves and abundant evidence from inclusions, such as mineral assemblage bulk compositions that have slab associations, trace element abundances, Sr, Pb and O isotopic compositions (e.g., Stachel et al. 2005; Pearson et al. 2007; Walter et al. 2008, 2011; Shirey et al. 2013, 2019; Ickert et al. 2015; Burnham et al. 2015; Thomson et al. 2016; Timmerman et al. 2019d).

While no *bona fide* single crystals of lower mantle minerals have been recovered, retrograde assemblages interpreted as lower mantle equivalents coming from both the crust and the mantle portion of the slab do exist (Harte et al. 1999; Stachel et al. 2000; Walter et al. 2011; Smith et al. 2018). There has been only one attempt at dating of inclusions from Letseng (Lesotho—Smith et al. 2017, 2021), and all the other dated inclusions are from the Juina area in Brazil, where the younger diamond ages may be associated with Mesoproterozoic to Phanerozoic subduction. Dating sublithospheric inclusions from other locations, such as Kankan, Monastery, Williamson, Jagersfontein, and DO27, is needed to determine if *'young'* sublithospheric diamond formation is a global phenomenon. Although the lack of older (>3 Ga) sublithospheric diamonds can easily be explained by the current limited dataset, potential geological reasons for the difference between sublithospheric and lithospheric diamond ages are discussed in the section below.

Currently, the most precise age for a sublithospheric inclusion in diamond is a 101 ± 7 Ma U–Pb age from a breyite / $CaTiO_3$-perovskite in the outer portion of a Collier-4 diamond (Bulanova et al. 2010). Although no matrix-matched standards were used during the SIMS analyses, the age of 101 ± 7 Ma seems accurate as it is close to the age of kimberlite eruption. Subsequent analysis on an eclogitic sulfide in the interior of this same Collier-4 diamond by Smit and Shirey (unpublished data) yielded a Neoproterozoic (650 ± 150 Ma) depleted mantle model age. This core–rim age difference leads to contrasting interpretations: either this is a Neoproterozoic diamond in which the U–Pb system in breyite remained open until kimberlite eruption or it is a Cretaceous diamond that incorporated a Neoproterozoic sulfide in the deep convecting mantle in which it grew. The former scenario is roughly consistent with Re–Os data (Hutchison et al. 2012) on a sulfide inclusion in an alluvial diamond also recovered from the Juina area. This eclogitic (based on Re, Os, and Ni content) sulfide produced a Re–Os mantle model age of ~1271 Ma. These two Proterozoic ages are significantly older than the kimberlitic magmatism in the Juina area (94–79 Ma; Davis 1977; Heaman et al. 1998; Kaminsky et al. 2010).

Uranium–Pb ratios from ICP-MS analyses in combination with Pb isotopic compositions give another young age estimate for a Collier-4 sublithospheric diamond (Timmerman et al. 2019d). Using a Stacey and Kramers (1975) Pb growth curve yields an average age of 42 Ma with a maximum of 162 Ma. Using a high common $^{207}Pb/^{206}Pb$ value of 1.17, as common Pb correction, results in a maximum U–Pb age of 660 Ma. While the diamond does contain substantial common Pb, these data provide further evidence for *'young'* sublithospheric diamond formation.

Another age estimate for sublithospheric diamonds that is younger than those from the continental lithospheric mantle comes from the pooled analysis of Sr and Nd isotopic compositions of around 40 majoritic garnet inclusions from Sao Luiz, Brazil (Harte and Richardson 2012). Two groups of pooled inclusions have Sr and Nd isotopic compositions that fall on the oceanic mantle Sr–Nd array between depleted MORB and enriched OIB endmembers. These isotopic compositions clearly retain younger oceanic mantle isotopic signatures—not those of the ancient continental lithospheric mantle. From these isotopic compositions, Harte and Richardson (2012) suggest diamond formation in subducted oceanic crust of Mesozoic age.

Sublithospheric diamonds that retain distinctive metallic inclusions—known as CLIPPIR diamonds (Smith et al. 2016)—present a yet unknown age story, since we only have one age determination to rely on so far (Smith et al. 2017, 2021). CLIPPIR diamonds have been consistently recovered from the Cullinan, Karowe and Letseng mines in southern Africa, where kimberlite eruption occurred at 1153 Ma, 93 Ma and 90 Ma, respectively. Thus, purely from their known occurrences, CLIPPIR diamonds show that diamond formation has been occurring in metallic domains of the sub-lithosphere/asthenosphere since at least the Mesoproterozoic (Smith et al. 2016). The sulfide portion of two metallic inclusions in a Letseng CLIPPIR diamond yielded an unradiogenic $^{187}Os/^{188}Os$ isotope composition of 0.111 that is equivalent to a circa 2.5 Ga old model age. While it is tempting to conclude that this diamond is Archean, Fe isotopic analyses on the metallic iron show that it is derived from the magnetite–awaruite assemblages created by low-temperature serpentinization of ocean-floor peridotite. As the current oceanic lithosphere contains common Proterozoic to even Neoarchean Os isotope signatures that result from prior depletion (e.g., Liu et al. 2008; Harvey et al. 2006; Scott et al. 2019) this old age is interpreted as inherited from the oceanic lithosphere (Smith et al. 2016, 2021).

**Diamond ages and implications for recycling of volatiles into the mantle**

As detailed above, diamond ages have placed important time constraints on the recycling of fluid mobile compounds and elements such as water, carbon, nitrogen, boron, and sulfur into the continental lithospheric mantle especially in relation to the geologic evolution of the continents. For sublithospheric diamonds, the lack of measured ages makes time constraints

on recycling somewhat speculative. But as there is no other way to trace the recycling of these volatiles far back in geologic time without the framework provided by diamond ages, some basic observations can be made.

For lithospheric diamonds, the comparison of their ages to the crustal rock geochronologic record provides evidence of a major change in the style of mantle geodynamics to produce differentiated, stable crust and attendant mantle keel from a vertical mode (e.g., Van Kranendonk 2010; Sizova et al. 2015; Fischer and Gerya 2016; Bédard 2020) to a horizontal mode (e.g., Jordan 1978; Shirey and Richardson 2011; Scott et al. 2019). The *vertical mode* encompasses mantle plume upwelling, thickening of the lithospheric mantle by underplating, vertical crustal tectonics, and internal (autochthonous) igneous crustal differentiation whereas the *horizontal mode* encompasses lateral oceanic lithosphere accretion, horizontal crustal tectonics, advective thickening, and external (allochthonous) igneous crustal differentiation. Looking at all cratons, examples of both modes exist from the Eoarchean to the Mesoarchean (e.g., Van Kranendonk et al. 2007, 2015; Reimink et al. 2019; Bauer et al. 2020; O'Neill et al. 2020). But since the latter mode looks more like modern plate tectonics, these essential questions are currently being vigorously debated: a) whether subduction/horizontal geodynamics became dominant in this time period (e.g., Stern 2018; Brown et al. 2020), b) if so when in this billion-year interval it became dominant (e.g., Van Kranendonk et al. 2007; Bauer et al. 2019; Capitanio et al. 2019; Bauer et al. 2020), and c) did it look like modern plate tectonics?

Using seismicity and specifically seismic tomography to image subduction (Wadati-Benioff) zones into the mantle transition zone and occasionally into the upper part of the lower mantle (e.g., Li et al. 2008), we can relate this style of plate subduction to modern plate tectonics and to the formation of the wide variety of sublithospheric diamonds (Shirey et al. 2021). Thus good, extensive sublithospheric diamond ages would provide one very important constraint on the onset of modern plate tectonics on Earth. As the 1153 Ma Premier kimberlite (Wu et al. 2013) contains CLIPPIR diamonds where metallic inclusions have heavy Fe isotopic compositions linked to serpentinite (Smith et al. 2021), we know that modern-style plate subduction extends at least to the Mesoproterozoic.

Most diamondiferous kimberlites are Mesozoic to Cenozoic, and though some are Paleozoic to even Proterozoic, it is highly unlikely that very old diamondiferous kimberlites are yet to be discovered. Only when we have a significant dataset of sublithospheric diamond ages, whose average age proves to be Mesoarchean to Paleoproterozoic will we be able to confidently extend deep slab subduction back this far. This circumstance rests entirely on the ability of sublithospheric diamonds to survive for more than 2 billion years in the mobile, convecting mantle and to fortuitously find their way to being sampled by erupting kimberlitic magma. These prospects seem geologically unlikely. More likely is the expectation that sublithospheric diamonds are geologically much younger than most lithospheric diamonds and that they and the kimberlites that bring them to the surface are both products of modern-style deep plate tectonics.

## HOW FAR HAVE WE COME AND WHERE SHOULD WE GO?

The last review on diamond dating with radiogenic isotopes by Pearson and Shirey (1999) outlined six main future directions for isotopic dating of diamonds. Below we briefly outline how far these suggestions have been met, along with some recommendations for future work.

### 1) Relationship between silicate and sulfide ages

A major analytical development since the last review is the ability to measure the low Rb–Sr and Sm–Nd content in single silicate inclusions (Timmerman et al. 2017). This development makes it possible to investigate the ages of a wider range of inclusion-bearing diamonds rather than the biased sample set of sulfide-bearing diamonds. Recently,

Gress et al. (2021b) showed that silicate (853 ± 55 Ma) and sulfide (786 ± 250 Ma) isochron ages from a single Letlhakane diamond agree within uncertainty. Further work from worldwide localities is needed to establish whether silicate and sulfide diamond formation always occurs contemporaneously, but unfortunately not all diamond suites contain both sets of inclusions. However, these results clearly validate the approach of using isochrons defined by mineral inclusions to date diamond formation.

**2) Isotopic dating of diamonds and their host rock**

Given that most diamonds are products of metasomatic fluids, ongoing evaluation of any age differences between the host rock and the diamonds is required. While diamond-dating research has strengthened the idea that diamonds form much younger than their host rocks, some studies have shown that older components from the host rock are likely included into the diamond fluid (e.g., Smit et al. 2016, 2019b; Aulbach et al. 2018). However there has not yet been a benchmark study of the age of diamonds and host minerals in the same mantle xenolith. Such a study requires an exceptional specimen: containing diamonds with sufficient inclusions to date, and with host rock minerals that are sufficiently pristine to yield geochronological information.

**3) Ability of the diamond-forming event to affect different isotopic systems**

A key issue remaining in diamond geochronology at the turn of the millennium was whether it was possible that diamond-formation ages could be reflected by protogenetic inclusions, allied with the question of how common protogenetic inclusions were. This concept has been addressed by isotopic studies (e.g., Westerlund et al. 2004; Smit et al. 2016, 2019b; Aulbach et al. 2018), crystallographic studies and Nd diffusion calculations (Nestola et al. 2019) and by Os diffusion calculations (Pamato et al. 2021). Crystallographic studies (Nestola et al. 2017) showed that the lattice orientations of many silicate inclusions were not parallel to the orientation of the diamond, raising the prospect that many inclusions, especially silicates, could be protogenetic. New modeling of diffusion and careful consideration of parent–daughter element isotope fractionation (e.g., Pamato et al. 2021) make convincing arguments that in most cases, the diamond formation event is sufficient to re-set isotope systematics in protogenetic inclusions. While the re-setting is not, in most cases, extensive enough to yield isochrons that pass rigorous statistical thresholds, it is sufficient for the arrays defined on isochron constructs to reflect the timing of diamond formation, for both Sm–Nd and Re–Os systems. More work is required to understand why the Rb–Sr system is generally not amenable to yielding isochron ages. In addition, the powerful $^{176}$Lu–$^{176}$Hf decay system has been under-exploited for constraining diamond formation ages. Increased instrumental sensitivity ought to lead to the exploitation of this decay system to date diamond formation as the parent–daughter element fractionations it displays in garnets are often significantly larger than the Sm–Nd system (e.g., Baxter and Scherer 2013)

**4) Experiments on Ar release from inclusions, meaning of Ar ages, and comparison of Ar ages with other isotopic systems such as U–Th/He**

Work by Phillips and Harris (2008; 2009) and others has demonstrated that argon contained in inclusions within diamonds is mobile under mantle temperature and pressure conditions and diffuses to the diamond/inclusion interface and/or inclusion defect sites over time. Definitive measurements of argon diffusivity parameters in inclusion minerals such as Cr-diopside and pyrope garnet remain outstanding, and therefore the argon closure temperature for these minerals is unknown. The consequence of argon mobility is that diamond formation ages are only attainable by analyzing totally encapsulated inclusions, either by laser drilling/fusion analyses or furnace step-heating/fusion analysis. Extraction or exposure of the inclusions results in partial or complete loss of pre-emplacement radiogenic argon. However, this behavior can be exploited to constrain the provenance of detrital diamonds (e.g., Phillips et al. 2018).

Improvement in trace element measurements recently resulted in U–Th/He isochron and model ages for fibrous diamonds (Timmerman et al. 2019c; Weiss et al. 2021). Based in part on their nitrogen-aggregation characteristics, these fluid-rich diamonds were previously assumed to form in association with proto-kimberlitic fluids/melts. These new U–Th/He ages have shown that this is not always the case, with fibrous diamonds forming up to several 100 m.y. (Timmerman et al. 2019c; Weiss et al. 2021) and possibly 1000 m.y. (2.5 Ga; Weiss et al. 2021) prior to kimberlite eruption. Future studies using U–Th/He isotopes may yield a much wider range of formation ages for fibrous diamonds and allow for improved understanding of any association of diamond-forming fluids with (proto-) kimberlitic melts in the lithosphere. Similarly, by the time of the next diamond-dating review, U–Th/He dating may have allowed us to demonstrate the variable formation ages of fibrous vs. monocrystalline diamonds.

**5) Future diamond inclusion dating studies need to be combined with detailed CL and FTIR studies of the diamonds prior to destruction**

This recommendation has now become routine procedure for diamond dating studies since it is essential to understand the relationship between inclusions and growth zones in each diamond. Similar to completed studies (Wiggers de Vries et al. 2013; Timmerman et al. 2017, 2019a; Smit et al. 2016, 2019a; Gress et al. 2021a,b; Howell et al. 2020), future studies should continue to combine age dating of inclusions with an attempt to determine the *composition of the diamond-forming fluid* to obtain a complete picture of diamond composition through time. This can be achieved through redox modelling of the diamond parental fluid (core-to-rim $\delta^{13}C$–N content profiles), trace element analyses of the diamond, as well as Raman and/or TEM identification of trapped fluid inclusions.

**6) Global studies of diamond ages to determine whether diamond formation can be linked to specific tectonic events and processes**

The advent of both single sulfide Re–Os dating (Pearson et al. 1998b) and single silicate Nd isotope dating (Timmerman et al. 2017) has led to step-wise increases in the number of diamond dating studies; allowing for meaningful reviews of global data, both in Howell et al. (2020) and this review. There are now numerous examples where diamond formation is linked to plate tectonic processes like subduction, collision and rifting.

The antiquity of diamonds and their formation in the continental lithospheric mantle has been established since the first diamond-dating study (Richardson et al. 1984). However, more robust constraints on the age of cool, deep lithospheric keels capable of hosting diamonds—as opposed to young, hot early cratonic nuclei—can be made if sufficient diamonds with suitable inclusions are found from Archean sediments (e.g., Timmerman et al. 2020). A focus of on-going studies is also on locations where continental lithospheric mantle is much younger—such as the predominantly Proterozoic Sask craton (Czas et al. 2020)—to further explore the apparent pulses of Proterozoic peridotitic diamond growth.

From a global perspective, there are currently no diamond ages available from the known deposits in the North Atlantic craton, the Wyoming craton, the Kola-Karelian cratons in the Baltic shield, or the cratons of India and China. Although diamonds from the Juina region are the focus of sublithospheric diamond dating, diamonds from other deposits in Brazil, and other areas in South America (São Francisco craton and Guyana shield) still need diamond-dating studies. These are obvious gaps in the database.

Lastly, new on-going studies are also focusing on establishing the age of sublithospheric diamonds to add geochronological data to the plethora of new information coming from studies of the transition zone and lower mantle (Shirey et al. 2021; Walter et al. 2022, this volume). There is much to look forward to in the next few years of diamond dating!

## ACKNOWLEDGEMENTS

The supplementary tables are available at *https://doi.org/10.7939/DVN/DRAJGT*. Janne Koornneef, Roberta Rudnick, and the editor Thomas Stachel provided constructive comments that helped us clarify the ideas presented in this chapter. S.T. acknowledges funding from the Natural Sciences and Engineering Research Council (NSERC) and the Government of Canada through a Banting post-doctoral fellowship. S.A. thanks the German Research Foundation for their continued support, currently via grant DFG AU356/11.

## REFERENCES

Agrosi G, Nestola F, Tempesta G, Bruno M, Scandale E, Harris J (2016) X-ray topographic study of a diamond from Udachnaya; implications for the genetic nature of inclusions. Lithos 248–251:153–159

Allègre CJ (2008) Isotope Geology. Cambridge University Press

Allègre CJ, Othman DB, Polve M, Richard P (1979) The Nd–Sr isotopic correlation in mantle materials and geodynamic consequences. Phys Earth Planet Sci 19:293–306

Aulbach S (2012) Craton nucleation and formation of thick lithospheric roots. Lithos 149:16–30

Aulbach S, Griffin WL, Pearson NJ, O'Reilly SY, Kivi K, Doyle BJ (2004) Mantle formation and evolution, Slave Craton: constraints from HSE abundances and Re–Os isotope systematics of sulfide inclusions in mantle xenocrysts. Chem Geol 208:61–88

Aulbach S, Shirey SB, Stachel T, Creighton S, Muehlenbachs K, Harris JW (2009a) Diamond formation episodes at the southern margin of the Kaapvaal Craton; Re–Os systematics of sulfide inclusions from the Jagersfontein Mine. Contrib Mineral Petrol 157:525–540

Aulbach S, Creaser RA, Pearson NJ, Simonetti SS, Heaman LM, Griffin WL, Stachel T (2009b) Sulfide and whole rock Re–Os systematics of eclogite and pyroxenite xenoliths from the Slave Craton, Canada. Earth Planet Sci Lett 283:48–58

Aulbach S, Stachel T, Creaser RA, Heaman LM, Shirey SB, Muehlenbachs K, Eichenberg D, Harris JW (2009c) Sulphide survival and diamond genesis during formation and evolution of Archaean subcontinental lithosphere; a comparison between the Slave and Kaapvaal Cratons. Lithos 112:747–757

Aulbach S, Stachel T, Heaman LM, Carlson JA (2011) Microxenoliths from the Slave Craton; archives of diamond formation along fluid conduits. Lithos 126:419–434

Aulbach S, Stachel T, Seitz H-M, Brey GP (2012) Chalcophile and siderophile elements in sulphide inclusions in eclogitic diamonds and metal cycling in a Paleoproterozoic subduction zone. Geochim Cosmochim Acta 93:278–299

Aulbach S, Mungall JE, Pearson DG (2016) Distribution and processing of highly siderophile elements in cratonic mantle lithosphere. Rev Mineral Geochem 81:239–304

Aulbach S, Creaser RA, Stachel T, Heaman LM, Chinn IL, Kong J (2018) Diamond ages from Victor (Superior Craton): Intra-mantle cycling of volatiles (C, N, S) during supercontinent reorganisation. Earth Planet Sci Lett 490:77–87

Aulbach S, Höfer HE, Gerdes A (2019) High-Mg and low-Mg mantle eclogites from Koidu (West African craton) linked by Neoproterozoic ultramafic melt metasomatism of subducted Archaean plateau-like oceanic crust. J Petrol 60:723–754

Banas A, Stachel T, Muehlenbachs K, McCandless TE (2007) Diamonds from the Buffalo Head Hills, Alberta: Formation in a non-conventional setting. Lithos 93:199–213

Barron LM, Lishmund S, Oakes G, Barron B (1998) Primary and related diamond occurrences within a Phanerozoic subduction regime in eastern New South Wales, Australia. International Kimberlite Conference: Extended Abstracts 7:46–48

Barron LM, Mernagh T, Barron B, Pogson R (2011) Spectroscopic research on ultrahigh pressure (UHP) macrodiamond at Copeton and Bingara NSW, Eastern Australia. Spectrochim Acta A 80:112–118

Barth MG, Rudnick RL, Carlson RW, Horn I, McDonough WF (2002) Re–Os and U–Pb geochronological constraints on the eclogite–tonalite connection in the Archean Man Shield, West Africa. Precambrian Res 118:267–283

Bassoo R, Befus KS, Liang P, Forman SL, Sharman G (2021) Deciphering the enigmatic origin of guyana's diamonds. Am Mineral 106:54–68

Bauer A, Reimink JR, Chacko T, Foley BJ, Shirey SB, Pearson G (2019) Zircon Hf isotope evidence for a global transition between stagnant-and mobile-lid tectonics. AGUFM 2019:V31G-0135

Bauer A, Reimink J, Chacko T, Foley B, Shirey S, Pearson D (2020) Hafnium isotopes in zircons document the gradual onset of mobile-lid tectonics. Geochem Perspect Lett 14:1–6, doi: 10.7185/geochemlet.2015

Baxter EF, Scherer EE (2013) Garnet geochronology: timekeeper of tectonometamorphic processes. Elements 9:433–438

Becker H (2000) Re–Os fractionation in eclogites and blueschists and the implications for recycling of oceanic crust into the mantle. Earth Planet Sci Lett 177:287–300

Becker H, Dale CW (2016) Re–Pt–Os isotopic and highly siderophile element behavior in oceanic and continental mantle tectonites. Rev Mineral Geochem 81:369–440

Bédard JH (2020) From the LIPS of a serial killer: Endogenic retardation of biological evolution on unstable stagnant-lid planets. Planet Space Sci 192:105068

Bekker YR, Bekasova NB, Ishkov AD (1970) Diamond-bearing placers in the Devonian rocks of the Northern Urals. Lithol Mineral Resour 4:421–430
Bluck BJ, Ward JD, de Wit MCJ (2005) Diamond mega-placers; Southern Africa and the Kaapvaal Craton in a global context. Geol Soc Spec Publ 248:213–245
Boyd FR, Gurney JJ (1986) Diamonds and the African lithosphere. Science 232:472–477
Boyd FR, Gurney JJ, Richardson SH (1985) Evidence for a 150–200-km thick Archaean lithosphere from diamond inclusion thermobarometry. Nature 315:387–389
Brenan JM, Cherniak DJ, Rose LA (2000) Diffusion of osmium in pyrrhotite and pyrite: implications for closure of the Re–Os isotopic system. Earth Planet Sci Lett 180:399–413
Broadley M, Byrne D, Kopylova MG, Thomassot E, Almayrac M, Marty B (2021) Determining the volatile composition of the ancient mantle through the analysis of Archean aged fibrous diamonds. Goldschmidt abstract, https://doi.org/10.7185/gold2021.7301
Brown M, Johnson T, Gardiner NJ (2020) Plate tectonics and the Archean Earth. Annu Rev Earth Planet Sci 48:291–320
Bulanova GP, Muchemwa E, Pearson DG, Griffin BJ, Kelley SP, Klemme S, Smith CB (2004) Syngenetic inclusions of yimengite in diamond from Sese Kimberlite (Zimbabwe); evidence for metasomatic conditions of growth. Lithos 77:181–192
Bulanova GP, Walter MJ, Smith CB, Kohn SC, Armstrong LS, Blundy J, Gobbo L (2010) Mineral inclusions in sublithospheric diamonds from Collier 4 kimberlite pipe, Juina, Brazil; subducted protoliths, carbonated melts and primary kimberlite magmatism. Contrib Mineral Petrol 160:489–510
Burgess R, Turner G, Harris JW (1992) $^{40}Ar$–$^{39}Ar$ laser probe studies of clinopyroxene inclusions in eclogitic diamonds. Geochim Cosmochim Acta 56:389–402
Burgess R, Turner G, Harris JW (1997) $^{40}Ar$–$^{39}Ar$ laser probe dating of diamonds. *In*: Seventh annual V M Goldschmidt conference. Vol 921. Lunar and Planetary Institute, Houston, TX, United States, p 37–38
Burgess R, Turner G, Laurenzi M, Harris JW (1989) $^{40}Ar$–$^{39}Ar$ laser probe dating of individual clinopyroxene inclusions in Premier eclogitic diamonds. Earth Planet Sci Lett 94:22–28
Burgess R, Kelley SP, Turner G, Harris JW (1994) Diamond formation and eruption ages by laser $^{40}Ar$– $^{39}Ar$ dating of syngenetic inclusions. *In*: Abstracts of the eighth international conference on Geochronology, cosmochronology, and isotope geology. Lanphere MA, Dalrymple GB, Turrin BD, (eds) U S Geological Survey, Reston, VA, USA, p 43
Burgess R, Johnson LH, Mattey DP, Harris JW, Turner G (1998) He, Ar and C isotopes in coated and polycrystalline diamonds. Chem Geol 146:205–217
Burgess R, Kiviets GB, Harris JW (2004) Ar–Ar age determinations of eclogitic clinopyroxene and garnet inclusions in diamonds from the Venetia and Orapa kimberlites. Lithos 77:113–124
Burgess R, Cartigny P, Harrison D, Hobson E, Harris J (2009) Volatile composition of microinclusions in diamonds from the Panda Kimberlite, Canada; implications for chemical and isotopic heterogeneity in the mantle. Geochim Cosmochim Acta 73:1779–1794
Burnham AD, Thomson AR, Bulanova GP, Kohn SC, Smith CB, Walter MJ (2015) Stable isotope evidence for crustal recycling as recorded by superdeep diamonds. Earth Planet Sci Lett 432:374–380
Capitanio F, Nebel O, Cawood P, Weinberg R, Clos F (2019) Lithosphere differentiation in the early Earth controls Archean tectonics. Earth Planet Sci Lett 525:115755
Carlson RW, Shirey SB, Schonbachler M (2008) Applications of PGE radioisotope systems in geo-and cosmochemistry. Elements 4:239–245
Caro G, Bennett VC, Bourdon B, Harrison TM, von Quadt A, Mojzsis SJ, Harris JW (2008) Application of precise $^{142}Nd/^{144}Nd$ analysis of small samples to inclusions in diamonds (Finsch, South Africa) and Hadean zircons (Jack Hills, Western Australia). Chem Geol 247:253–265
Cartigny P, Farquhar J, Thomassot E, Harris JW, Wing B, Masterson A, McKeegan K, Stachel T (2009) A mantle origin for Paleoarchean peridotitic diamonds from the Panda kimberlite, Slave Craton; evidence from $^{13}C$, $^{15}N$ and $^{33,34}S$ stable isotope systematics. Lithos 112:852–864
Cherepanova Y, Artemieva I (2015) Density heterogeneity of the cratonic lithosphere: a case study of the Siberian craton. Gondwana Res 28:1344–1360
Chinn IL (1995) A study of unusual diamonds from the George Creek K1 kimberlite dyke, Colorado. PhD thesis, University of Cape Town, Cape Town, South Africa
Clifford TN (1966) Tectono-metallogenic units and metallogenic provinces of Africa. Earth Planet Sci Lett 1:421–434
Creaser R, Papanastassiou D, Wasserburg G (1991) Negative thermal ion mass spectrometry of osmium, rhenium and iridium. Geochim Cosmochim Acta 55:397–401
Cumming G, Richards J (1975) Ore lead isotope ratios in a continuously changing Earth. Earth Planet Sci Lett 28:155–171
Czas J, Pearson DG, Stachel T, Kjarsgaard BA, Read GH (2020) A Palaeoproterozoic diamond-bearing lithospheric mantle root beneath the Archean Sask Craton, Canada. Lithos 356:105301
Davies RM, O'Reilly SY, Griffin WL (2002) Multiple origins of alluvial diamonds from New South Wales, Australia. Econ Geol Bull Soc Econ Geol 97:109–123
Davies GR, van den Heuvel Q, Matveev S, Drury MR, Chinn IL, Gress MU (2018) A combined cathodoluminescence and electron backscatter diffraction examination of the growth relationships between Jwaneng diamonds and their eclogitic inclusions. Mineral Petrol 112:231–242

Davis GL (1977) The ages and uranium contents of zircons from kimberlites and associated rocks. International Kimberlite Conference: Extended Abstracts 2:67–69
Davis G, Sobolev N, Kharkiv A (1980) New data on the age of Yakutian kimberlites (U–Pb zircon method). Doklady Akademii Nauk SSSR 254:175–179
De Stefano A, Lefebvre N, Kopylova M (2006) Enigmatic diamonds in Archean calc-alkaline lamprophyres of Wawa, southern Ontario, Canada. Contrib Mineral Petrol 151:158–173
de Wit M (1999) Post-Gondwana drainage and the development of diamond placers in western South Africa. Econ Geol 94:721–740
de Wit MCJ (1993) Cainozoic evolution of the drainage systems in the north-western Cape. PhD thesis, Univeristy of Cape Town, Cape Town, South Africa
de Wit MC (2016) Early Permian diamond-bearing proximal eskers in the Lichtenburg/Ventersdorp area of the North West Province, South Africa. S Afr J Geol 119:585–606
de Wit MJ, de Ronde CE, Tredoux M, Roering C, Hart RJ, Armstrong RA, Green RW, Peberdy E, Hart RA (1992) Formation of an Archaean continent. Nature 357:553–562
DePaolo D, Wasserburg G (1979) Sm–Nd age of the Stillwater Complex and the mantle evolution curve for neodymium. Geochim Cosmochim Acta 43:999–1008
Deines P, Harris JW (1995) Sulfide inclusion chemistry and carbon isotopes of African diamonds. Geochim Cosmochim Acta 59:3173–3188
Dobrzhinetskaya L, Wirth R, Green H (2014) Diamonds in Earth's oldest zircons from Jack Hills Conglomerate, Australia, are contamination. Earth Planet Sci Lett 387:212–218
Dodson MH, Compston W, Williams IS, Wilson JF (1988) A search for ancient detrital zircons in Zimbabwean sediments. J Geol Soc London 145:977–983
Doucet LS, Ionov DA, Golovin AV (2015) Paleoproterozoic formation age for the Siberian cratonic mantle: Hf and Nd isotope data on refractory peridotite xenoliths from the Udachnaya kimberlite. Chem Geol 391:42–55
Dunai T, Roselieb K (1996) Sorption and diffusion of helium in garnet: implications for volatile tracing and dating. Earth Planet Sci Lett 139:411–421
Dunn DP (2003) Diamond economics of the Prairie Creek Lamproite, Murfreesboro, AR, USA. Ore Geol Rev 22:251–262
Ebel D, Naldrett A (1997) Crystallization of sulfide liquids and the interpretation of ore composition. Can J Earth Sci 34:352–365
Eldridge CS, Compston W, Williams IS, Harris JW, Bristow JW (1991) Isotope evidence for the involvement of recycled sediments in diamond formation. Nature 353:649–653
Farley KA (2002) (U–Th)/He dating: Techniques, calibrations, and applications. Rev Mineral Geochem 47:819–844
Farquhar J, Wing BA, McKeegan KD, Harris JW, Cartigny P, Thiemens MH (2002) Mass-independent sulfur of inclusions in diamond and sulfur recycling on early Earth. Science 298:2369–2372
Fischer R, Gerya T (2016) Early Earth plume-lid tectonics: A high-resolution 3D numerical modelling approach. J Geodyn 100:198–214
Fleet M, Crocket J, Stone W (1996) Partitioning of platinum-group elements (Os, Ir, Ru, Pt, Pd) and gold between sulfide liquid and basalt melt. Geochim Cosmochim Acta 60:2397–2412
Foley SF, Fischer TP (2017) An essential role for continental rifts and lithosphere in the deep carbon cycle. Nat Geosci 10:897–902
Foley SF, Barth MG, Jenner GA (2000) Rutile/melt partition coefficients for trace elements and an assessment of the influence of rutile on the trace element characteristics of subduction zone magmas. Geochim Cosmochim Acta 64:933–938
Giuliani A, Phillips D, Maas R, Woodhead JD, Kendrick MA, Greig A, Armstrong RA, Chew D, Kamenetsky VS, Fiorentini ML (2014) LIMA U–Pb ages link lithospheric mantle metasomatism to Karoo magmatism beneath the Kimberley region, South Africa. Earth Planet Sci Lett 401:132–147
Gladkochub D, Pisarevsky S, Donskaya T, Natapov L, Mazukabzov A, Stanevich A, Sklyarov E (2006) The Siberian Craton and its evolution in terms of the Rodinia hypothesis. Episodes 29:169–174
Green BL, Collins AT, Breeding CM (2022) Diamond spectroscopy, defect centers, color, and treatments. Rev Mineral Geochem 88:637–688
Gress MU, Koornneef JM, Thomassot E, Chinn I, van Zuilen K, Davies GR (2021a) Sm–Nd isochron ages coupled with CN isotope data of eclogitic diamonds from Jwaneng, Botswana. Geochim Cosmochim Acta 293:1–17
Gress MU, Pearson DG, Chinn IL, Thomassot E, Davies GR (2021b) Mesozoic to Paleoproterozoic diamond growth beneath Botswana recorded by Re–Os ages from individual eclogitic and websteritic inclusions. Lithos 388–389:106058
Gress MU, Timmerman S, Chinn I, Koornneef JM, Thomassot E, van der Valk EAS, van Zuilen K, Bouden N, Davies GR (2021c) Two billion years of episodic and simultaneous websteritic and eclogitic diamond formation beneath the Orapa kimberlite cluster, Botswana. Contrib Mineral Petrol 176:54
Griffin WL, Doyle BJ, Ryan CG, Pearson NJ, O'Reilly SY, Davies R, Kivi K, Van Achterbergh E, Natapov LM (1999) Layered mantle lithosphere in the Lac de Gras area, Slave Craton: Composition, structure and origin. J Petrol 40:705–727
Griffin T, Page R, Sheppard S, Tyler I (2000) Tectonic implications of Palaeoproterozoic post-collisional, high-K felsic igneous rocks from the Kimberley region of northwestern Australia. Precambrian Res 101:1–23

Gurney JJ, Switzer GS (1973) The discovery of garnets closely related to diamonds in the Finsch Pipe, South Africa. Contrib Mineral Petrol 39:103–116
Haggerty SE (1986) Diamond genesis in a multiply-constrained model. Nature 320:34–38
Hamilton MA, Stern R, Pearson DG, Harris JW, Shirey SB (1997) Dating diamond growth: SHRIMP II ion microprobe Pb isotopic analyses of syngenetic sulphide inclusions from Koffiefontein diamonds. GAC-MAC:A62
Hamilton MA, Sobolev NV, Stern RA, Pearson DG (2003) SHRIMP U–Pb dating of a perovskite inclusion in diamond: evidence for a syneruption age for diamond formation, Sytykanskaya kimberlite pipe, Yakutia region, Siberia. International Kimberlite Conference: Extended Abstracts, 8. https://doi.org/10.29173/ikc3245
Hancock S, Rutland R (1984) Tectonics of an early Proterozoic geosuture: the Halls Creek orogenic sub-province, northern Australia. J Geodynamics 1:387–432
Hanson R, Crowley J, Bowring S, Ramezani J, Gose W, Dalziel I, Pancake J, Seidel E, Blenkinsop T, Mukwakwami J (2004) The age of the Umkondo Group, eastern Zimbabwe, and implications for palaeomagnetic correlations. Science 304:1126–1129
Harlow GE (1997) K in clinopyroxene at high pressure and temperature; an experimental study. Am Mineral 82:259–269
Harlow GE, Veblen DR (1991) Potassium in clinopyroxene inclusions from diamonds. Science 251:652–655
Harris JW (1968) The relative orientation of solid mineral inclusions in diamond
Harris JW, Gurney JJ (1979) Inclusions in diamond. *In*: The Properties of Diamond. Field JE (ed) Acad Press, London, UK, p 555–591
Harris JW, Smit KV, Fedortchouk Y, Moore M (2022) Morphology of monocrystalline diamond and its inclusions. Rev Mineral Geochem 88:119–166
Harte B, Richardson S (2012) Mineral inclusions in diamonds track the evolution of a Mesozoic subducted slab beneath west Gondwanaland. Gondwana Res 21:236–245
Harte B, Harris JW, Hutchison MT, Watt GR, Wilding MC (1999) Lower mantle mineral associations in diamonds from Sao Luiz, Brazil. *In*: Mantle Petrology; Field Observations and High-pressure Experimentation; a Tribute to Francis R (Joe) Boyd. Vol 6. Fei Y, Bertka Constance M, Mysen Bjorn O, (eds). Geochemical Society - University of Houston, Department of Chemistry, Houston, TX, United States, p 125–153
Harvey J, Gannoun A, Burton KW, Rogers NW, Alard O, Parkinson IJ (2006) Ancient melt extraction from the oceanic upper mantle revealed by Re Os isotopes in abyssal peridotites from the Mid-Atlantic ridge. Earth Planet Sci Lett 244:606–621
Harvey J, Warren JM, Shirey SB (2016) Mantle sulfides and their role in Re–Os and Pb isotope geochronology. Rev Mineral Geochem 81:579–649
Haugaard R, Wateron P, Ootes L, Pearson DG, Luo Y, Konhauser K (2021) Detrital chromites reveal Slave craton's missing komatiite. Geology 49:1079–1083
Hayman PC, Kopylova MG, Kaminsky FV (2005) Lower mantle diamonds from Rio Soriso (Juina area, Mato Grosso, Brazil). Contrib Mineral Petrol 149:430–445
Heaman L, Teixeira N, Gobbo L, Gaspar J (1998) U–Pb mantle zircon ages for kimberlites from the Juina Paranatinga Provinces, Brazil. International Kimberlite Conference: Extended Abstracts 7:322–324
Helmstaedt HH, Schulze DJ (1989) Evidence for subduction and spreading in the Archean rock record; implications for Archean tectonic style and the evolution of the subcontinental lithosphere. *In*: Workshop on the Archean Mantle. Vol 89–05. Ashwal Lewis D, (ed) Lunar and Planetary Institute, Houston, TX, USA, p 42–44
Helmstaedt HH, Gurney JJ, Richardson SH (2010) Ages of cratonic diamond and lithosphere evolution; constraints on Precambrian tectonics and diamond exploration. Can Mineral 48:1385–1408
Herzberg C, Rudnick R (2012) Formation of cratonic lithosphere: an integrated thermal and petrological model. Lithos 149:4–15
Hoffman PF, Bally A, Palmer A (1989) Precambrian geology and tectonic history of North America. Chapter 16 *In:* The Geology of North America—An Overview,. Geol Soc Am p 447–512
Holwell D, McDonald I, Butler I (2011) Precious metal enrichment in the Platreef, Bushveld Complex, South Africa: evidence from homogenized magmatic sulfide melt inclusions. Contrib Mineral Petrol 161:1011–1026
Honda M, Reynolds JH, Roedder E, Epstein S (1987) Noble gases in diamonds; occurrences of solarlike helium and neon. J Geophys Res B 92; 12:12507–12521
Howell D, Stachel T, Stern R, Pearson D, Nestola F, Hardman M, Harris JW, Jaques A, Shirey S, Cartigny P (2020) Deep carbon through time: Earth's diamond record and its implications for carbon cycling and fluid speciation in the mantle. Geochim Cosmochim Acta 275:99–122
Hutchison M (1997) Constitution of the deep transition zone and lower mantle shown by diamonds and their inclusions. PhD thesis, University of Edinburgh, Edinburgh, United Kingdom
Hutchison MT, Dale CW, Nowell GM, Laiginhas FA, Pearson DG (2012) Age constraints on ultra-deep mantle petrology shown by Juina diamonds. International Kimberlite Conference: Extended Abstracts, 10. https://doi.org/10.29173/ikc3733
Ickert RB, Stachel T, Stern RA, Harris JW (2015) Extreme 18O-enrichment in majorite constrains a crustal origin of transition zone diamonds. Geochem Perspect Lett 1:65–74

Ionov DA, Doucet LS, Carlson RW, Golovin AV, Korsakov RV (2015) Post-Archean formation of the lithospheric mantle in the central Siberian craton: Re–Os and PGE study of peridotite xenoliths from the Udachnaya kimberlite. Geochim Cosmochim Acta 165:466–483

Jacob DE, Mikhail S (2022) Polycrystalline diamonds from kimberlites: Snapshots of rapid and episodic diamond formation in the lithospheric mantle. Rev Mineral Geochem 88:167–190

Jacobsen SB, Wasserburg G (1980) Sm–Nd isotopic evolution of chondrites. Earth Planet Sci Lett 50:139–155

Jaques AL, O'Neill HSC, Smith CB, Moon J, Chappell BW (1990) Diamondiferous peridotite xenoliths from the Argyle (AK1) lamproite pipe, Western Australia. Contrib Mineral Petrol 104:255–276

Jordan TH (1978) Composition and development of the continental tectosphere. Nature 274:544–548

Kaminsky FV, Khachatryan GK, Andreazza P, Araujo DP, Griffin WL (2009) Super-deep diamonds from kimberlites in the Juina area, Mato Grosso State, Brazil. Lithos 112:833–842

Kaminsky FV, Sablukov SM, Belousova EA, Andreazza P, Tremblay M, Griffin WL (2010) Kimberlitic sources of super-deep diamonds in the Juina area, Mato Grosso State, Brazil. Lithos 114:16–29

Katayama I, Karato S-I (2008) Effects of water and iron content on the rheological contrast between garnet and olivine. Phys Earth Planet Inter 166:57–66

Kemppinen LI, Kohn SC, Parkinson IJ, Bulanova GP, Howell D, Smith CB (2018) Identification of molybdenite in diamond-hosted sulphide inclusions: Implications for Re–Os radiometric dating. Earth Planet Sci Lett 495:101–111

Kennedy W (1964) The structural differentiation of Africa in the Pan-African (+/-500 m.y.) tectonic episode. *In:* University of Leeds, Research Institute of African Geology, Annual Report on Scientific Results, p 48–49

Kinny PD, Meyer HOA (1994) Zircon from the mantle; a new way to date old diamonds. J Geol 102:475–481

Kjarsgaard BA, de Wit M, Heaman LM, Pearson DG, Stiefenhofer J, Janusczcak N, Shirey SB (2022) A review of the geology of global diamond mines and deposits. Rev Mineral Geochem 88:1–118

Klein-BenDavid O, Pearson DG, Nowell GM, Ottley C, McNeill JCR, Cartigny P (2010) Mixed fluid sources involved in diamond growth constrained by Sr–Nd–Pb–C–N isotopes and trace elements. Earth Planet Sci Lett 289:123–133

Klein-BenDavid O, Pearson DG, Nowell GM, Ottley C, McNeill JC, Logvinova A, Sobolev NV (2014) The sources and time-integrated evolution of diamond-forming fluids–Trace elements and isotopic evidence. Geochim Cosmochim Acta 125:146–169

Koornneef J, Bouman C, Schwieters J, Davies G (2014) Measurement of small ion beams by thermal ionisation mass spectrometry using new $10^{13}$ Ohm resistors. Analytica Chimica Acta 819:49–55

Koornneef JM, Gress MU, Chinn IL, Jelsma HA, Harris JW, Davies GR (2017) Archaean and Proterozoic diamond growth from contrasting styles of large-scale magmatism. Nat Commun 8:1–8

Kopylova MG, Afanasiev VP, Bruce LF, Thurston PC, Ryder J (2011) Metaconglomerate preserves evidence for kimberlite, diamondiferous root and medium grade terrane of a pre-2.7 Ga Southern Superior protocraton. Earth Planet Sci Lett 312:213–225

Kramers JD (1979) Lead, uranium, strontium, potassium and rubidium in inclusion-bearing diamonds and mantle-derived xenoliths from southern Africa. Earth Planet Sci Lett 42:58–70

Kramers J, Smith C (1983) A feasibility study of U–Pb and Pb–Pb dating of kimberlites using groundmass mineral fractions and whole-rock samples. Chem Geol 41:23–38

Krebs M, Pearson D, Stachel T, Laiginhas F, Woodland S, Chinn I, Kong J (2019) A common parentage-low abundance trace element data of gem diamonds reveals similar fluids to fibrous diamonds. Lithos 324:356–370

Kuiper K, Deino A, Hilgen F, Krijgsman W, Renne P, Wijbrans JR (2008) Synchronizing rock clocks of Earth history. Science 320:500–504

Kukharenko A (1955) Diamonds of the Urals. PhD thesis, Gosgeolizdat, Moscow, Russia

Kurz MD, Gurney JJ, Jenkins WJ, Lott III DE (1987) Helium isotopic variability within single diamonds from the Orapa kimberlite pipe. Earth Planet Sci Lett 86:57–68

Laiginhas FA, Pearson DG, Phillips D, Burgess R, Harris JW (2009) Re–Os and $^{40}Ar/^{39}Ar$ isotope measurements of inclusions in alluvial diamonds from the Ural Mountains; constraints on diamond genesis and eruption ages. Lithos 112:714–723

Lal D (1989) An important source of $^{4}He$ (and $^{3}He$) in diamonds. Earth Planet Sci Lett 96:1–7

Lee J-Y, Marti K, Severinghaus JP, Kawamura K, Yoo H-S, Lee JB, Kim JS (2006) A redetermination of the isotopic abundances of atmospheric Ar. Geochim Cosmochim Acta 70:4507–4512

Lippolt HJ, Leitz M, Wernicke RS, Hagedorn B (1994) (Uranium+ thorium)/helium dating of apatite: experience with samples from different geochemical environments. Chem Geol 112:179–191

Liu C-Z, Snow JE, Hellebrand E, Brügmann G, von der Handt A, Büchl A, Hofmann AW (2008) Ancient, highly heterogeneous mantle beneath Gakkel ridge, Arctic Ocean. Nature 452:311–316

Lorand J (1989) Abundance and distribution of CuFeNi sulfides, sulfur, copper and platinum-group elements in orogenic-type spinel lherzolite massifs of Ariege (Northeastern Pyrenees, France). Earth Planet Sci Lett 93:50–64

Lorand J-P, Grégoire M (2006) Petrogenesis of base metal sulphide assemblages of some peridotites from the Kaapvaal craton (South Africa). Contrib Mineral Petrol 151:521

Lorand J-P, Luguet A (2016) Chalcophile and siderophile elements in mantle rocks: Trace elements controlled by trace minerals. Rev Mineral Geochem 81:441–488

Luguet A, Pearson G (2019) Dating mantle peridotites using Re–Os isotopes: The complex message from whole rocks, base metal sulfides, and platinum group minerals. Am Mineral 104:165–189
Luguet A, Reisberg L (2016) Highly siderophile element and $^{187}Os$ signatures in non-cratonic basalt-hosted peridotite xenoliths: Unravelling the origin and evolution of the post-Archean lithospheric mantle. Rev Mineral Geochem 81:305–367
Luguet A, Jaques AL, Pearson DG, Smith CB, Bulanova GP, Roffey SL, Rayner MJ, Lorand JP (2009) An integrated petrological, geochemical and Re/Os isotope study of peridotite xenoliths from the Argyle lamproite, Western Australia and implications for cratonic diamond occurrences. Lithos 112:1096–1108
Lytwyn J, Burke K, Culver S (2006) The nature and location of the suture zone in the Rokelide orogen, Sierra Leone: Geochemical evidence. J Afr Earth Sci 46:439–454
Maree B (1988) Outeur se antwoord op bespreking. S Afr J Geol 91:421–422
Maree BD (1987) Die afsetting en verspreiding van spoeldiamante in Suid-Afrika Translated Title: The deposition and distribution of alluvial diamonds in South Africa. Verhandelinge van die Geologiese Vereniging van Suid Afrika [Trans Geol Soc S Afr] 90:428–447
Mazzone P, Haggerty S (1986) Corganites and corgaspinites. Two new types of aluminous assemblages from the Jagersfontein kimberlite pipe. International Kimberlite Conference: Extended Abstracts 4:279–281
McCallum ME, Huntley PM, Falk RW, Otter ML (1991) Morphological, resorption and etch feature trends of diamonds from kimberlites within the Colorado-Wyoming state line district, USA International Kimberlite Conference: Extended Abstracts 5:261–263
McDonald I, Hughes HSR, Butler IB, Harris JW, Muir D (2017) Homogenisation of sulphide inclusions within diamonds; a new approach to diamond inclusion geochemistry. Geochim Cosmochim Acta 216:335–357
McDougall I, Harrison TM (1999) Geochronology and Thermochronology by the $^{40}Ar/^{39}Ar$ Method. Oxford University Press
McNeill J, Pearson D, Klein-BenDavid O, Nowell G, Ottley C, Chinn I (2009) Quantitative analysis of trace element concentrations in some gem-quality diamonds. J Phys Condens Matter 21:364207
Meisel T, Horan MF (2016) Analytical methods for the highly siderophile elements. Rev Mineral Geochem 81:89–106
Melton GL, McNeill J, Stachel T, Pearson DG, Harris JW (2012) Trace elements in gem diamond from Akwatia, Ghana and DeBeers Pool, South Africa. Chem Geol 314–317:1–8
Menneken M, Nemchin AA, Geisler T, Pidgeon RT, Wilde SA (2007) Hadean diamonds in zircon from Jack Hills, Western Australia. Nature 448:917–920
Menzies AH, Carlson RW, Shirey SB, Gurney JJ (2003) Re–Os systematics of diamond-bearing eclogites from the Newlands Kimberlite. Lithos 71:323–336
Meyer HOA, McCallum ME (1993) Diamonds and their sources in the Venezuelan portion of the Guyana Shield. Econ Geol Bull Soc Econ Geol 88:989–998
Meyer NA, Wenz MD, Walsh JP, Jacobsen SD, Locock AJ, Harris JW (2019) Goldschmidtite,(K, REE, Sr)(Nb, Cr) $O_3$: A new perovskite supergroup mineral found in diamond from Koffiefontein, South Africa. Am Mineral 104:1345–1350
Miller CE, Kopylova MG, Ryder J (2012) Vanished diamondiferous cratonic root beneath the Southern Superior province: evidence from diamond inclusions in the Wawa metaconglomerate. Contrib Mineral Petrol 164:697–714
Mitchell RS, Giardini AA (1953) Oriented olivine inclusions in diamond. Am Mineral 38:136–138
Mitchell RH, Keays RR (1981) Abundance and distribution of gold, palladium and iridium in some spinel and garnet lherzolites: implications for the nature and origin of precious metal-rich intergranular components in the upper mantle. Geochim Cosmochim Acta 45:2425–2442
Moore A, Cotterill F, Broderick T, Plowes D (2009) Landscape evolution in Zimbabwe from the Permian to present, with implications for kimberlite prospecting. S Afr J Geol 112:65–88
Moore JM, Moore AE (2004) The roles of primary kimberlitic and secondary Dwyka glacial sources in the development of alluvial and marine diamond deposits in Southern Africa. J Afr Earth Sci 38:115–134
Nägler TF, Kramers JD, Kamber BS, Frei R, Prendergast MDA (1997) Growth of sub- continental lithospheric mantle beneath Zimbabwe started at or before 3.8 Ga: Re–Os study on chromites. Geology 25:983–986
Nair R, Chacko T (2008) Role of oceanic plateaus in the initiation of subduction and origin of continental crust. Geology 36:583–586
Navon O (1999) Diamond formation in the Earth's mantle. *In*: Proceedings of the 7th International Kimberlite conference. Vol 2. Gurney John J, Gurney James L, Pascoe Michelle D, Richardson Stephen H, (eds). Red Roof Publishing, Cape Town, p 584–604
Navon O, Hutcheon ID, Rossman GR, Wasserburg GJ (1988) Mantle-derived fluids in diamond micro-inclusions. Nature 335:784–789
Nestola F, Nimis P, Angel RJ, Milani S, Bruno M, Prencipe M, Harris JW (2014) Olivine with diamond-imposed morphology included in diamonds; syngenesis or protogenesis? Int Geol Rev 56:1658–1667
Nestola F, Jung H, Taylor LA (2017) Mineral inclusions in diamonds may be synchronous but not syngenetic. Nat Commun 8:14168
Nestola F, Jacob DE, Pamato MG, Pasqualetto L, Oliveira B, Greene S, Perritt S, Chinn I, Milani S, Kueter N (2019) Protogenetic garnet inclusions and the age of diamonds. Geology 47:431–434

Niespolo EM, Rutte D, Deino AL, Renne PR (2017) Intercalibration and age of the Alder Creek sanidine $^{40}Ar/^{39}Ar$ standard. Quat Geochron 39:205–213

Nimis P (2022) Pressure and temperature data for diamonds. Rev Mineral Geochem 88:533–566

Nimis P, Alvaro M, Nestola F, Angel RJ, Marquardt K, Rustioni G, Harris JW, Marone F (2016) First evidence of hydrous silicic fluid films around solid inclusions in gem quality diamonds. Lithos 260:384–389

O'Neill C, Marchi S, Bottke W, Fu R (2020) The role of impacts on Archaean tectonics. Geology 48:174–178

Oosterveld M (2003) Evaluation of alluvial diamond deposits. *In*: Workshop Alluvial Diamonds in South Africa. Vol 2, p 1–7

Otter ML (1989) Diamonds and their mineral inclusions from the Sloan diatremes of the Colorado-Wyoming State Line kimberlite district, North America. PhD thesis, University of Cape Town, Cape Town, South Africa

Ozima M, Zashu S, Tomura K, Matsuhisa Y (1991) Constraints from noble-gas contents on the origin of carbonado diamonds. Nature 351:472–474

Pamato MG, Novella D, Jacob DE, Oliveira B, Pearson DG, Greene S, Afonso JC, Favero M, Stachel T, Alvaro M, Nestola F (2021) Protogenetic sulfide inclusions in diamonds date the diamond formation event using Re–Os isotopes. Geology 49:941–945

Patten C, Barnes S-J, Mathez EA, Jenner FE (2013) Partition coefficients of chalcophile elements between sulfide and silicate melts and the early crystallization history of sulfide liquid: LA-ICP-MS analysis of MORB sulfide droplets. Chem Geol 358:170–188

Pearson DG (1999) The age of continental roots. Lithos 48:171–194

Pearson DG, Shirey SB (1999) Isotopic dating of diamonds. *In*: Application of radiogenic isotopes to ore deposit research and exploration. Vol 12. Lambert David D, Ruiz J (eds) Soc Econ Geol, Boulder, CO, USA, p 143–171

Pearson DG, Wittig N (2008) Formation of Archaean continental lithosphere and its diamonds; the root of the problem. J Geol Soc London 165:895–914

Pearson DG, Carlson RW, Shirey SB, Boyd FR, Nixon PH (1995) Stabilisation of Archaean lithospheric mantle; a Re–Os isotope study of peridotite xenoliths from the Kaapvaal Craton. Earth Planet Sci Lett 134:341–357

Pearson DG, Davies R, Shirey SB, Carlson RW, Griffin W (1998a) The age and origin of eastern Australian diamonds: Re–Os isotope evidence from sulfide inclusions in two diamonds from Wellington, New South Wales. International Kimberlite Conference: Extended Abstracts 7:664–666

Pearson DG, Shirey SB, Harris JW, Carlson RW (1998b) Sulphide inclusions in diamonds from the Koffiefontein kimberlite, S Africa; constraints on diamond ages and mantle Re–Os systematics. Earth Planet Sci Lett 160:311–326

Pearson DG, Shirey SB, Bulanova GP, Carlson RW, Milledge HJ (1999a) Re–Os isotope measurements of single sulfide inclusions in a Siberian diamond and its nitrogen aggregation systematics. Geochim Cosmochim Acta 63:703–711

Pearson DG, Shirey SB, Bulanova GP, Carlson RW, Milledge HJ (1999b) Dating and paragenetic distinction of diamonds using the Re–Os isotope system; application to some Siberian diamonds. *In*: Proceedings of the 7th International Kimberlite Conference. Vol 2. Gurney John J, Gurney James L, Pascoe Michelle D, Richardson Stephen H, (eds). Red Roof Publishing, Cape Town, p 637–643

Pearson DG, Irvine G, Carlson RW, Kopylova M, Ionov D (2002) The development of lithospheric keels beneath the earliest continents: time constraints using PGE and Re–Os isotope systematics. Geol Soc London Spec Publ 199:65–90

Pearson DG, Harlou R, Hayman P, Cartigny P, Kopylova M (2007) Sr isotopic compositions of ultra-deep inclusions in diamonds; implications for mantle chemical structure and evolution. Geochim Cosmochim Acta 71:A769

Pearson DG, Smith C, Liu J, Mather K, Krebs M, Bulanova G, Kobussen A (2018) Characteristics and origin of the mantle root beneath the Murowa diamond mine: Implications for craton and diamond formation. Chapter 19 *In:* Geoscience and Exploration of the Argyle, Bunder, Diavik and Murowa Diamond Deposit. Davy AT, Smith CB, Helmstaedt H, Jaques AL, Gurney JJ (eds) Spec Publ Soc Econ Geol Vol 20, p 403–424

Pearson DG, Scott JM, Liu J, Schaeffer A, Wang LH, Van Hunen J, Szilas K, Chacko T, Kelemen PB (2021) Deep continental roots and cratons. Nature 592:199–210

Pernet-Fisher JF, Barry PH, Day JM, Pearson DG, Woodland S, Agashev AM, Pokhilenko LN, Pokhilenko NP (2019) Heterogeneous kimberlite metasomatism revealed from a combined Re–Os isotope study of Siberian megacrystalline dunite xenoliths. Geochim Cosmochim Acta 266:220–236

Petts DC, Stachel T, Stern RA, Hunt L, Fomradas G (2016) Multiple carbon and nitrogen sources associated with the parental mantle fluids of fibrous diamonds from Diavik, Canada, revealed by SIMS microanalysis. Contrib Mineral Petrol 171:17

Peucker-Ehrenbrink B, Bach W, Hart SR, Blusztajn JS, Abbruzzese T (2003) Rhenium-osmium isotope systematics and platinum group element concentrations in oceanic crust from DSDP/ODP Sites 504 and 417/418. Geochem Geophys Geosystems 4:8911

Phillips D, Harris JW (2008) Provenance studies from $^{40}Ar/^{39}Ar$ dating of mineral inclusions in diamonds; methodological tests on the Orapa Kimberlite, Botswana. Earth Planet Sci Lett 274:169–178

Phillips D, Harris JW (2009) Diamond provenance studies from $^{40}Ar/^{39}Ar$ dating of clinopyroxene inclusions; an example from the west coast of Namibia. Lithos 112:793–805

Phillips D, Onstott TC, Harris JW (1989) $^{40}Ar/^{39}Ar$ laser-probe dating of diamond inclusions from Premier kimberlite. Nature 340:460–462

Phillips D, Harris JW, Kiviets GB (2004) $^{40}Ar/^{39}Ar$ analyses of clinopyroxene inclusions in African diamonds; implications for source ages of detrital diamonds. Geochim Cosmochim Acta 68:151–165
Phillips D, Matchan E, Honda M, Kuiper K (2017) Astronomical calibration of $^{40}Ar/^{39}Ar$ reference minerals using high-precision, multi-collector (ARGUSVI) mass spectrometry. Geochim Cosmochim Acta 196:351–369
Phillips D, Harris JW, de Wit MC, Matchan EL (2018) Provenance history of detrital diamond deposits, West Coast of Namaqualand, South Africa. Mineral Petrol 112:259–273
Pidgeon RT (1989) Archaean diamond xenocrysts in kimberlites; how definitive is the evidence? *In*: Kimberlites and Related Rocks. Vol 14; 2. Ross J, Jaques AL, Ferguson J, Green DH, Y ORS, Danchin RV, Janse AJA, (eds). Geological Society of Australia, Sydney NSW, Australia, p 1006–1011
Raal FA (1969) A study of some gold mine diamonds. Am Mineral 54:292–296
Rayner MJ, Jaques A, Boxer G, Smith C, Lorenz V, Moss SW, Webb K, Ford D (2018) The geology of the Argyle (AK1) diamond deposit, Western Australia. Chapter 4 *In:* Geoscience and Exploration of the Argyle, Bunder, Diavik and Murowa Diamond Deposit. Davy AT, Smith CB, Helmstaedt H, Jaques AL, Gurney JJ (eds).Spec Publ Soc Econ Geol Vol 20, p 89–117
Regier M, Miškovic A, Ickert RB, Pearson DG, Stachel T, Stern RA, Kopylova M (2018) An oxygen isotope test for the origin of Archean mantle roots. Geochem Perspect Lett 9:6–10
Reimink JR, Chacko T, Stern RA, Heaman LM (2014) Earth's earliest evolved crust generated in an Iceland-like setting. Nat Geosci 7:529–533
Reimink J, Pearson D, Shirey S, Carlson R, Ketchum J (2019) Onset of new, progressive crustal growth in the central Slave craton at 3.55 Ga. Geochem Perspect Lett 10:8–13
Reiners PW, Carlson RW, Renne PR, Cooper KM, Granger DE, McLean NM, Schoene B (2018) Geochronology and Thermochronology. John Wiley and Sons
Reis NJ, Nadeau S, Fraga LM, Betiollo LM, Faraco MTL, Reece J, Lachhman D, Ault R (2017) Stratigraphy of the Roraima Supergroup along the Brazil–Guyana border in the Guiana shield, Northern Amazonian Craton-results of the Brazil-Guyana geology and geodiversity mapping project. Brazilian J Geol 47:43–57
Reisberg L (2021) Osmium isotope constraints on formation and refertilization of the non-cratonic continental mantle lithosphere. Chem Geol 574:120245
Reisberg L, Lorand J-P (1995) Longevity of sub-continental mantle lithosphere from osmium isotope systematics in orogenic peridotite massifs. Nature 376:159–162
Richardson SH (1986) Latter-day origin of diamonds of eclogitic paragenesis. Nature 322:623–626
Richardson SH (1989) As definitive as ever: A Reply to Archean diamond xenocrysts in kimberlites; how definitive is the evidence? by R T Pidgeon. *In*: Kimberlites and Related Rocks. Vol 14; 2. Ross J, Jaques AL, Ferguson J, Green DH, O'Reilly SY, Danchin RV, Janse AJA, (eds). Geol Soc Aust, Sydney NSW, Australia, p 1070–1072
Richardson SH, Shirey SB (2008) Continental mantle signature of Bushveld magmas and coeval diamonds. Nature 453:910–913
Richardson SH, Gurney JJ, Erlank AJ, Harris JW (1984) Origin of diamonds in old enriched mantle. Nature 310:198–202
Richardson SH, Erlank AJ, Harris JW, Hart SR (1990) Eclogitic diamonds of Proterozoic age from Cretaceous kimberlites. Nature 346:54–56
Richardson SH, Harris JW, Gurney JJ (1993) Three generations of diamonds from old continental mantle. Nature 366:256–258
Richardson SH, Harris JW (1997) Antiquity of peridotitic diamonds from the Siberian Craton. Earth Planet Sci Lett 151:271–277
Richardson SH, Chinn IL, Harris JW (1998) Age and origin of eclogitic diamonds from the Jwaneng kimberlite, Botswana. International Kimberlite Conference: Extended Abstracts 7:734–736
Richardson SH, Chinn IL, Harris JW (1999) Age and origin of eclogitic diamonds from the Jwaneng Kimberlite, Botswana. *In*: Proceedings of the 7th International Kimberlite Conference. Vol 2. Gurney John J, Gurney James L, Pascoe Michelle D, Richardson Stephen H, (eds). Red Roof Publishing, Cape Town, p 709–713
Richardson SH, Shirey SB, Harris JW, Carlson RW (2001) Archean subduction recorded by Re–Os isotopes in eclogitic sulfide inclusions in Kimberley diamonds. Earth Planet Sci Lett 191:257–266
Richardson SH, Shirey SB, Harris JW (2004) Episodic diamond genesis at Jwaneng, Botswana, and implications for Kaapvaal Craton evolution. Lithos 77:143–154
Richardson SH, Poeml PF, Shirey SB, Harris JW (2009) Age and origin of peridotitic diamonds from Venetia, Limpopo Belt, Kaapvaal-Zimbabwe Craton. Lithos 112:785–792
Rotenberg E, Davis DW, Amelin Y, Ghosh S, Bergquist BA (2012) Determination of the decay-constant of $^{87}Rb$ by laboratory accumulation of $^{87}Sr$. Geochim Cosmochim Acta 85:41–57
Rudnick RL, Walker RJ (2009) Interpreting ages from Re–Os isotopes in peridotites. Lithos 112:1083–1095
Rudnick RL, Eldridge CS, Bulanova GP (1993) Diamond growth history from in situ measurement of Pb and S isotopic compositions of sulfide inclusions; with Suppl. Data 9305. Geology 21:13–16
Rutherford E (1905) Radio-activity. Cambridge University Press
Saal A, Takazawa E, Frey F, Shimizu N, Hart S (2001) Re–Os isotopes in the Horoman peridotite: evidence for refertilization? J Petrol 42:25–37

Schärer U, Corfu F, Demaiffe D (1997) U–Pb and Lu–Hf isotopes in baddeleyite and zircon megacrysts from the Mbuji-Mayi kimberlite: constraints on the subcontinental mantle. Chem Geol 143:1–16
Schmidberger SS, Simonetti A, Heaman LM, Creaser RA, Whiteford S (2007) Lu–Hf, in-situ Sr and Pb isotope and trace element systematics for mantle eclogites from the Diavik diamond mine; evidence for Paleoproterozoic subduction beneath the Slave Craton, Canada. Earth Planet Sci Lett 254:55–68
Schmitt AK, Zack T, Kooijman E, Logvinova AM, Sobolev NV (2019) U–Pb ages of rare rutile inclusions in diamond indicate entrapment synchronous with kimberlite formation. Lithos 350:105251
Schmitz MD, Bowring SA, de Wit MJ, Gartz V (2004) Subduction and terrane collision stabilize the western Kaapvaal craton tectosphere 2.9 billion years ago. Earth Planet Sci Lett 222:363–376
Schrauder M, Koeberl C, Navon O (1996) Trace element analyses of fluid-bearing diamonds from Jwaneng, Botswana. Geochim Cosmochim Acta 60:4711–4724
Scoates JS, Friedman RM (2008) Precise age of the platiniferous Merensky Reef, Bushveld Complex, South Africa, by the U–Pb zircon chemical abrasion ID-TIMS technique. Econ Geol 103:465–471
Scott J, Liu J, Pearson D, Harris G, Czertowicz T, Woodland S, Riches A, Luth R (2019) Continent stabilisation by lateral accretion of subduction zone-processed depleted mantle residues; insights from Zealandia. Earth Planet Sci Lett 507:175–186
Selby D, Creaser RA, Stein HJ, Markey RJ, Hannah JL (2007) Assessment of the $^{187}$Re decay constant by cross calibration of Re–Os molybdenite and U–Pb zircon chronometers in magmatic ore systems. Geochim Cosmochim Acta 71:1999–2013
Shee SR, Gurney JJ, Robinson DN (1982) Two diamond-bearing peridotite xenoliths from the Finsch Kimberlite, South Africa. Contrib Mineral Petrol 81:79–87
Shelkov DA, Verchovsky AB, Milledge HJ, Pillinger CT (1998) The radial distribution of implanted and trapped $^{4}$He in single diamond crystals and implications for the origin of carbonado. Chem Geol 149:109–116
Shigley JE, Chapman J, Ellison RK (2001) Discovery and mining of the Argyle diamond deposit, Australia. Gems Gemol 37:26–41
Shimizu N, Richardson SH (1987) Trace element abundance patterns of garnet inclusions in peridotite-suite diamonds. Geochim Cosmochim Acta 51:755–758
Shimizu N, Sobolev NV (1995) Young peridotitic diamonds from the Mir kimberlite pipe. Nature 375:394–397
Shimizu N, Pokhilenko NP, Boyd FR, Pearson DG (1997) Geochemical characteristics of mantle xenoliths from the Udachnaya kimberlite pipe. Russ Geol Geophys 38:205–217
Shirey SB, Richardson SH (2011) Start of the Wilson cycle at 3 Ga shown by diamonds from subcontinental mantle. Science 333:434–436
Shirey SB, Walker RJ (1998) The Re–Os isotope system in cosmochemistry and high-temperature geochemistry. Annu Rev Earth Planet Sci 26:423–500
Shirey SB, Harris JW, Carlson RW (1999) Re–Os systematics of sulfide inclusions in diamonds from the Orapa Kimberlite, Botswana; implications for multiple generations of diamond growth. Eos Trans Am Geophys Union 80 suppl 46:1191
Shirey SB, Carlson RW, Richardson SH, Menzies A, Gurney JJ, Pearson DG, Harris JW, Wiechert U (2001) Archean emplacement of eclogitic components into the lithospheric mantle during formation of the Kaapvaal Craton. Geophys Res Lett 28:2509–2512
Shirey SB, Harris JW, Richardson SH, Fouch MJ, James DE, Cartigny P, Deines P, Viljoen F (2002) Diamond genesis, seismic structure, and evolution of the Kaapvaal-Zimbabwe Craton. Science 297:1683–1686
Shirey SB, Richardson SH, Harris JW (2004) Integrated models of diamond formation and craton evolution. Lithos 77:923–944
Shirey SB, Cartigny P, Frost DJ, Keshav S, Nestola F, Nimis P, Pearson DG, Sobolev NV, Walter MJ (2013) Diamonds and the geology of mantle carbon. Rev Mineral Geochem 75:355–421
Shirey SB, Smit KV, Pearson DG, Walter MJ, Aulbach S, Brenker FE, Bureau H, Burnham AD, Cartigny P, Chacko T, Frost DJ, Hauri EH, Jacob DE, Jacobsen SD, Kohn SC, Luth RW, Mikhail S, Navon O, Nestola F, Nimis P, Palot M, Smith EM, Stachel T, Stagno V, Steele A, Stern RA, Thomassot E, Thomson AR, Weiss Y (2019) Diamonds and the mantle geodynamics of carbon: deep mantle carbon evolution from the diamond record. *In*: Deep Carbon: Past to Present. Orcutt BN, Daniel I, Dasgupta R, (eds). Cambridge University Press, Cambridge, p 89–128
Shirey SB, Wagner LS, Walter MJ, Pearson DG, van Keken PE (2021) Slab transport of fluids to deep focus earthquake depths—thermal modeling constraints and evidence from diamonds. AGU Adv 2: e2020AV000304
Simon NSC, Carlson RW, Pearson DG, Davies GR (2007) The origin and evolution of the Kaapvaal cratonic lithospheric mantle. J Petrol 48:589–625
Sizova E, Gerya T, Stüwe K, Brown M (2015) Generation of felsic crust in the Archean: a geodynamic modeling perspective. Precambrian Res 271:198–224
Smit KV, Milne SEM, Richardson SH, Timmerman S, Pearson DG (2021) Radiogenic isotope compositions of inclusions in diamond. https://doi.org/10.7939/DVN/DRAJGT, Scholars Portal Dataverse, V1
Smit KV, Shirey SB, Richardson SH, le Roex AP, Gurney JJ (2010) Re/Os isotopic composition of peridotitic sulphide inclusions in diamonds from Ellendale, Australia; age constraints on Kimberley cratonic lithosphere. Geochim Cosmochim Acta 74:3292–3306

Smit KV, Shirey SB, Wang W (2016) Type Ib diamond formation and preservation in the West African lithospheric mantle; Re/Os age constraints from sulphide inclusions in Zimmi diamonds. Precambrian Res 286:152–166
Smit KV, Stachel T, Luth RW, Stern RA (2019a) Evaluating mechanisms for eclogitic diamond growth: An example from Zimmi Neoproterozoic diamonds (West African craton). Chem Geol 520:21–32
Smit KV, Shirey SB, Hauri EH, Stern RA (2019b) Sulfur isotopes in diamonds reveal differences in continent construction. Science 364:383–385
Smith CB (1983) Pb, Sr and Nd isotopic evidence for sources of southern African Cretaceous kimberlites. Nature 304:51–54
Smith CB, Gurney JJ, Harris JW, Otter ML, Kirkley MB, Jagoutz E (1991) Neodymium and strontium isotope systematics of eclogite and websterite paragenesis inclusions from single diamonds, Finsch and Kimberley Pool, RSA. Geochim Cosmochim Acta 55:2579–2590
Smith CB, Pearson DG, Bulanova GP, Beard AD, Carlson RW, Wittig N, Sims K, Chimuka L, Muchemwa E (2009) Extremely depleted lithospheric mantle and diamonds beneath the southern Zimbabwe Craton. Lithos 112:1120–1132
Smith EM, Kopylova MG, Nowell GM, Pearson DG, Ryder J (2012) Archean mantle fluids preserved in fibrous diamonds from Wawa, Superior craton. Geology 40:1071–1074
Smith EM, Kopylova MG, Frezzotti ML, Afanasiev VP (2014) N-rich fluid inclusions in octahedrally-grown diamond. Earth Planet Sci Lett 393:39–48
Smith EM, Shirey SB, Nestola F, Bullock ES, Wang J, Richardson SH, Wang W (2016) Large gem diamonds from metallic liquid in Earth's deep mantle. Science 354:1403–1405
Smith EM, Richardson SH, Shirey SB, Wang W (2017) Old unradiogenic Os in deep mantle metallic liquid from large gem IIa diamonds. International Kimberlite Conference: Extended Abstracts, 11. https://doi.org/10.29173/ikc3990
Smith EM, Shirey SB, Richardson SH, Nestola F, Bullock ES, Wang J, Wang W (2018) Blue boron-bearing diamonds from Earth's lower mantle. Nature 560:84–87
Smith EM, Ni P, Shirey SB, Richardson S, Wang W, Shahar A (2021) Heavy iron in large gem diamonds traces deep subduction of serpentinized ocean floor. Sci Adv 7:eabe9773
Smith EM, Krebs MY, Genzel P-T, Brenker FE (2022) Raman identification of inclusions in diamond. Rev Mineral Geochem 88:451–474
Sobolev NV (1977). Deep-seated Inclusions in Kimberlites and the Problem of the Composition of the Upper Mantle. (Translated from the Russian edition 1974). AGU, Washington, 279 pp
Sobolev NV (1985) Ultramafic and eclogitic types of paragenesis of diamonds. Conference extended abstract: Native elements formation in endogenic processes, Acad Sci USSR, Siberian Division, Yakutsk (not paginated)
Spencer LK, Dikinis SD, Keller PC, Kane RE (1988) The diamond deposits of Kalimantan, Borneo. Gems Gemol 24:67–80
Spetsius ZV, Belousova E, Griffin WL, O'Reilly SY, Pearson N (2002) Archean sulfide inclusions in Paleozoic zircon megacrysts from the Mir kimberlite, Yakutia: implications for the dating of diamonds. Earth Planet Sci Lett 199:111–126
Stacey Jt, Kramers J (1975) Approximation of terrestrial lead isotope evolution by a two-stage model. Earth Planet Sci Lett 26:207–221
Stachel T (2014) Diamond. Geology of Gem Deposits. Groat LA (ed) Mineral Assoc Canada, Short Course Ser 44:1–28
Stachel T, Harris JW (2008) The origin of cratonic diamonds; constraints from mineral inclusions. Ore Geol Rev 34:5–32
Stachel T, Luth RW (2015) Diamond formation; where, when and how? Lithos 220–223:200–220
Stachel T, Viljoen KS, Brey G, Harris JW (1998) Metasomatic processes in lherzolitic and harzburgitic domains of diamondiferous lithospheric mantle; REE in garnets from xenoliths and inclusions in diamonds. Earth Planet Sci Lett 159:1–12
Stachel T, Harris JW, Brey GP, Joswig W (2000) Kankan diamonds (Guinea) II: lower mantle inclusion parageneses. Contrib Mineral Petrol 140 :16–27
Stachel T, Brey GP, Harris JW (2005) Inclusions in sublithospheric diamonds; glimpses of deep earth. Elements 1:73–87
Stachel T, Harris J, Hunt L, Muehlenbachs K, Kobussen A, EIMF (2018a) Argyle diamonds-how subduction along the Kimberley craton edge generated the world's biggest diamond deposit. Chapter 6 *In:* Geoscience and Exploration of the Argyle, Bunder, Diavik and Murowa Diamond Deposit. Davy AT, Smith CB, Helmstaedt H, Jaques AL, Gurney JJ (eds).Spec Publ Soc Econ Geol Vol 20, p 145–167
Stachel T, Banas A, Aulbach S, Smit KV, Wescott P, Chinn IL, Kong J (2018b) The Victor Mine (Superior Craton, Canada): Neoproterozoic lherzolitic diamonds from a thermally-modified cratonic root. Mineral Petrol 112:325–336
Stachel T, Aulbach S, Harris JW (2022a) Mineral inclusions in lithospheric diamonds. Rev Mineral Geochem 88:307–392
Stachel T, Cartigny P, Chacko T, Pearson DG (2022b) Carbon and nitrogen in mantle-derived diamonds. Rev Mineral Geochem 88:809–876
Stachel T, Banas A, Muehlenbachs K, Kurszlaukis S, Walker EC (2006) Archean diamonds from Wawa (Canada); samples from deep cratonic roots predating cratonization of the Superior Province. Contrib Mineral Petrol 151:737–750
Steiger RH, Jäger E (1977) Subcommission on geochronology: convention on the use of decay constants in geo-and cosmochronology. Earth Planet Sci Lett 36:359–362
Stern RJ (2018) The evolution of plate tectonics. Philos Trans R Soc A 376:20170406
Strutt RJ (1905) On the radio-active minerals. Proc R Soc London Ser A 76:88–101

Sutherland FL, Raynor LR, Pogson RE (1994) Spinel to garnet lherzolite transition in relation to high temperature palaeogeotherms, eastern Australia. Aust J Earth Sci 41:205–220

Taylor WR (1990) A reappraisal of the nature of fluids included by diamond; a window to deep-seated mantle fluids and redox conditions. *In*: Proceedings of the Conference on Stable Isotopes and Fluid Processes in Mineralization. Vol 23. Herbert Hugh K, Ho Susan E, (eds). University of Western Australia, Geology Department and Extension Service. Perth, West, Aust., Australia, p 333–349

Taylor WR, Bulanova G, Milledge HJ (1995) Quantitative nitrogen aggregation study of some Yakutian diamonds; constraints on the growth, thermal, and deformation history of peridotitic and eclogitic diamonds. International Kimberlite Conference: Extended Abstracts 6:608–610

Taylor LA, Anand M, Promprated P, Floss C, Sobolev NV (2003) The significance of mineral inclusions in large diamonds from Yakutia, Russia. Am Mineral 88:912–920

Thomassot E, Cartigny P, Harris JW, Lorand JP, Rollion-Bard C, Chaussidon M (2009) Metasomatic diamond growth; a multi-isotope study ($^{13}C$, $^{15}N$, $^{33}S$, $^{34}S$) of sulphide inclusions and their host diamonds from Jwaneng (Botswana). Earth Planet Sci Lett 282:79–90

Thomson AR, Kohn SC, Bulanova GP, Smith CB, Araujo DP, Walter MJ, Shirey SB (2016) Trace element composition of silicate inclusions in sub-lithospheric diamonds from the Juina-5 kimberlite; evidence for diamond growth from slab melts. Lithos 265:108–124

Timmerman S (2018) Diamonds-Time capsules of volatiles and the key to dynamic Earth evolution. PhD thesis, Australian National University, Canberra, Australia

Timmerman S, Koornneef JM, Chinn IL, Davies GR (2017) Dated eclogitic diamond growth zones reveal variable recycling of crustal carbon through time. Earth Planet Sci Lett 463:178–188

Timmerman S, Krebs MY, Pearson DG, Honda M (2019a) Diamond-forming media through time–Trace element and noble gas systematics of diamonds formed over 3 billion years of Earth's history. Geochim Cosmochim Acta 257:266–283

Timmerman S, Honda M, Zhang X, Jaques A, Bulanova G, Smith C, Burnham A (2019b) Contrasting noble gas compositions of peridotitic and eclogitic monocrystalline diamonds from the Argyle lamproite, Western Australia. Lithos 344:193–206

Timmerman S, Yeow H, Honda M, Howell D, Jaques AL, Krebs MY, Woodland S, Pearson DG, Ávila JN, Ireland TR (2019c) U–Th/He systematics of fluid-rich 'fibrous' diamonds–Evidence for pre-and syn-kimberlite eruption ages. Chem Geol 515:22–36

Timmerman S, Honda M, Burnham A, Amelin Y, Woodland S, Pearson DG, Jaques A, Le Losq C, Bennett V, Bulanova G (2019d) Primordial and recycled helium isotope signatures in the mantle transition zone. Science 365:692–694

Timmerman S, Pearson G, Nestola F, Banas A, Stachel T, Stern RA, Reimink JR, Vezinet A, Ielpi A, Mircea C (2020) Diamond-bearing metasediments point to thick, cool lithospheric root established by the Mesoarchean beneath parts of the Slave Craton (Canada). AGUFM:DI020-0002

Tirone M, Ganguly J, Dohmen R, Langenhorst F, Hervig R, Becker H-W (2005) Rare earth diffusion kinetics in garnet: experimental studies and applications. Geochim Cosmochim Acta 69:2385–2398

Tyler I, Page R, Griffin T (1999) Depositional age and provenance of the Marboo Formation from SHRIMP U–Pb zircon geochronology: implications for the early Palaeoproterozoic tectonic evolution of the Kimberley region, Western Australia. Precambrian Res 95:225–243

van Achterbergh E, Griffin WL, Stiefenhofer J (2001) Metasomatism in mantle xenoliths from the Letlhakane kimberlites: estimation of element fluxes. Contrib Mineral Petrol 141:397–414

van Acken D, Becker H, Hammerschmidt K, Walker RJ, Wombacher F (2010) Highly siderophile elements and Sr–Nd isotopes in refertilized mantle peridotites—a case study from the Totalp ultramafic body, Swiss Alps. Chem Geol 276:257–268

Van Kranendonk MJ (2010) Two types of Archean continental crust: Plume and plate tectonics on early Earth. Am J Sci 310:1187–1209

Van Kranendonk MJ, Kirkland CL (2016) Conditioned duality of the Earth system: Geochemical tracing of the supercontinent cycle through Earth's history. Earth Sci Rev 160:171–187

Van Kranendonk MJ, Smithies RH, Hickman AH, Champion D (2007) secular tectonic evolution of Archean continental crust: interplay between horizontal and vertical processes in the formation of the Pilbara Craton, Australia. Terra Nova 19:1–38

Van Kranendonk MJ, Smithies RH, Griffin WL, Huston DL, Hickman AH, Champion DC, Anhaeusser CR, Pirajno F (2015) Making it thick: a volcanic plateau origin of Palaeoarchean continental lithosphere of the Pilbara and Kaapvaal cratons. Geol Soc London Spec Publ 389:83–111

Van Orman JA, Grove TL, Shimizu N, Layne GD (2002) Rare earth element diffusion in a natural pyrope single crystal at 2.8 GPa. Contrib Mineral Petrol 142:416–424

Van Wyk JP, Pienaar LF (1986) Diamondiferous gravels of the Lower Orange River, Namaqualand. *In*: Mineral deposits of Southern Africa. Anhaeusser CR, Maske S, (eds). Geol Soc S Afr, Johannesburg, South Africa, p 2309–2321

Vermeesch P (2010) HelioPlot, and the treatment of overdispersed (U–Th–Sm)/He data. Chem Geol 271:108–111

Vermeesch P (2018) IsoplotR: A free and open toolbox for geochronology. Geosci Front 9:1479–1493

Viljoen KS, Smith CB, Sharp ZD (1996) Stable and radiogenic isotope study of eclogite xenoliths from the Orapa kimberlite, Botswana. Chem Geol 131:235–255

Viljoen KS, Harris JW, Ivanic T, Richardson SH, Gray K (2014) Trace element chemistry of peridotitic garnets in diamonds from the Premier (Cullinan) and Finsch kimberlites, South Africa; contrasting styles of mantle metasomatism. Lithos 208–209:1–15
Völkening J, Walczyk T, Heumann KG (1991) Osmium isotope ratio determinations by negative thermal ionization mass spectrometry. Int J Mass Spectrom Ion Processes 105:147–159
Wagner PA (1914) The Diamond Fields of Southern Africa. Johannesburg: The Transvaal Leader; London: The Technical Book-Shop
Walker R, Carlson R, Shirey S, Boyd F (1989) Os, Sr, Nd, and Pb isotope systematics of southern African peridotite xenoliths: implications for the chemical evolution of subcontinental mantle. Geochim Cosmochim Acta 53:1583–1595
Walker R, Horan M, Morgan J, Becker H, Grossman J, Rubin A (2002) Comparative $^{187}$Re–$^{187}$Os systematics of chondrites: Implications regarding early solar system processes. Geochim Cosmochim Acta 66:4187–4201
Walter M, Bulanova G, Armstrong L, Keshav S, Blundy J, Gudfinnsson G, Lord O, Lennie A, Clark S, Smith C (2008) Primary carbonatite melt from deeply subducted oceanic crust. Nature 454:622–625
Walter MJ, Kohn SC, Araujo D, Bulanova GP, Smith CB, Gaillou E, Wang J, Steele A, Shirey SB (2011) Deep mantle cycling of oceanic crust; evidence from diamonds and their mineral inclusions. Science 334:54–57
Walter MJ, Thomson AR, Smith EM (2022) Geochemistry of silicate and oxide inclusions in sublithospheric diamonds. Rev Mineral Geochem 88:393–450
Wang H, van Hunen J, Pearson DG (2018) Making Archean cratonic roots by lateral compression: a two-stage thickening and stabilization model. Tectonophysics 746:562–571
Warnock A, Zeitler P, Wolf R, Bergman S (1997) An evaluation of low-temperature apatite UTh/He thermochronometry. Geochim Cosmochim Acta 61:5371–5377
Wass SY, Rogers N (1980) Mantle metasomatism—precursor to continental alkaline volcanism. Geochim Cosmochim Acta 44:1811–1823
Weiss Y, Cazs J, Navon O (2022a) Fluid inclusions in fibrous diamonds. Rev Mineral Geochem 88:475–532
Weiss Y, Czas J, Navon O (2022b) Global published compositions of high-density fluids (HDFs) in fibrous diamonds, Version 1.0. Interdisciplinary Earth Data Alliance (IEDA), doi: 10.26022/IEDA/112016
Weiss Y, Kiro Y, Class C, Winckler G, Harris JW, Goldstein SL (2021) Helium in diamonds unravels over a billion years of craton metasomatism. Nat Commun 12:2667
Welke HJ, Allsopp HL, Harris JW (1974) Measurements of K, Rb, U, Sr and Pb in diamonds containing inclusions. Nature 252:35–37
Westerlund KJ, Gurney JJ (2004) Silicate and oxide inclusion characteristics and infra-red absorption analysis of diamonds from the Klipspringer kimberlites, South Africa. S Afr J Geol 107:131–146
Westerlund KJ, Gurney JJ, Carlson RW, Shirey SB, Hauri EH, Richardson SH (2004) A metasomatic origin for late Archean eclogitic diamonds; implications from internal morphology of diamonds and Re–Os and S isotope characteristics of their sulfide inclusions from the Late Jurassic Klipspringer kimberlites. S Afr J Geol 107:119–130
Westerlund KJ, Shirey SB, Richardson SH, Carlson RW, Gurney JJ, Harris JW (2006) A subduction wedge origin for Paleoarchean peridotitic diamonds and harzburgites from the Panda Kimberlite, Slave Craton; evidence from Re–Os isotope systematics. Contrib Mineral Petrol 152:275–294
Wetherill GW (1956) Discordant uranium–lead ages I. Eos, Trans Am Geophys Union 37:320–326
White LT, Graham I, Tanner D, Hall R, Armstrong RA, Yaxley G, Barron L, Spencer L, van Leeuwen TM (2016) The provenance of Borneo's enigmatic alluvial diamonds; a case study from Cempaka, SE Kalimantan. Gondwana Res 38:251–272
Wiggers de Vries DF, Pearson DG, Bulanova GP, Smelov AP, Pavlushin AD, Davies GR (2013) Re–Os dating of sulphide inclusions zonally distributed in single Yakutian diamonds; evidence for multiple episodes of Proterozoic formation and protracted time scales of diamond growth. Geochim Cosmochim Acta 120:363–394
Williams AF (1932) The genesis of the diamond. London Ernest Benn
Wilson JF (1990) A craton and its cracks: some of the behaviour of the Zimbabwe block from the Late Archaean to the Mesozoic in response to horizontal movements, and the significance of some of its mafic dyke fracture patterns. J Afr Earth Sci 10:483–501
Wolf R, Farley K, Silver L (1996) Helium diffusion and low-temperature thermochronometry of apatite. Geochim Cosmochim Acta 60:4231–4240
Wu F, Mitchell RH, Li Q, Sun J, Liu C, Yang Y (2013) In situ U–Pb age determination and Sr–Nd isotopic analysis of perovskite from the Premier (Cullinan) kimberlite, South Africa. Chem Geol 353:83–95
Zegers TE, de Keijzer M, Passchier CAW, White SH (1998) The Mulgandinnah shear zone, and Archean crustal-scale strike-slip zone, eastern Pilbara, Western Australia. Precambrian Res 88:233–248
Zeh A, Stern RA, Gerdes A (2014) The oldest zircons of Africa—their U–Pb–Hf–O isotope and trace element systematics, and implications for Hadean to Archean crust–mantle evolution. Precambrian Res 241:203–230